5-1-2011

Characterization of tissue mimicking materials for testing of microwave medical devices

Mary Virginia Dancsisin

CHARACTERIZATION OF TISSUE MIMICKING MATERIALS FOR TESTING OF MICROWAVE MEDICAL DEVICES

By

Mary Virginia Dancsisin

A Thesis
Submitted to the Faculty of
Mississippi State University
in Partial Fulfillment of the Requirements
for the Degree of Masters of Arts
in Biomedical Engineering
in the Department of Agricultural and Biological Engineering

Mississippi State, MS

August 2011

CHARACTERIZATION OF TISSUE MIMICKING MATERIALS FOR TESTING OF MICROWAVE MEDICAL DEVICES

By

Mary Virginia Dancsisin

Approved:

Erdem Topsakal Associate Professor of Electrical and Computer Engineering (Director of Thesis)	Steven Elder Professor of Agricultural and Biological Engineering (Graduate Coordinator)
Jun Liao Associate Professor of Agricultural and Biological Engineering (Committee Member)	Robert Cooper Associate Dean and COO of MSU College of Veterinary Medicine (Committee Member)

Sarah A. Rajala
Dean of the Bagley College of Engineering

Name: Mary Virginia Dancsisin

Date of Degree: August 6, 2011

Institution: Mississippi State University

Major Field: Biomedical Engineering

Major Professor: Dr. Erdem Topsakal

Title of Study: CHARACTERIZATION OF TISSUE MIMICKING MATERIALS FOR TESTING OF MICROWAVE MEDICAL DEVICES

Pages in Study: 102

Candidate for Degree of Master of Science

The driving force behind this thesis was the need for developing tissue mimicking materials that can mimic the dielectric properties of various biological soft tissues to aid in the development and testing of electromagnetic medical devices. Materials that can mimic the dielectric properties of human skin, adipose, muscle, malignant and healthy fibroglandular tissue, liver, pancreas, and kidney within the frequency range of 500 MHz to 20 GHz have been characterized and tested. The tissue mimicking materials are used to construct biological phantoms for studies that involve the investigation of wireless medical telemetry and a microwave breast cancer detection device.

TABLE OF CONTENTS

LIST OF TABLES

LIST OF FIGURES

CHAPTER I

INTRODUCTION

The application of electromagnetics in medicine is emerging as it shows great potential in present and upcoming medical technology and procedures. The electromagnetic fields can be transmitted or received for imaging, communications, or heating purposes without having direct contact with the point of interest [1]. Some of these applications that are being used or researched today include cardiac pacemakers, glucose monitoring, microwave imaging systems, and microwave hyperthermia [2-5]. The testing stage is vital in guaranteeing the proper functioning of the new, developed equipment. Because *in vivo* testing of electromagnetic medical devices on humans is not practical during the design process, and such measurements are subject to strict regulations enforced by the Food and Drug Administration, there is a need for developing *in vitro* testing techniques that consist of synthetic materials that can mimic the dielectric properties of the tissue of interest.

In the past, different tissue mimicking phantom materials have been synthesized and used throughout several studies as an alternative to testing electromagnetic equipment on human subjects [6-10]. The core ingredient varies with each phantom causing the material to acquire three different forms: liquid, solid, and semi-solid. Most liquid phantoms are composed of saline mixtures or similar body fluid equivalent materials. They have been used on several applications regarding antenna and RF

equipments to simulate and measure the specific absorption rate (SAR) of the tissue once exposed to electromagnetic radiation [6-10]. Because of the liquid phantoms form a state, there are limitations on their use by prohibiting the creation of complex phantoms. Liquid phantoms are required to be kept in a container and therefore cannot be implemented to create a phantom that mimics a complex biological construct with multiple tissue layers and a dynamic shape. For this reason, the tissue mimicking material needs to be in a solid or semi-solid form to acquire realistic tissue equivalent models. In addition, testing the device in liquids can be messy and quite cumbersome. The solid phantoms synthesized in previous research consisted of plastics, polyethylene powder and saline, silicon rubber, ceramic powder and resin, and strontium titanate powder and resin [11-17]. Solid body phantoms have been used throughout several studies to measure SAR at radio frequencies [15-19]. The solid phantoms are intended for mimicking the average dielectric properties among various tissues rather than of each individual tissue. Consequently, phantoms with multiple layers of tissue cannot be synthesized. The solution to this is the implementation of semi-solid mimicking materials. The core ingredients for tissue mimicking semi-solid phantoms that other researchers have used are polyacrylamide, TX-150, cryogel, and gelatin [20-29].

In our research we concentrate on gelatin based semi-solid tissue mimicking phantoms for the purpose of *in vitro* testing of implantable medical telemetry, microwave breast cancer detection technique, and microwave hyperthermia. The advantages of using a gelatin base material include the following: contain very few ingredients, does not require elaborated steps and expensive facilities to be characterized, composed of inexpensive materials, and is a simple and quick process when compared to *in vivo*

testing. Materials have been characterized that mimic the electrical properties of the following human tissues: skin, adipose tissue, muscle, malignant and nonmalignant fibroglandular tissue that contains 0-30% adipose tissue, malignant and nonmalignant fibroglandular tissue that contains 31-84% adipose tissue, liver, pancreas, and kidney. These materials are characterized to be applied to implantable medical telemetry, breast cancer detection system, and microwave hyperthermia.

CHAPTER II

ELECTRICAL PROPERTIES OF BIOLOGICAL TISSUES AND MEASUREMENT TECHNIQUES

2.1 Electrical Properties of Biological Tissues

The electrical properties of biological tissues play a large role in several new and upcoming electromagnetic medical applications such as medical telemetry devices, microwave imaging, and radio frequency hyperthermia. The electrical properties of interest are relative permittivity and conductivity. Permittivity describes the material's ability to store charges or rotate dipoles by an applied external field [30]. Permittivity, ε, is described by:

$$\varepsilon = \varepsilon_r \varepsilon_o \tag{2-1}$$

where:

ε_r = relative permittivity

ε_o = permittivity of free space (8.85×10^{-12} F/m).

Relative permittivity, ε_r, is the permittivity of a material relative to that of free space. It is of interest when evaluating the effects of biological tissues under an applied field. Relative permittivity is composed of real and imaginary elements which can be described by:

$$\varepsilon_r = \varepsilon_r' + i\varepsilon_r'' \tag{2-2}$$

where,

$$\varepsilon_r'' = \frac{\sigma}{\omega\varepsilon_o}$$

= the imaginary element of relative permittivity

ε_r' = the real element of relative permittivity

σ = conductivity

ω = angular frequency.

Conductivity, σ, is the measure of a material's ability to conduct or transport electrical charges by an applied electric field, thus it is also of interest when evaluating the effects of biological tissues under an applied field. Both conductivity and relative permittivity are functions of vector coordinates, frequency, and temperature. This characteristic is called dispersion and occurs in biological tissues. At frequencies below 10 kHz, called α region, the permittivity is high while the conductivity is low. This is because of the ability of the dipoles to change orientation due to an applied electric field. As the frequency increases to the MHz frequency range, β region, and the GHz frequency range, γ region, the polarization disappears because the dipoles are less likely to change because of the applied force. This causes the permittivity to decrease. Within relatively higher frequencies, charged carriers are least likely to be trapped and thus the conductivity is increased [30]. The dispersion effect among a large frequency range is shown is Figure 2.1 [30].

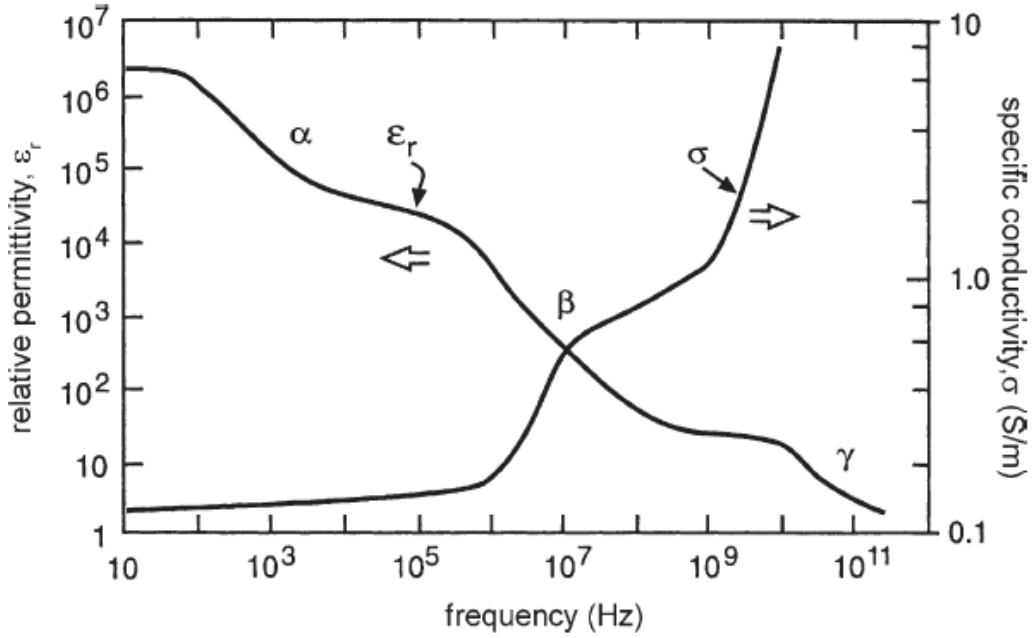

Figure 2.1

Dispersion of Biological Tissues

2.2 Measurement Tools and Techniques

The characterization of tissue mimicking gels involves the testing of the material's electrical properties through the use of the Agilent Technologies® E8362B PNA Network Analyzer and Agilent Technologies® 85070E Dielectric Probe Kit. The PNA network analyzer is a measurement platform used to analyze various properties of electrical networks that are associated with electrical signal reflection, signal transmission, amplitude, and phase. The PNA network analyzer along with the dielectric probe is shown in Figure 2.2.

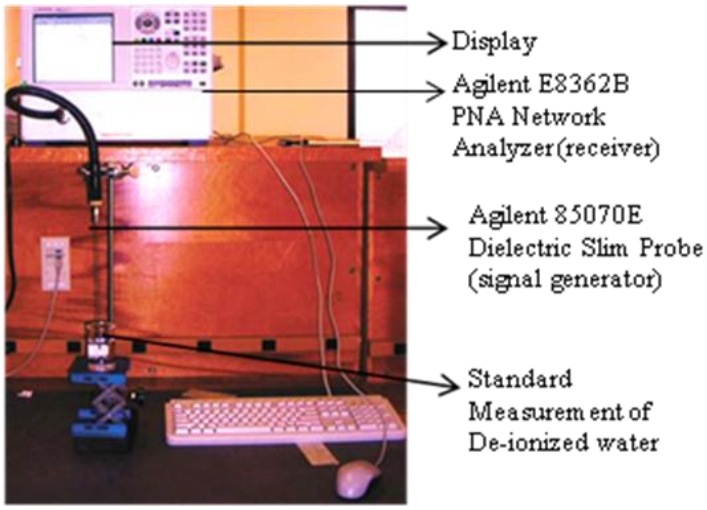

Figure 2.2

PNA Network Analyzer and Dielectric Probe Kit Set-Up

The network analyzer operates from 10 MHz to 20 GHz and consists of a signal generator, receiver, and a display. Shown in Figure 2.2, the dielectric properties of a material are measures at real time by the dielectric probe (the signal generator) transmitting a microwave signal at a single frequency into the material, while the network analyzer (the receiver) measures the material's response to the microwave energy by detecting the reflected and transmitted signals from the material. The measurement is then repeated at the next stepped frequency until it reaches the assigned final frequency. The measured data is displayed in a chart form which is easily exported into MATLAB® for graphing and analysis.

The network analyzer can calculate a material's relative permittivity, dielectric loss factor, loss tangent, or Cole-Cole parameters. For the majority of our case studies, the dielectric constant, ε', and the dielectric loss factor, ε'', was utilized to obtain the

material's dielectric properties. Once the dielectric loss of the material is measured, it is implemented into Equation 2.3 to calculate the material's conductivity, σ.

$$\sigma = \omega \varepsilon'' \varepsilon_0 \tag{2-3}$$

The dielectric probe kit contains three probe designs: performance, high temperature, and slim form. The performance probe kit, shown in Figure 2.3(a), works over a frequency range of 500 MHz to 50 GHz and withstands a -40°C to 200°C temperature range. The broad operating temperature range allows for dielectric measurements versus both frequency and temperature. The probe can be autoclaved so it is useful in food, medical and chemical industry applications. The high temperature probe kit, shown in Figure 2.3(b), works over a frequency range of 200 MHz to 50 GHz and withstands a -40°C to 200°C temperature range that allows for dielectric measurements versus both frequency and temperature. The probe is resistant to corrosive or abrasive materials, and its large flange makes it appropriate to measuring flat surface solids and liquids. The slim probe kit, shown in Figure 2.3(c), is used for the majority of our studies. It operates over a frequency range of 500 MHz to 50 GHz and withstands a 0°C to 125°C temperature range. To perform the measurements, the probe is either immerged in a liquid or placed on the surface of a semi-solid. The slim probe is best used for small sample sizes that are either liquid or semi-solids. For accurate measurements, 5mm of the material to be measured must be below and around the tip of the probe.

(a) (b) (c)

Figure 2.3

(a) Performance Probe, (b) High Temperature Probe, and (c) Slim Probe

Before measurements are made on the material, the probe must be calibrated to improve the accuracy of the measurements by removing any systematic errors. During calibration, three known standards are measured to compensate for the systematic errors: air, short circuit, and de-ionized water. The main sources of error that can affect measurement accuracy is the stability of the cable, air bubbles in the sample or at the tip of the probe, air gap between the probe and material, and the dimensions of the sample. Calibration is performed in every study before measuring each material. The calibration set-up is shown in Figure 2.2.

The network analyzer is also used to measure the electrical signal reflection and signal transmission through various tissue mimicking materials. This is important to measure the absorption of power by biological tissues that are radiated with electrical signals.

CHAPTER III

CHARACTERIZATION OF TISSUE MIMICKING MATERIALS

3.1 Skin Mimicking Material

3.1.1 Characterization of Skin Mimicking Material

A skin material is characterized by mixing de-ionized water, vegetable oil, Gelatin A, Ultra Ivory® hand soap, polyethylene glycol mono phenyl ether (Triton X-100), sodium chloride (Morton® popcorn salt), and pink food coloring. An investigation of the electrical properties of each ingredient showed that vegetable oil has the lowest electrical properties among all ingredients, while de-ionized water holds the highest. Varying the proportions of these two ingredients allows the mimicking of both low and high water content human soft tissues. Salt is used to increase the conductivity of the material while decreasing the relative permittivity. Salt also causes the permittivity to decrease rapidly from 500 MHz to 1 GHz and then slowly decrease from 1 GHz to 20 GHz. Gelatin A, Triton-X, food coloring, and hand soap all have small effects on the electrical properties of the material because of the composition of the material or its small content within the total mixture. Each human soft tissue mimicking material is characterized based on these facts. Table 3.1 shows the list of ingredients along with their percent volume, while Figure 3.1 shows the equipment that is used during the process.

Table 3.1

Recipe for Skin Mimicking Material

Ingredient	Percent Volume
De-ionized Water	68.33
Vegetable Oil	20.68
Gelatin A	8.99 (ρ=1.2 g/mL)
Ultra Ivory Soap	0.899
Triton X-100	0.899
Sodium Chloride	0.166 (ρ=2.165 g/mL)
Pink Food Coloring	0.037 (1 drop= 0.042 mL)

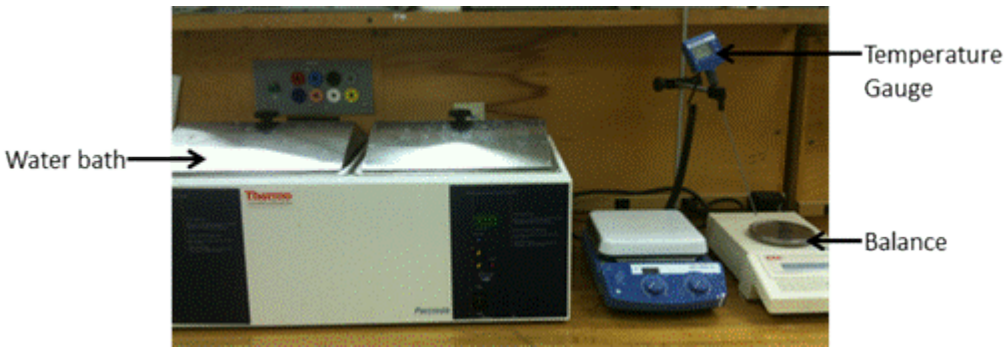

Figure 3.1

Equipment for Characterization of Tissue Mimicking Material

First, sodium chloride is mixed in a beaker with the total required amount of de-ionized water. The beaker is covered with Syran® wrap and placed in an 80ºC water bath until all of the salt granules are dissolved. In a separate beaker, Triton X-100 is mixed with the Gelatin A until all the gelatin granules are coated. Triton X-100 is a wetting agent that alleviates the mixing of Gelatin A with aqueous solutions. Gelatin A is a gelling agent used to solidify the mixture. Once the sodium chloride granules are dissolved in the water, the saline solution is poured into the beaker that contains the Gelatin A compound. While stirring, pink food coloring is added to the mixture. The

beaker is then covered with Syran® wrap and placed in an 80ºC water bath for 20 minutes. Gelatin A is soluble in water at high temperatures and sets as a gel at or above room temperature. The total required amount of vegetable oil is poured in a separate beaker, covered with Syran® wrap, and placed in an 80°C water bath for 20 minutes. The oil needs to be at the same temperature as the Gelatin A compound when they are mixed together so that the gelatin does not prematurely form before the mixture is thoroughly mixed. Once the gelatin and oil mixtures have both reached 80°C, the vegetable oil and Gelatin mixtures are mixed with Ultra Ivory® hand soap in a 500 mL Whip Mix Vac-U-Mixer. The hand soap acts as a surfactant that allows the oil to mix into the water. Once the lid is sealed, the mixer's drive nut is inserted into the Whip-Mix Combination Vacuum Mixer Unit's drive chuck. The gel should be mixed for 15 seconds. Figure 3.2 shows the equipment used in the mixing process.

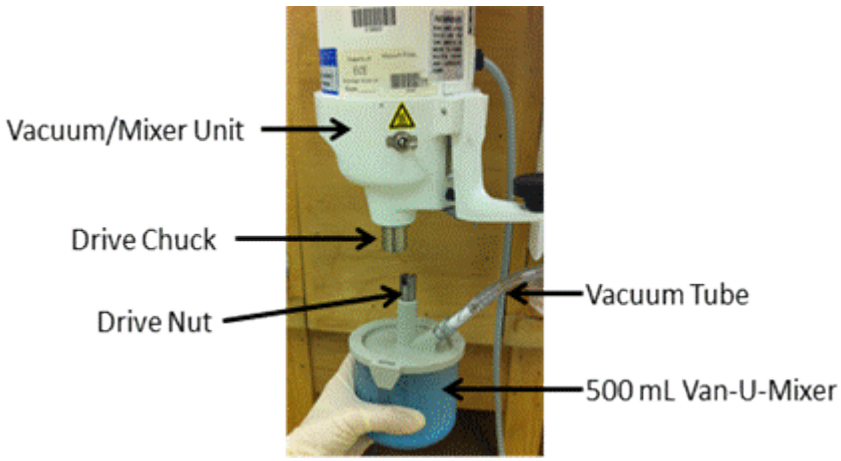

Figure 3.2

Whip Mix Combination Vacuum Mixer Unit and Vac-U-Mixer

Figure 3.3

Characterized Skin Mimicking Material

Obtaining a mixture without air bubbles is vital to achieve accurate electrical property measurements. The machine has a vacuum system; therefore, almost no air bubbles are made within the gel during the mixing process. The mixture is poured into a beaker and set to form in the refrigerator for 30 minutes. Producing air bubbles should be avoided while pouring the material into the beaker. The Figure 3.3 shows the skin mimicking material once it is completely formed.

3.1.2 Skin Mimicking Material Dielectric Probe Measurements

Once the skin mimicking material has gelatinized, the relative permittivity and conductivity is measured from 500 MHz to 20 GHz using Agilent Technologies® E8362B PNA Network Analyzer and Agilent Technologies® 85070E Dielectric Slim Probe Kit. The experimental set-up for electrical property measurements is demonstrated in Figure 3.4.

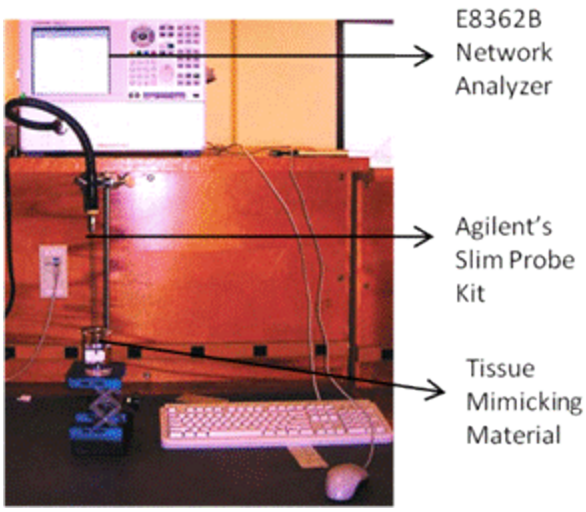

Figure 3.4

Dielectric Probe Measurement Set-Up

Any air bubbles that are obtained within the material rise to the top of the mixture during the forming process. To obtain a mixture with absolutely no air bubbles, approximately 1 cm of the top of the gel is cut off. As shown in Figure 3.5, this procedure is done to all of the tissue mimicking gels characterized. To ensure data reliability, six different points on the material are measured with the Agilent slim probe: one on the top, one on the bottom, and four on the side where each measurement is at a 90º angle from the previous measurement. Figure 3.6 shows a diagram of the areas in which the measurements are taken.

Figure 3.5

Top Slices of Gels to Avoid Air Bubbles

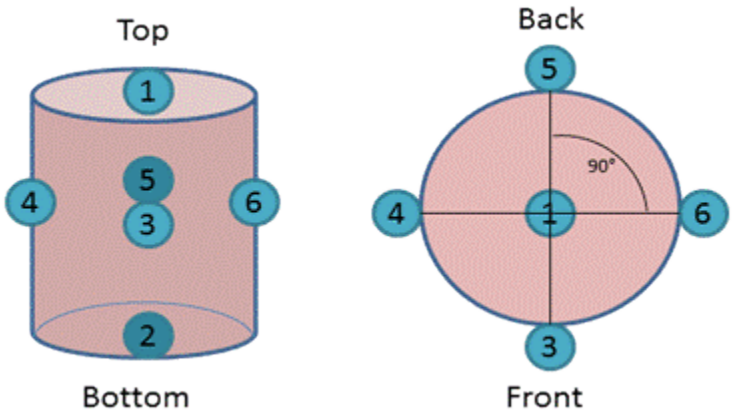

(a) (b)

Figure 3.6

Points of Measurements where (a) Shows the Side View and
(b) Shows the Top View of the Material

Once the measurements are performed, the data of the electrical properties is graphed in MATLAB®. The average of the six sets of measured properties is compared with the human wet skin reference data obtained from [34-35]. In [34] a comprehensive literature survey of previously measured electrical properties of different tissues either excised from humans or animals is provided. In [35] the electrical property measurements of different tissues from 10 Hz to 20 GHz are given. The measurements are taken from (i)

excised animal tissue mostly from freshly killed ovine and some porcine; (ii) human autopsy materials and (iii) human skin and tongue *in vivo*. The human tissues are obtained 24 to 48 hours after death while the animal tissues are measured 2 hours after death. This data is implemented into a website that will allow users to obtain the electrical properties of various tissues within the frequency range of interest. Figure 3.7 and Figure 3.8 show a graphical comparison between skin's relative permittivity and conductivity of each point of measurements, the average of the six points, and reference data in [34-35], respectively.

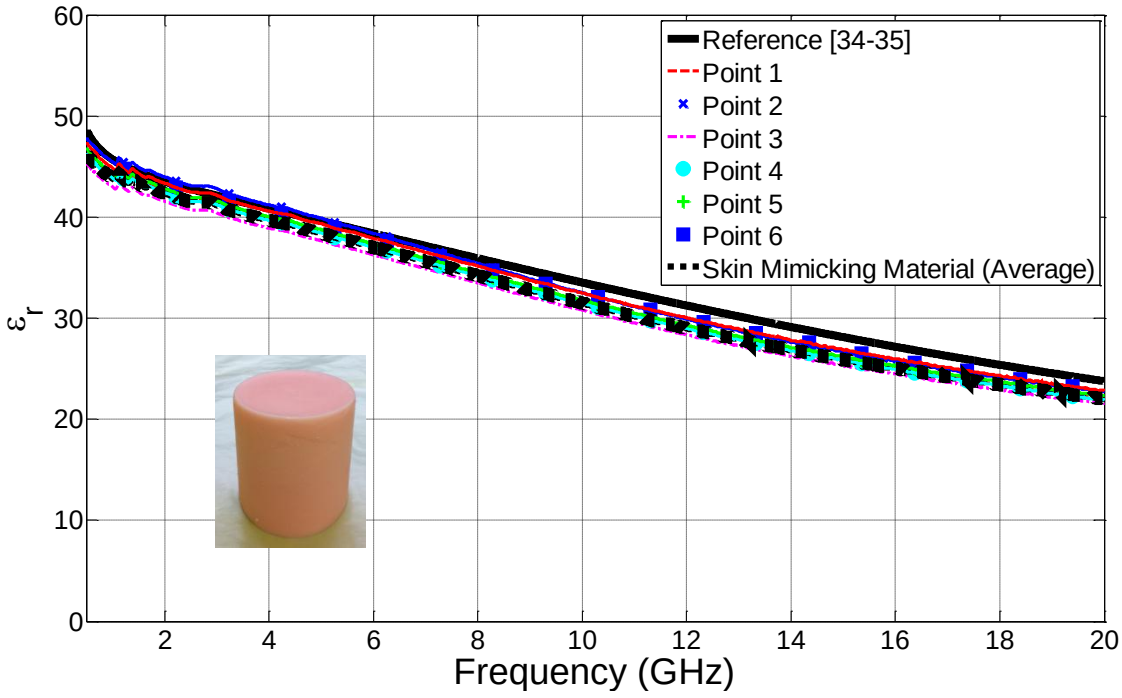

Figure 3.7

Relative Permittivity Comparison of Skin Mimicking Material to Reference Data

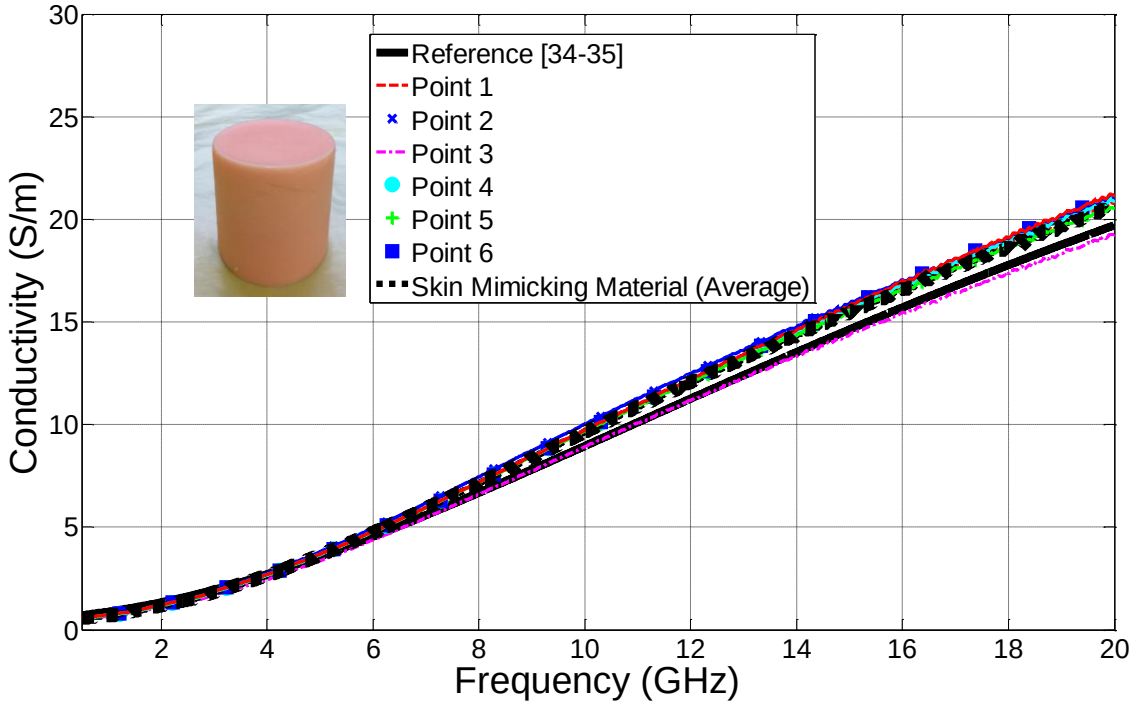

Figure 3.8

Conductivity Comparison of Skin Mimicking Material to Reference Data

As shown in the figures, a consistent agreement is obtained between the reference data in [34-35] and the measurements of the skin mimicking material. It is important to obtain a maximum deviation that is less than 10% of the data found in [34-35] at a set frequency. The characterized skin mimicking gel maximum deviation from the reference data from 500 MHz to 20 GHz is

$$\Delta\varepsilon_r = \varepsilon_{r_{reference}} - \varepsilon_{r_{material}} = 2.35 \tag{3-1}$$

for relative permittivity and

$$\Delta\sigma = \sigma_{reference} - \sigma_{material} = 1.02 \tag{3-2}$$

for conductivity.

The maximum deviation falls under 10% of the data given in literature, thus the material can be used to accurately investigate the interaction between the electromagnetic waves and skin tissue at 500 MHz to 20 GHz. This comparison is performed during the characterization process of all of the tissue mimicking materials until a desirable recipe is reached. Please note that since the maximum deviation of all of the tissue mimicking materials fall under 10% of the data given in literature, only the maximum deviation will be given for all remaining materials.

3.1.3 Shelf Life Study of the Skin Mimicking Material

Once the skin mimicking gel is characterized, the shelf life of the material is studied for a period of eight weeks. Two identical skin mimicking gel samples are created and kept covered in Syran® wrap to study the effects refrigeration has on the electrical properties of the mimicking material. One of the samples is kept in the refrigerator during the 8 week study, while the other sample is kept at room temperature. Every week the relative permittivity and conductivity are measured at room temperature from 500 MHz to 20 GHz using Agilent Technologies® E8362B PNA Network Analyzer and Agilent Technologies® 85070E Dielectric Slim Probe Kit. Approximately 1 cm of the top of the gel is cut off each week **t**o obtain the electrical properties within layers of the gel. Six measurements are made at different locations as shown in Figure 3.6. Figures 3.9-3.12 show the electrical properties of the refrigerated and non-refrigerated material.

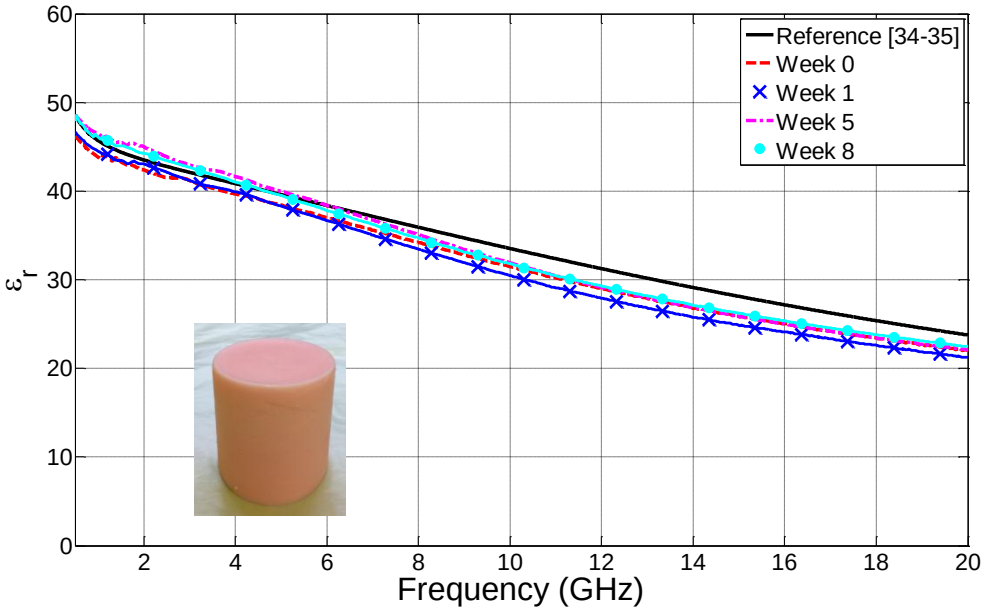

Figure 3.9

Relative Permittivity of Refrigerated Skin Mimicking Material

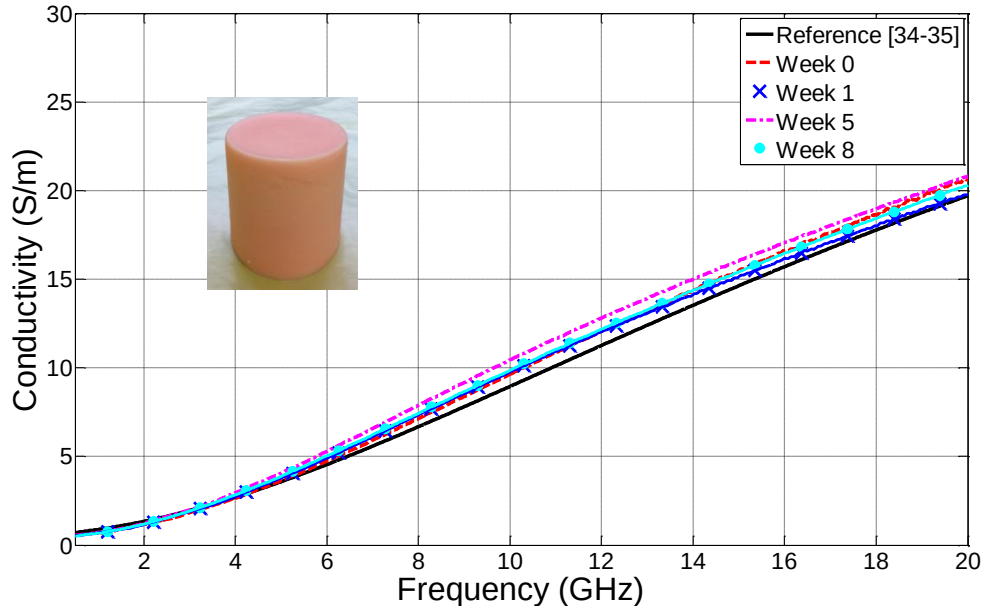

Figure 3.10

Conductivity of Refrigerated Skin Mimicking Material

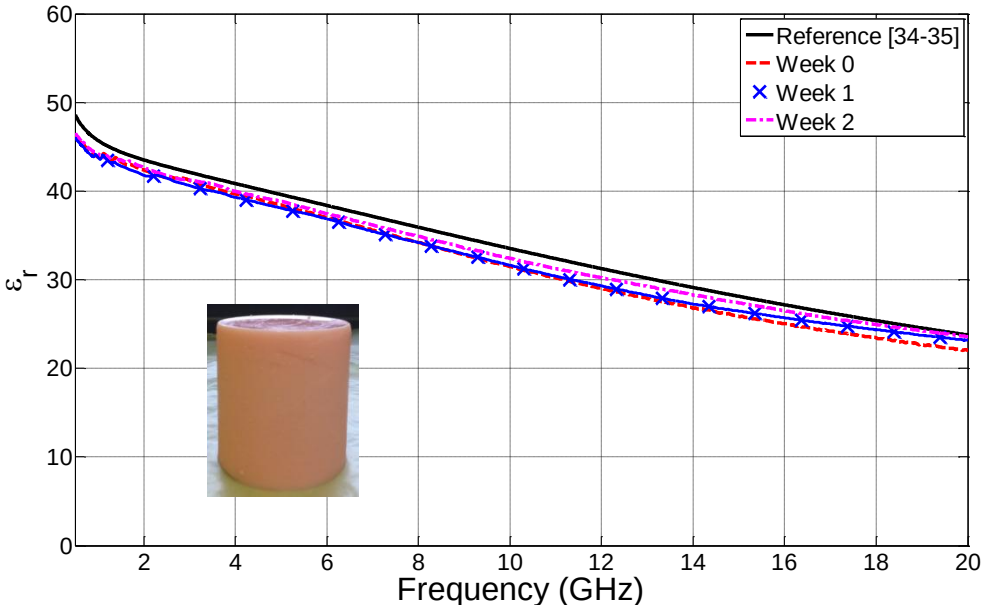

Figure 3.11

Relative Permittivity of Non-Refrigerated Skin Mimicking Material

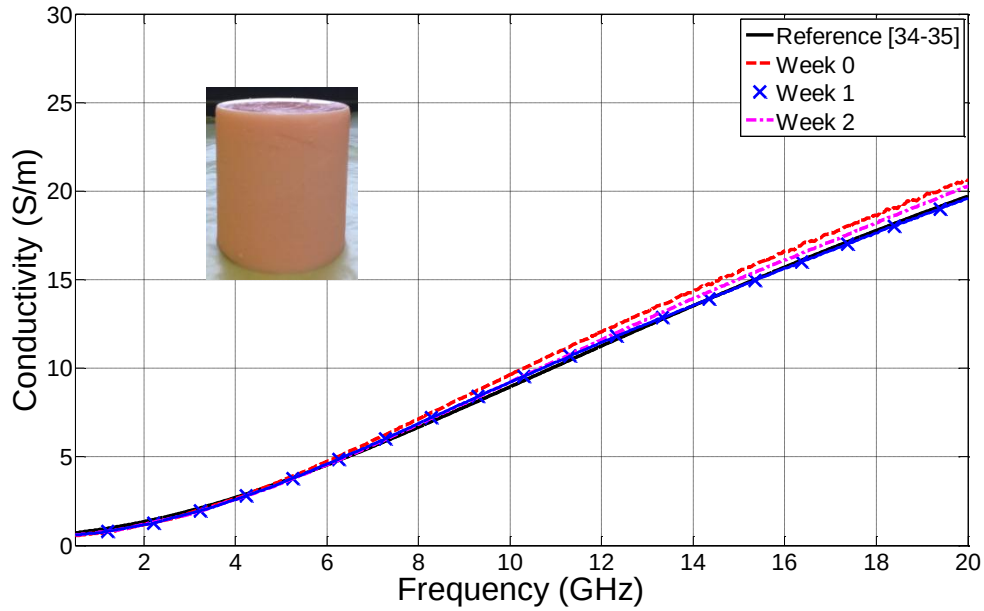

Figure 3.12

Conductivity of Non-Refrigerated Skin Mimicking Material

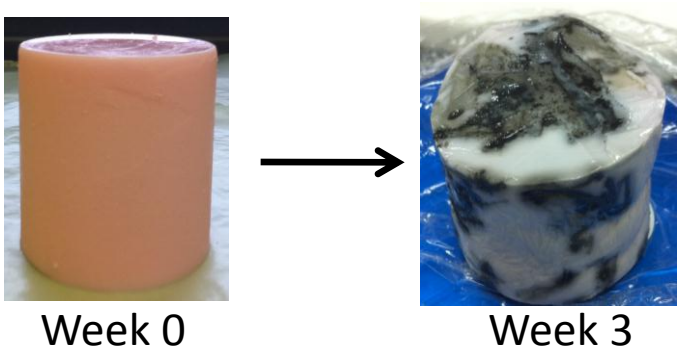

Figure 3.13

Molding of the Non-Refrigerated Material

After week 2, the unrefrigerated skin mimicking material spoiled by becoming infected with mold. Because of this, the measurements on the non-refrigerated sample are not performed for the weeks following. Figure 3.13 shows the appearance of the non-refrigerated skin mimicking material at week 0 and week 3, respectively. The spoiling of the skin mimicking material after two weeks of not being refrigerated shows the importance of refrigeration. The refrigerated gel does not spoil during the eight week period and the electrical properties are consistent.

3.1.4 Absorption of the Skin Mimicking Material

In order to study the absorption characteristics of the tissue mimicking materials, the following measuring set-up is performed. Two horn antennas that operate at 7-11 GHz are connected to the Agilent Technologies® E8362B PNA Network Analyzer to measure the absorption of power because of the interference or presence of a square skin mimicking gel sample. For both horn antennas, the waveguide length is 9 cm, the height is 5.8 cm, and the thickness is 8.2 cm, while the antennas' length is 4.5 cm, the height is 1.2 cm, and the thickness is 2.5 cm. The dimensions of the square sample are 26.5 cm in height, 26.5 cm in length, and 1.02 cm in thickness. The horn antennas are placed 9.5 cm apart, and the sample is placed between the horns. Figure 3.14 shows the measurement set-up with and without a skin mimicking gel sample.

(a) (b)

Figure 3.14

S12 and S21 Measurement Set-Up (a) Without Interference of a Skin Mimicking Sample and (b) With Interference of a Skin Mimicking Sample

Figure 3.15 shows S12 and S21 from 7-11 GHz of the antennas with and without the interference of the skin mimicking sample. These measurements are performed using Agilent Technologies® E8362B PNA Network Analyzer. The difference of the S12 and S21 of the antennas with and without the sample provides the amount of energy absorbed by the material. The absorption by the skin mimicking material is shown in Figure 3.16.

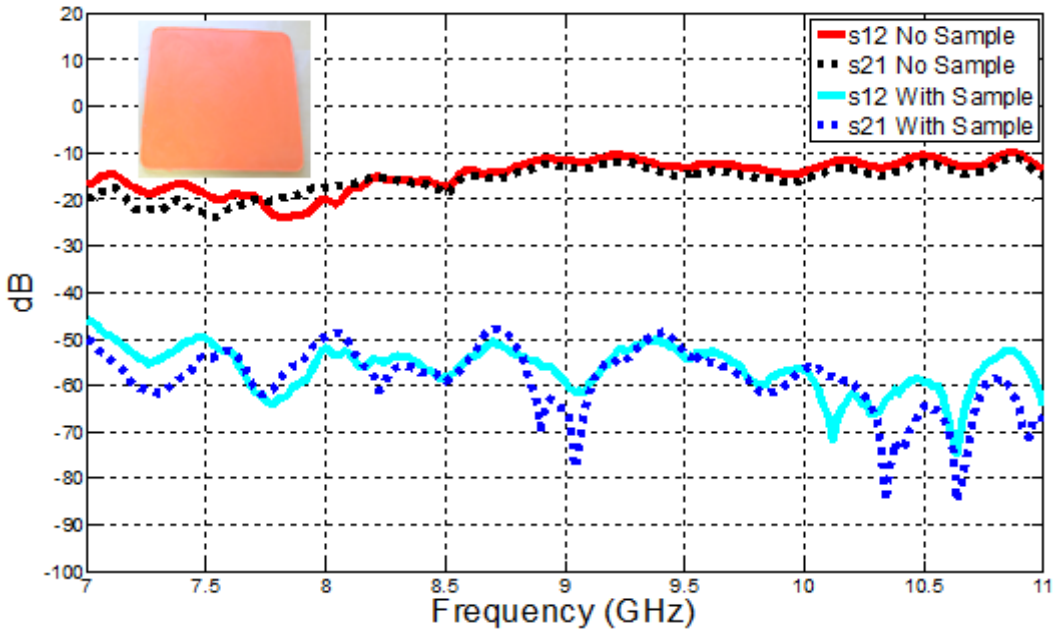

Figure 3.15

S12 and S21 With and Without the Interference of the Skin Mimicking Sample

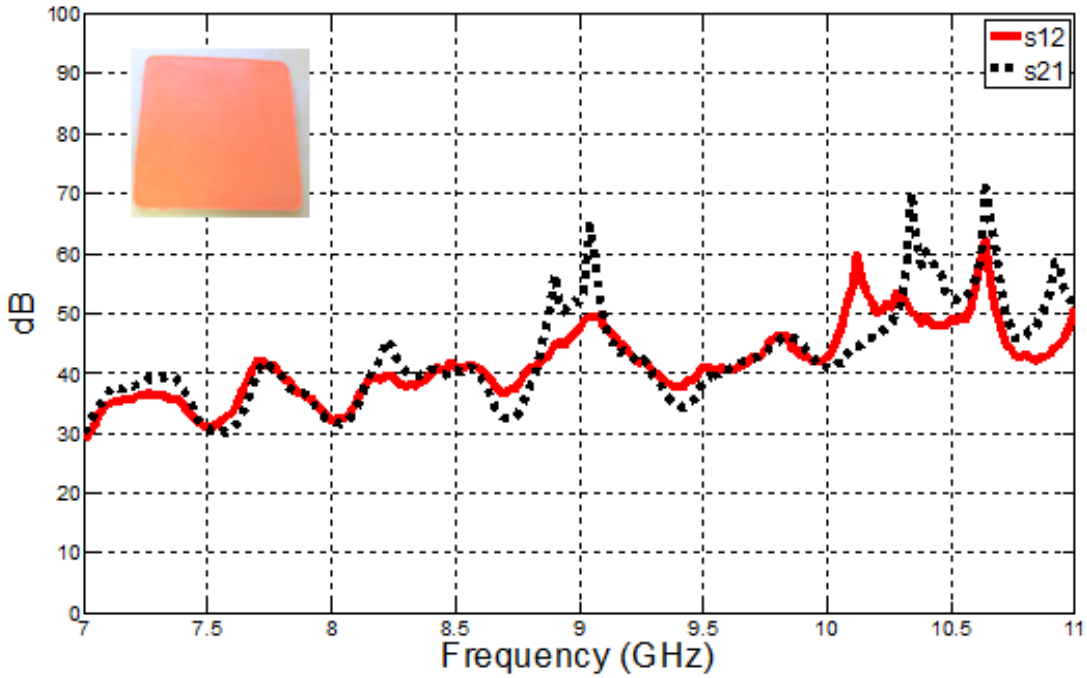

Figure 3.16

Absorption of the Skin Mimicking Material

3.2 Adipose Tissue Mimicking Material

3.2.1 Characterization of Adipose Tissue Mimicking Material

An adipose tissue mimicking material is characterized by mixing de-ionized water, vegetable oil, Ultra Ivory® hand soap, Gelatin B, Triton X-100, and yellow food coloring. Gelatin B is a gelling agent used to solidify the mixture. Table 3.2 shows the list of ingredients along with their percent volume.

Table 3.2

Recipe for Adipose Tissue Mimicking Material

Ingredient	Percent Volume
De-ionized Water	11.38
Vegetable Oil	83.44
Gelatin B	2.84 (ρ=1.2 g/mL)
Ultra Ivory Soap	1.52
Triton X-100	0.76
Yellow Food Coloring	0.06 (1 drop= 0.0417 mL)

In a beaker, the Gelatin B granules are coated with Triton X-100. Then the total required amount of de-ionized water and food coloring is stirred into the mixture. This beaker is covered with Syran® wrap and placed an 80ºC water bath for 20 minutes. The total required amount of vegetable oil is placed in a separate beaker, covered with Syran® wrap, and put in an 80°C water bath for 20 minutes. The Gelatin B mixture along with Ultra Ivory® hand soap is poured into a bowl. A hand mixer is used to stir the material. As the material is mixing, the oil is slowly poured into the mixture. Lastly, the homogeneous mixture is poured into a beaker and set to form in the refrigerator for 30 minutes. The formed adipose tissue mimicking gel is shown in the Figure 3.17.

Figure 3.17

Characterized Adipose Tissue Mimicking Material

3.2.2 Adipose Tissue Mimicking Material Dielectric Probe Measurements

Once the adipose tissue mimicking material has formed, the relative permittivity and conductivity are measured from 500 MHz to 20 GHz using Agilent Technologies® E8362B PNA Network Analyzer and Agilent Technologies® 85070E Dielectric Slim Probe Kit. As previously described in Figure 3.6, six different points on the material are measured with the Agilent slim probe. The average of the obtained measurements is compared with the human breast fat reference data obtained from [34-35]. Figure 3.18 and 3.19 show a graphical comparison between an adipose tissue's relative permittivity and conductivity of measured and reference data in [34-35] respectively.

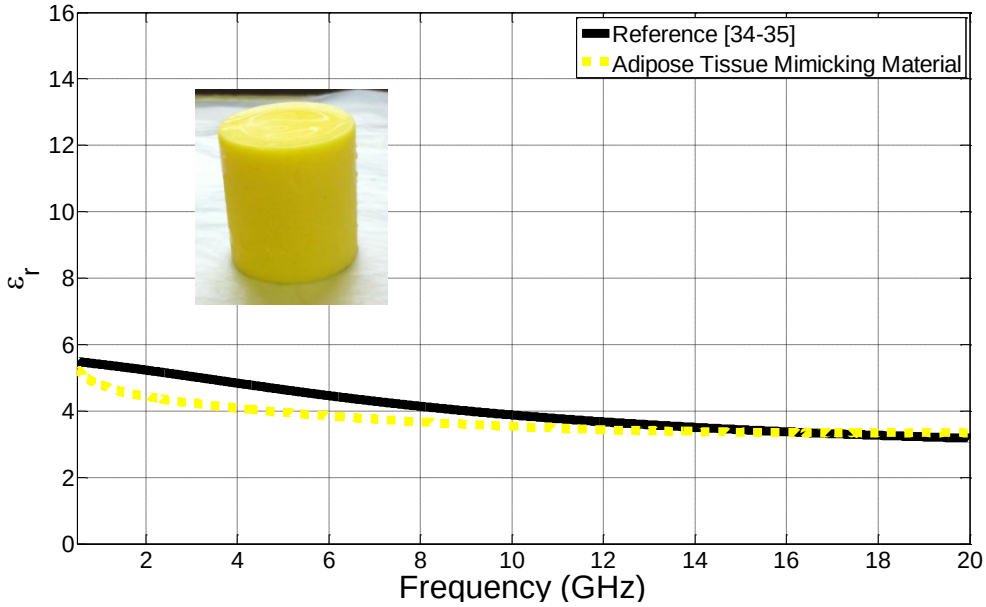

Figure 3.18

Relative Permittivity Comparison of Adipose Tissue Mimicking Material to Reference Data

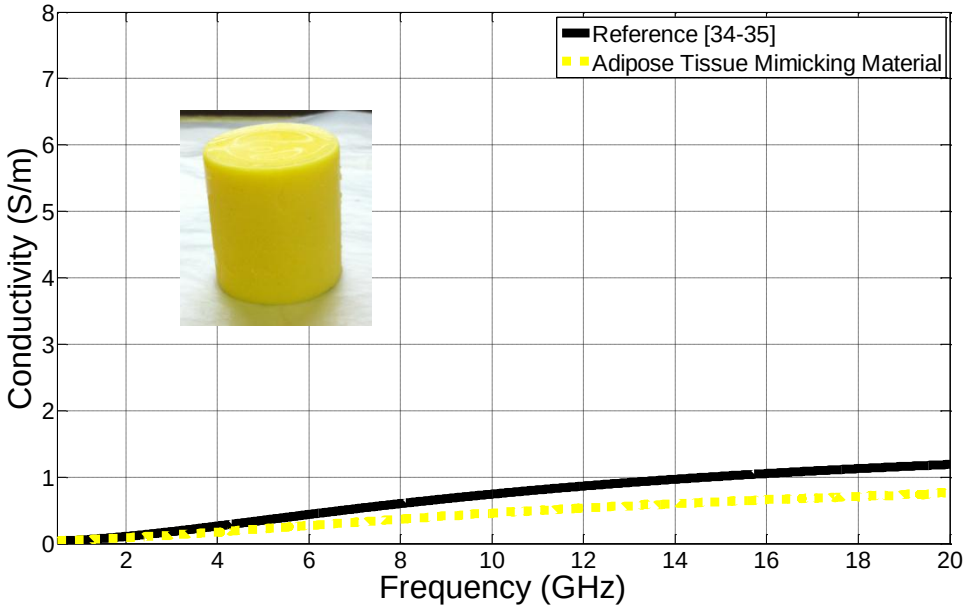

Figure 3.19

Conductivity Comparison of Adipose Tissue Mimicking Material
to Reference Data

The graph shows that a consistent agreement obtained between reference data in [34-35] and measurements of the adipose tissue mimicking material. The characterized adipose tissue mimicking gel maximum deviation from the reference data from 500 MHz to 20 GHz is 0.82 for the relative permittivity and 0.44 S/m for conductivity.

3.2.3 Shelf Life Study of the Adipose Tissue Mimicking Material

The shelf life of the adipose tissue mimicking material is studied for a period of eight weeks. The steps previously described in Chapter 3.1.3 for the skin is applied to the two adipose tissue mimicking materials to investigate the material's shelf life and the effects refrigeration has on the electrical properties of the characterized adipose tissue mimicking material. Figures 3.20-3.23 show the electrical properties throughout the 8 week study of both the refrigerated and non-refrigerated material, respectively.

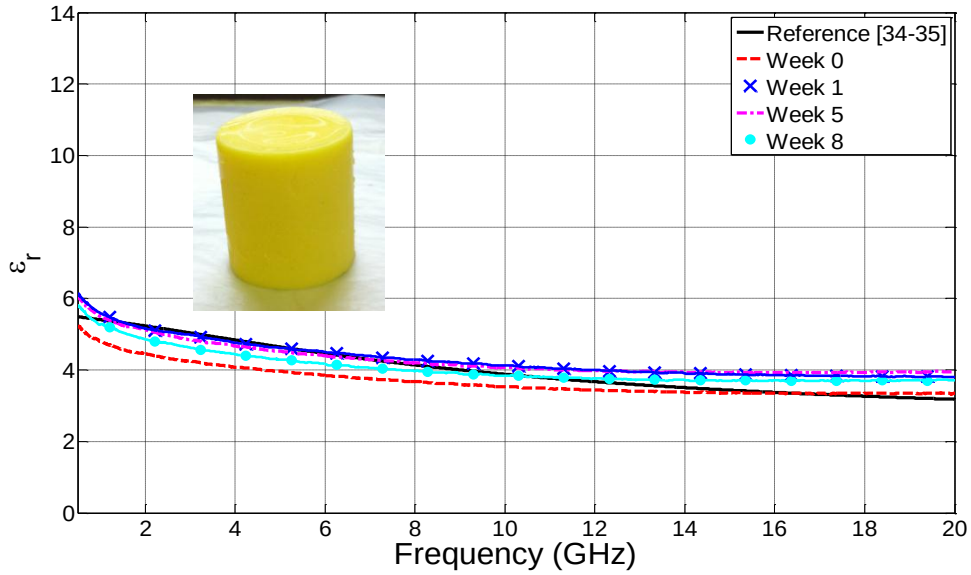

Figure 3.20

Relative Permittivity of Refrigerated Adipose Tissue Mimicking Material

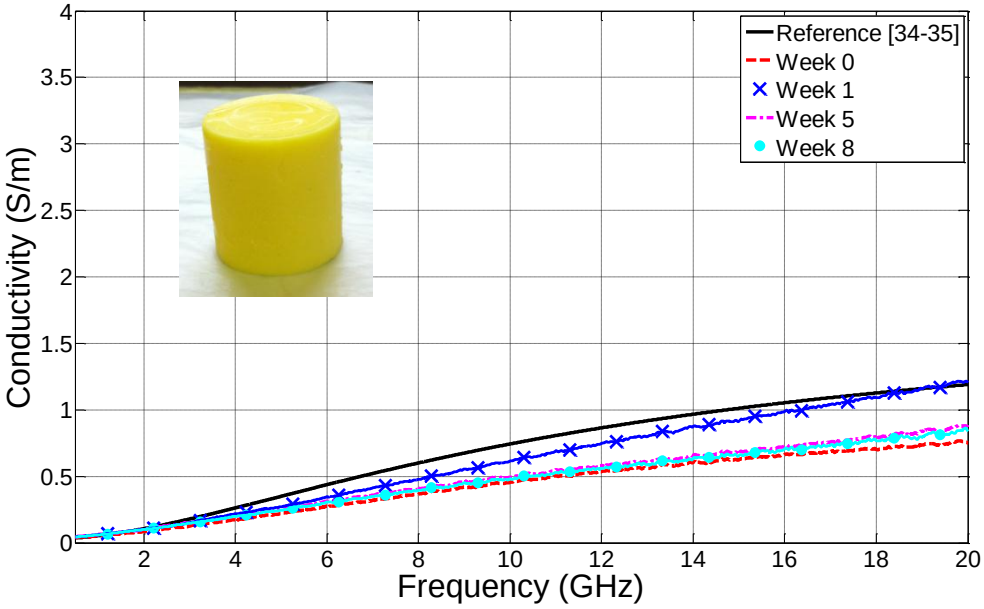

Figure 3.21

Conductivity of Refrigerated Adipose Tissue Mimicking Material

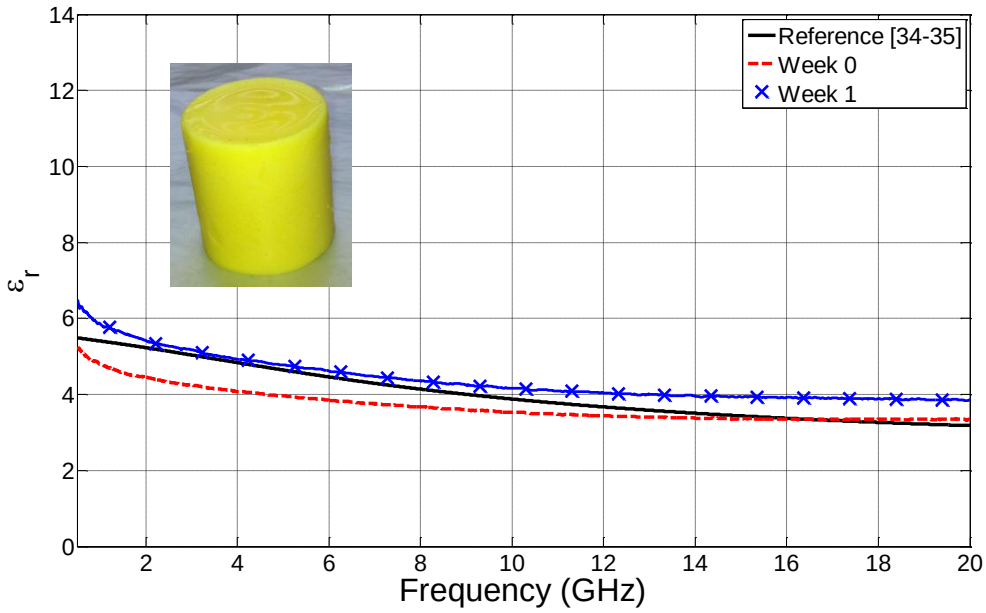

Figure 3.22

Relative Permittivity of Non-Refrigerated Adipose Tissue Mimicking Material

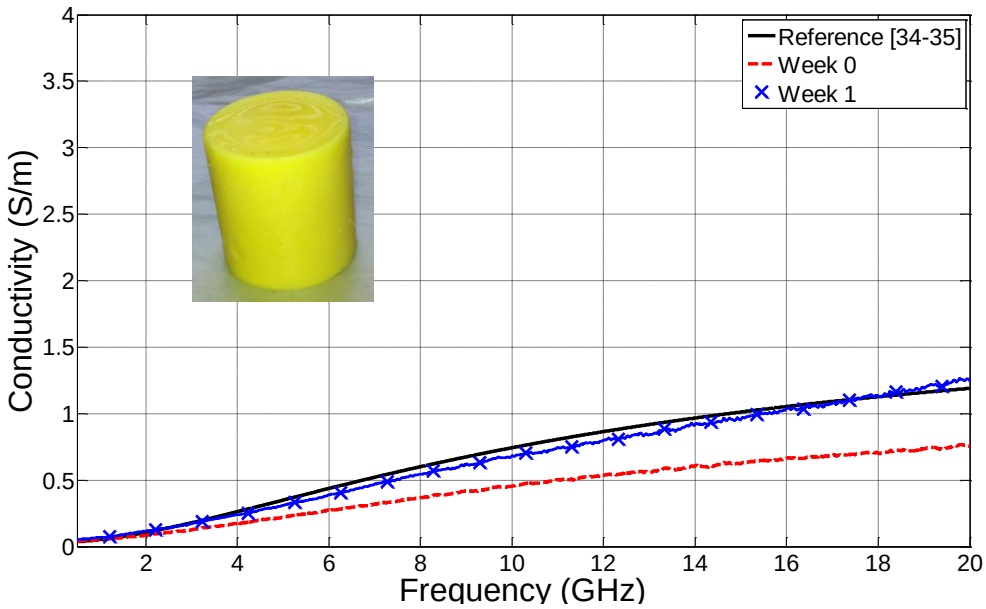

Figure 3.23

Conductivity of Non-Refrigerated Adipose Tissue Mimicking Material

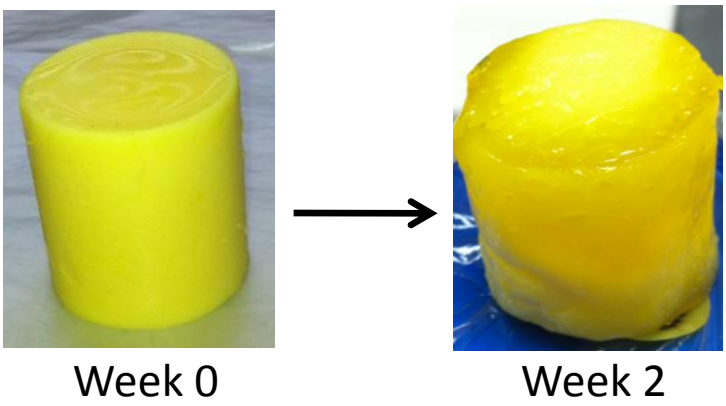

Figure 3.24

Spoiling of the Non-Refrigerated Material

After week 1, the non-refrigerated adipose tissue mimicking material spoiled. Because of this, the measurements on the non-refrigerated sample are not performed for the weeks following. Figure 3.24 shows the appearance of the non-refrigerated adipose tissue mimicking material at week 0 and week 2.

3.2.4 Absorption of the Adipose Tissue Mimicking Material

The horn antenna set-up described in Chapter 3.1.4 is used to measure the absorption of power by the presence of a square adipose tissue mimicking gel sample. The dimensions of the square sample are 15.5 cm in height, 9.5 cm in length, and 1.3 cm in thickness. The measurement set-up with the adipose tissue mimicking sample is shown in Figure 3.25. Figure 3.26 shows S12 and S21 from 7-11 GHz of the antennas with and without the interference of the adipose tissue mimicking gel sample. The absorption by the adipose tissue mimicking material is shown in Figure 3.27.

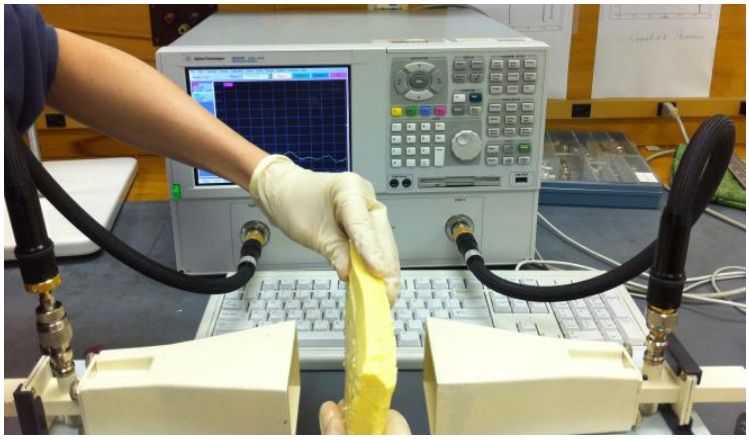

Figure 3.25

S12 and S21 Measurement Set-Up

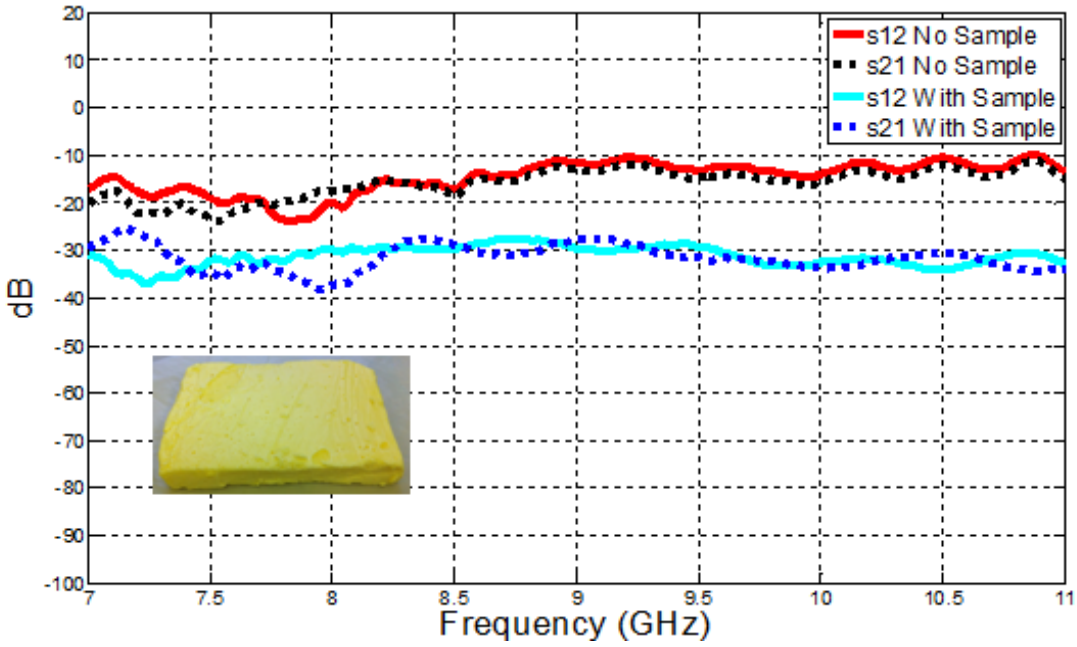

Figure 3.26

S12 and S21 With and Without the Interference of the
Adipose Tissue Mimicking Sample

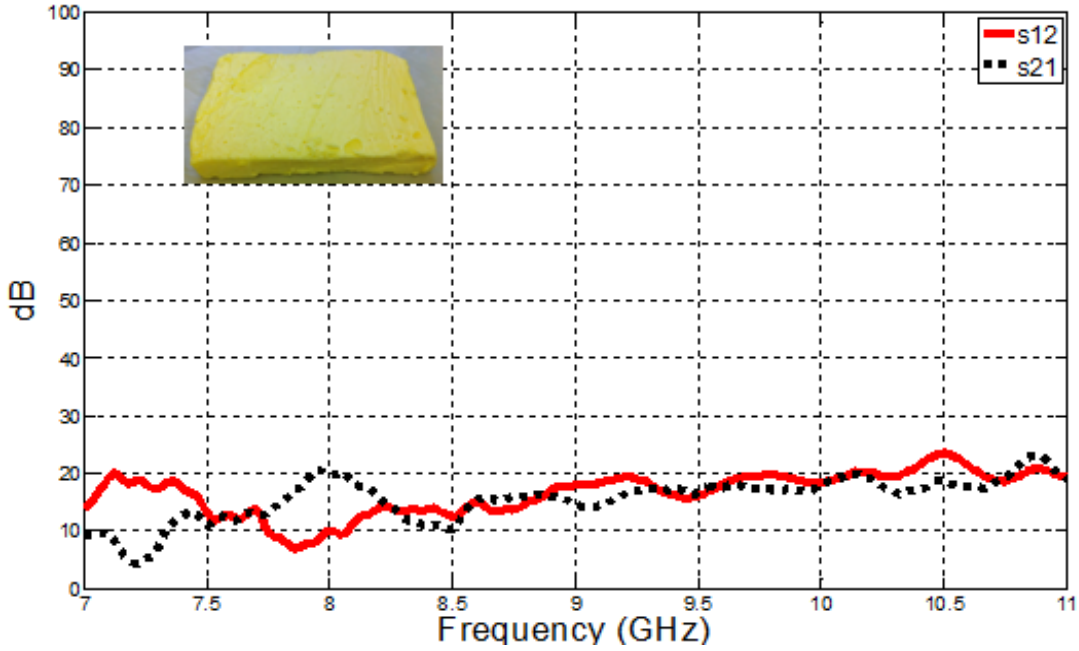

Figure 3.27

Absorption of Adipose Tissue Mimicking Material

3.3 Muscle Mimicking Material

3.3.1 Characterization of Muscle Mimicking Material

A muscle mimicking material is characterized by mixing de-ionized water, vegetable oil, Ultra Ivory® hand soap, Gelatin A, Triton X-100, Sodium Chloride, and red food coloring. Table 3.3 shows the list of ingredients along with their percent volume. The steps described in Chapter 3.1.1 are followed to characterize the muscle mimicking material. The formed muscle mimicking gel is shown in Figure 3.28.

Table 3.3

Recipe for Muscle Mimicking Material

Ingredient	Percent Volume
De-ionized Water	72.47
Vegetable Oil	13.59
Gelatin A	9.06 (ρ=1.2 g/mL)
Ultra Ivory Soap	2.72
Triton X-100	0.91
Sodium Chloride	0.13 (ρ=2.165 g/mL)
Red Food Coloring	1.13 (1 drop= 0.042 mL)

Figure 3.28

Characterized Muscle Mimicking Material

3.3.2 Muscle Mimicking Material Dielectric Probe Measurements

The relative permittivity and conductivity are measured from 500 MHz to 20 GHz. As described in Chapter 3.1.3, six different points on the material are measured with the Agilent slim probe. The average of the obtained measurements is compared with the human muscle reference data obtained from [34-35]. Figure 3.29 and Figure 3.30 show a graphical comparison between a muscle's relative permittivity and conductivity of measured and reference data in [34-35], respectively.

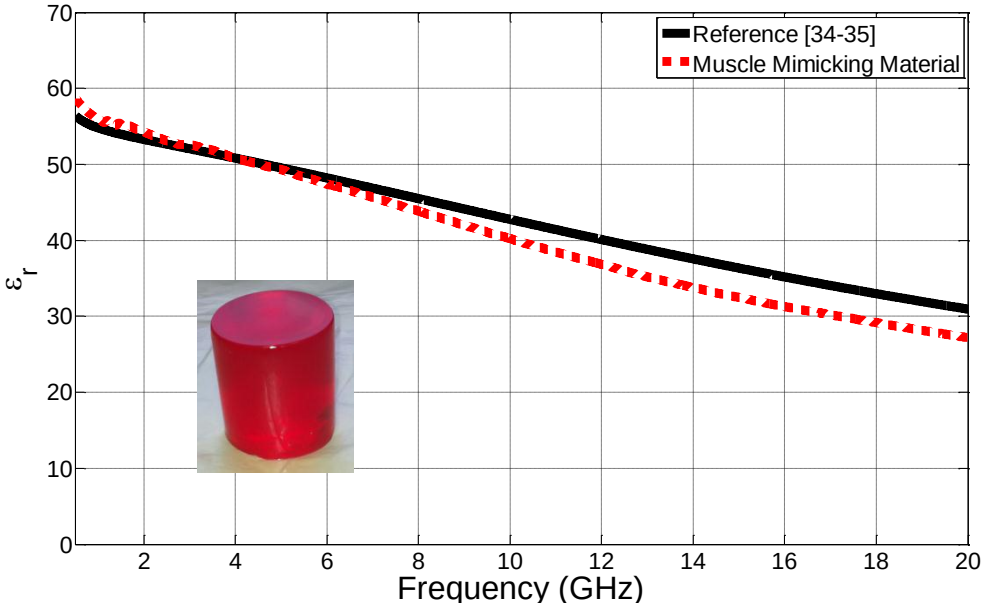

Figure 3.29

Relative Permittivity Comparison of Muscle Mimicking Material to Reference Data

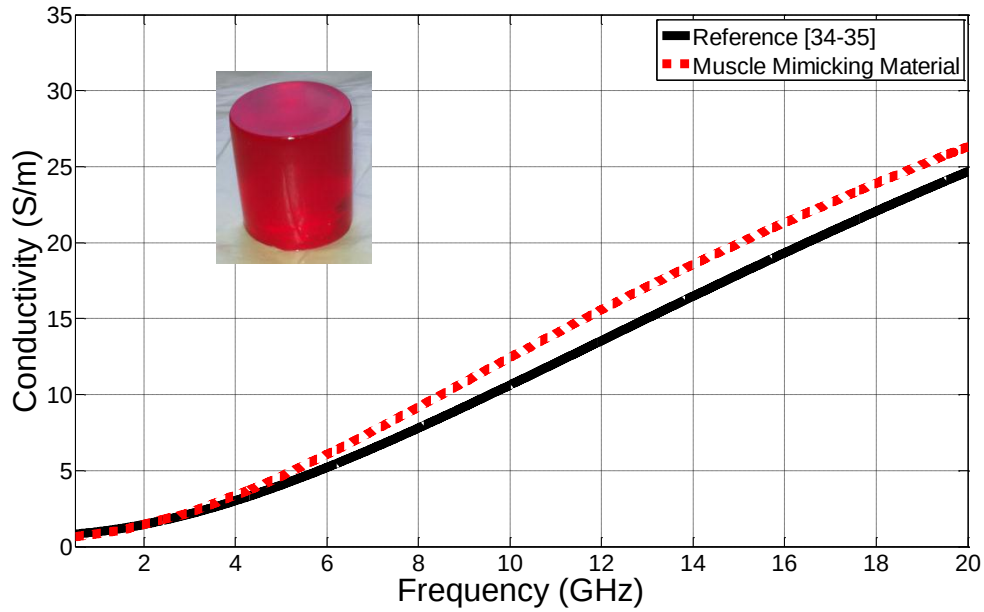

Figure 3.30

Conductivity Comparison of Muscle Mimicking Material to Reference Data

A good agreement is obtained between reference data in [34-35] and measurements of the muscle mimicking material. The characterized muscle mimicking material maximum deviation from the reference data from 500 MHz to 20 GHz is 3.94 for the relative permittivity and 0.57 S/m for conductivity.

3.3.3 Shelf Life Study of the Muscle Mimicking Material

The shelf life of the muscle mimicking material is studied for a period of eight weeks. The steps previously described in Chapter 3.1.3 are applied to two muscle mimicking materials to investigate the material's shelf life and the effects refrigeration has on the electrical properties of the tissue mimicking material. Figures 3.31-3.34 show the electrical properties throughout the 8 week study of both the refrigerated and non-refrigerated material, respectively.

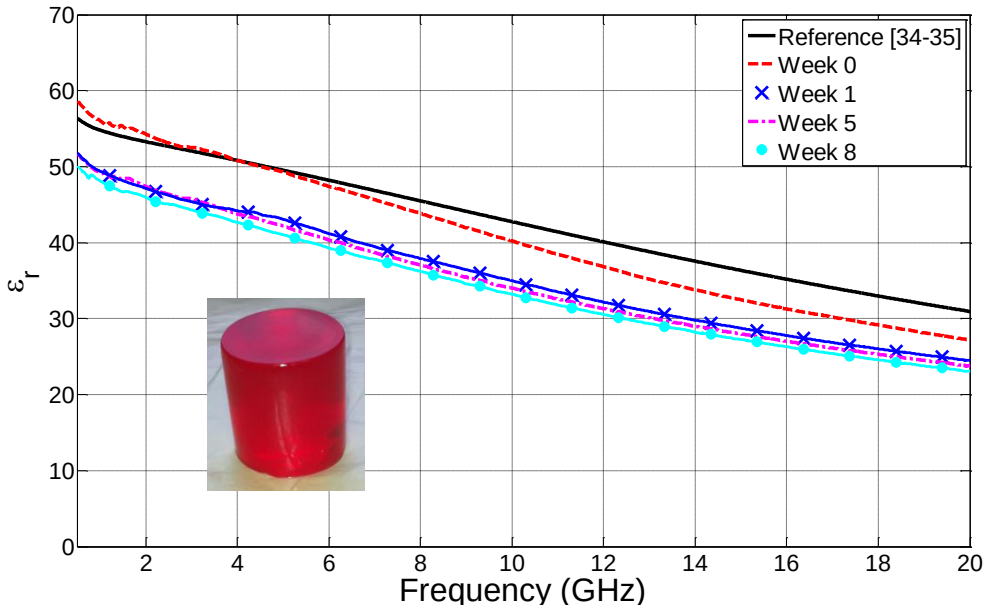

Figure 3.31

Relative Permittivity of Refrigerated Muscle Mimicking Material

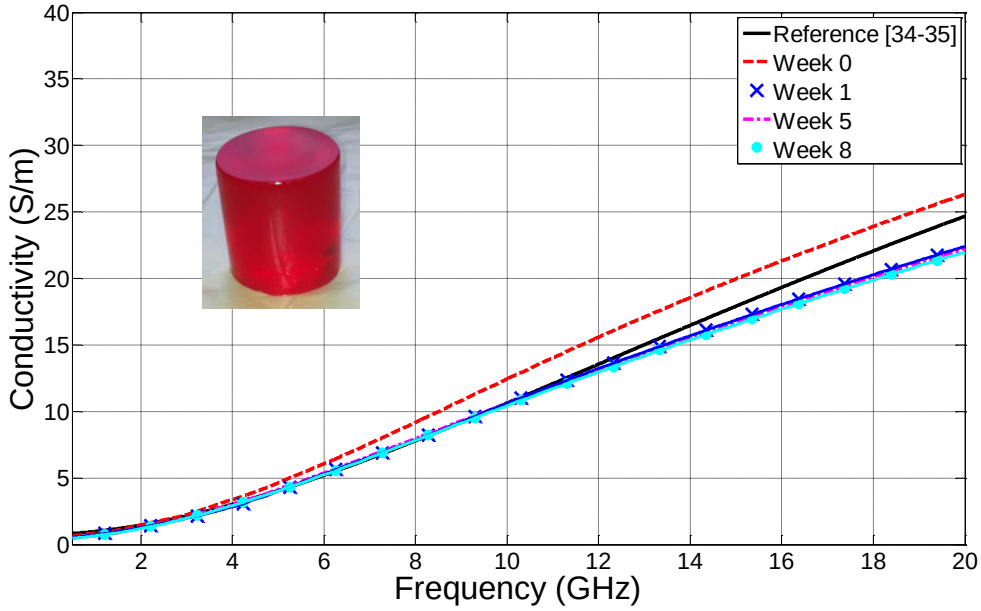

Figure 3.32

Conductivity of Refrigerated Muscle Mimicking Material

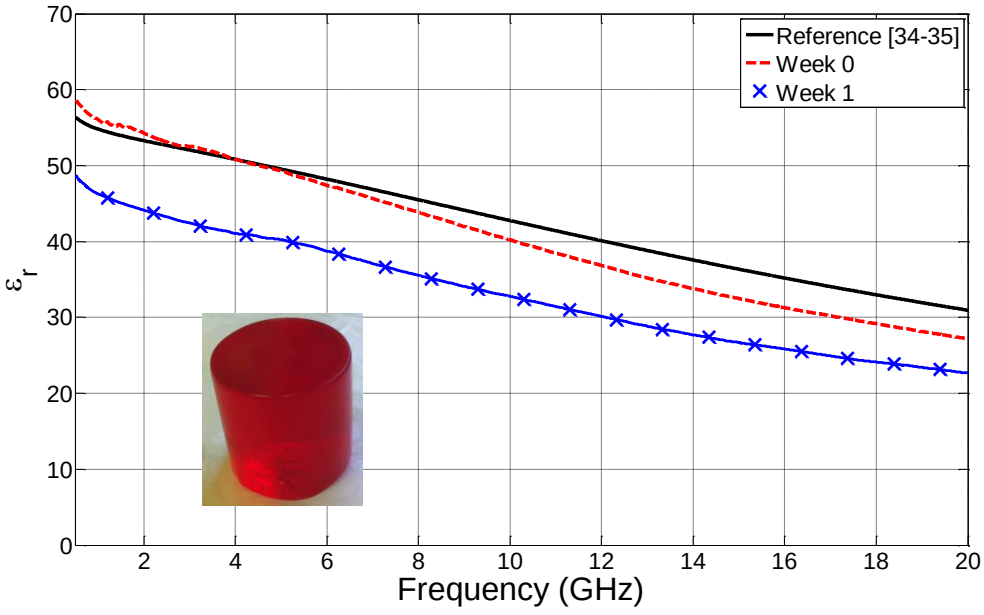

Figure 3.33

Relative Permittivity of Non-Refrigerated Muscle Mimicking Material

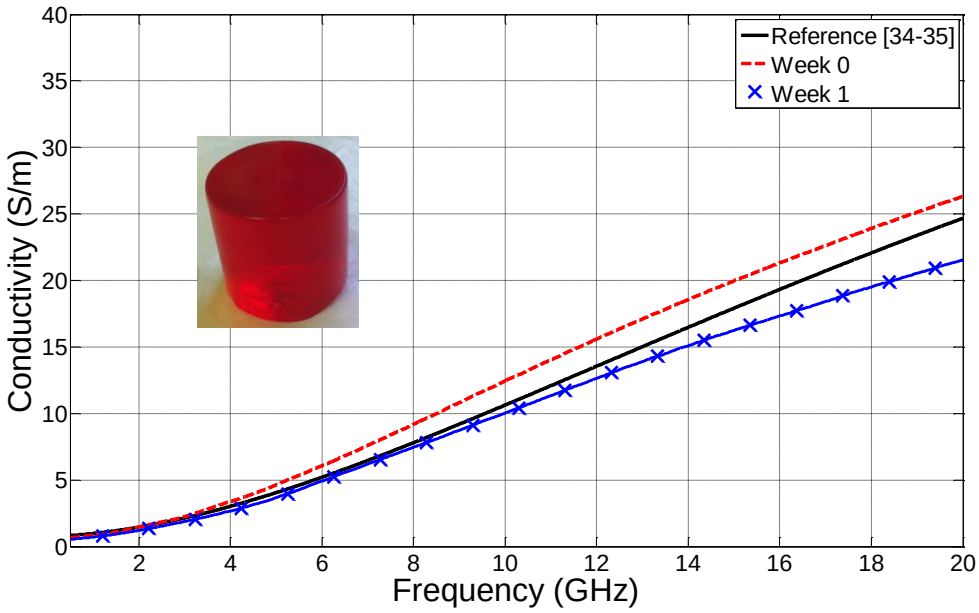

Figure 3.34

Conductivity of Non-Refrigerated Muscle Mimicking Material

After week 1, the non-refrigerated muscle mimicking material spoiled. Because of this, the measurements on the non-refrigerated sample are not performed for the weeks following. Figure 3.35 shows the appearance of the non-refrigerated muscle mimicking gel at week 0 and week 2.

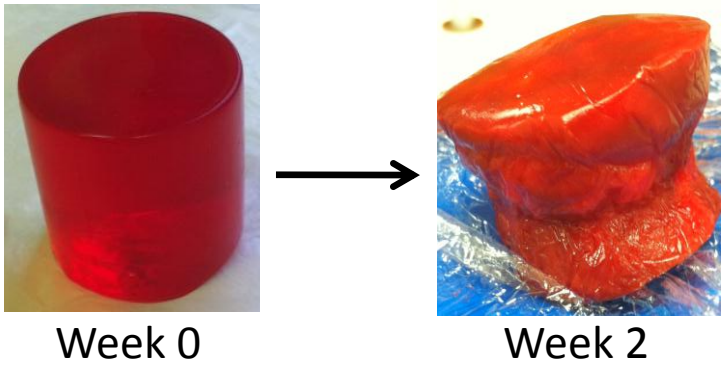

Figure 3.35

Spoiling of the Non-Refrigerated Material

3.3.4 Absorption of the Muscle Mimicking Material

The horn antenna set-up described in Chapter 3.1.4 is used to measure the absorption of power by the presence of a square muscle mimicking gel sample. The dimensions of the square sample are 26.5 cm in height, 26.5 cm in length, and 1.3 cm in thickness. The measurement set-up with the muscle mimicking gel sample is shown in Figure 3.36. Figure 3.37 shows S12 and S21 from 7-11 GHz of the antennas with and without the interference of the muscle mimicking gel sample, while the absorption by the muscle mimicking material is shown in Figure 3.38.

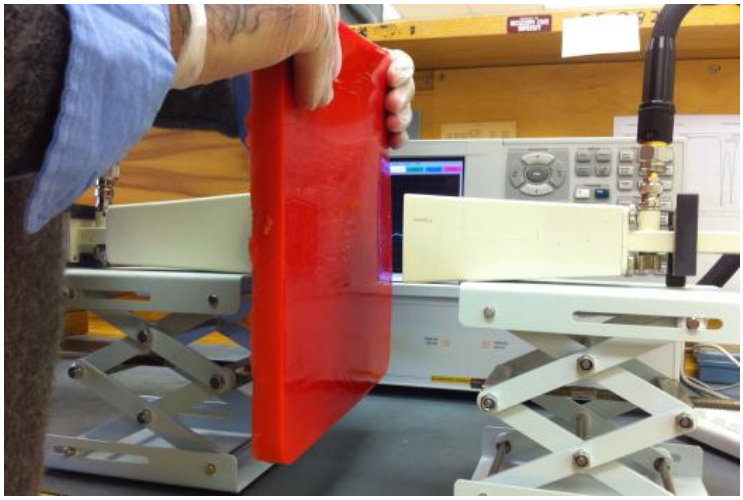

Figure 3.36

S12 and S21 Measurement Set-Up

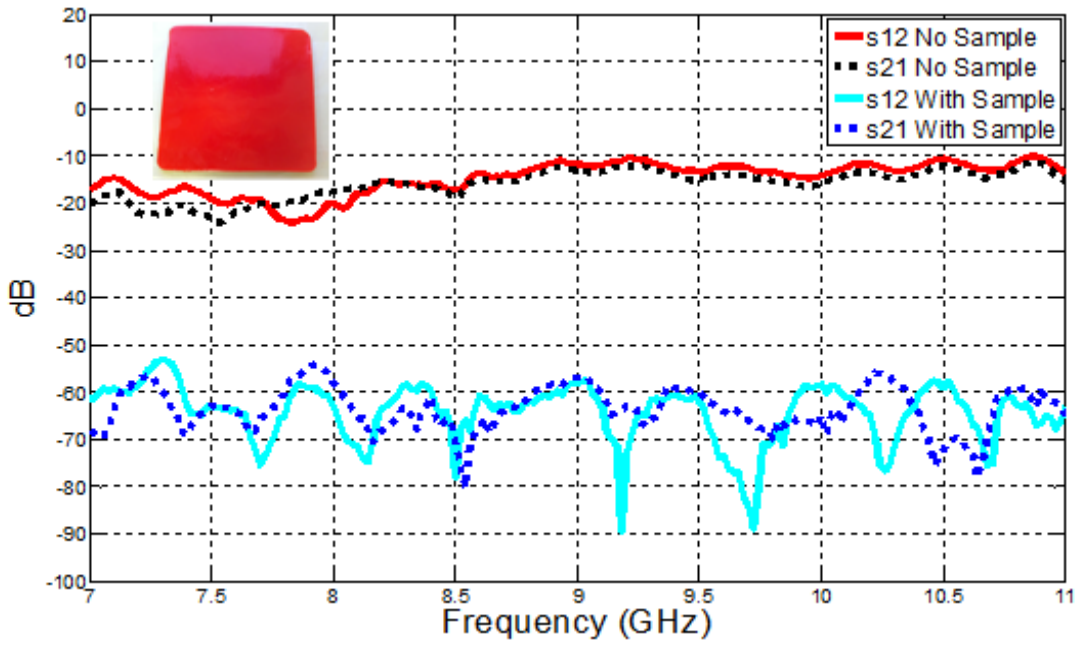

Figure 3.37

S12 and S21 With and Without the Interference of the Muscle Mimicking Sample

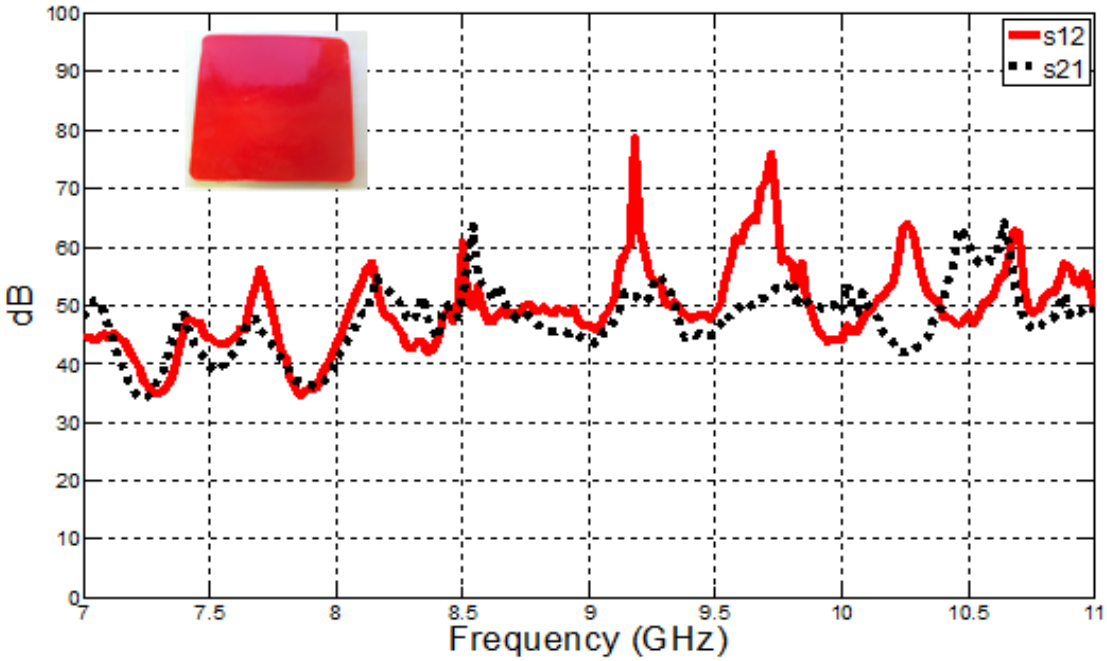

Figure 3.38

Absorption of Muscle Mimicking Material

3.4 Fibroglandular Tissue Mimicking Material with 0-30% Adipose Tissue

3.4.1 Characterization of Fibroglandular Tissue Mimicking Material with 0-30% Adipose Tissue

A material that mimics fibroglandular tissue with 0-30% adipose tissue is characterized by mixing de-ionized water, vegetable oil, Ultra Ivory® hand soap, Gelatin A, Triton X-100, and purple food coloring. Table 3.4 shows the list of ingredients along with their percent volume. In a beaker, Gelatin A granules are coated with Triton X-100. Then the total required amount of de-ionized water and food coloring is stirred into the mixture. This beaker is covered with Syran® wrap and placed an 80ºC water bath for 20 minutes. The total required amount of vegetable oil is placed in a separate beaker, covered with Syran® wrap, and put in an 80°C water bath for 20 minutes. The vegetable oil and Gelatin A mixture is mixed with Ultra Ivory® hand soap for 15 seconds. The mixture is poured into a beaker and set to form in the refrigerator for 30 minutes. The formed fibroglandular tissue mimicking gel is shown in the Figure 3.39.

Table 3.4

Recipe for Fibroglandular Tissue Mimicking Material with 0-30% Adipose Tissue

Ingredient	Percent Volume
De-ionized Water	73.02
Vegetable Oil	12.17
Gelatin A	12.17 (ρ=1.2 g/mL)
Ultra Ivory Soap	1.22
Triton X-100	1.22
Purple Food Coloring	0.202 (1 drop= 0.0417 mL)

Figure 3.39

Characterized Fibroglandular Tissue Mimicking Material

3.4.2 Fibroglandular Tissue Mimicking Material with 0-30% Adipose Tissue Dielectric Probe Measurements

Once the fibroglandular tissue mimicking material is formed, the relative permittivity and conductivity is measured from 500 MHz to 20 GHz as described in 3.1.2. The average of the six sets of measured electrical properties is compared with the human fibroglandular tissue with 0-30% adipose tissue average reference data obtained from [36]. In [36] the electrical property measurements from 500 MHz to 20 GHz of three types of fibroglandular tissue defined by percentage adipose tissue present in samples are given: 0-30% adipose, 31-84% adipose, and 85-100% adipose fat. The measurements are taken from normal breast tissue obtained from 93 patients undergoing breast reduction surgery. Figure 3.40 and Figure 3.41 show a graphical comparison between muscle's relative permittivity and conductivity of measured and reference data in [36], respectively.

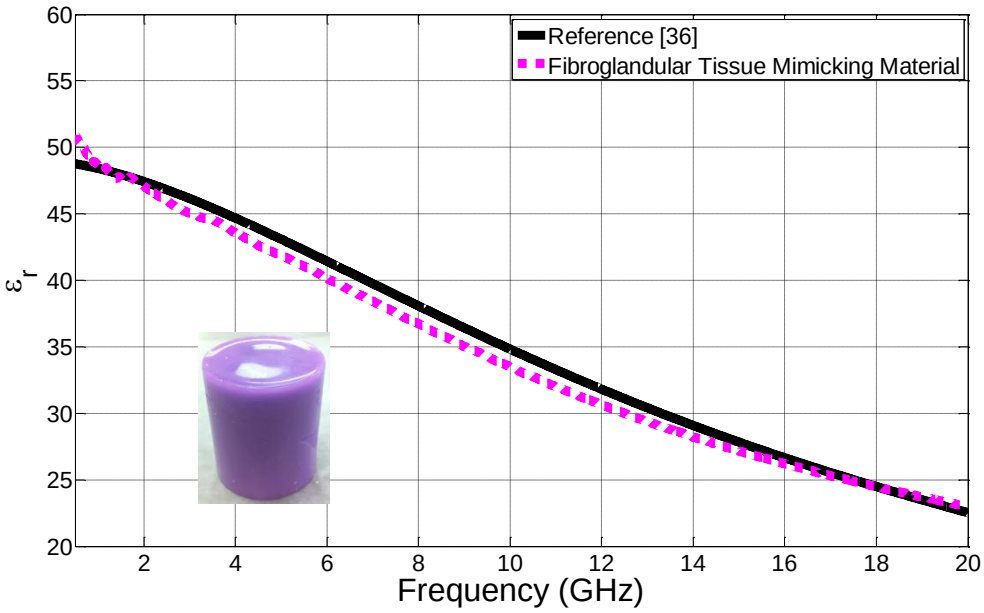

Figure 3.40

Relative Permittivity Comparison of Fibroglandular Tissue Mimicking Material to Reference Data

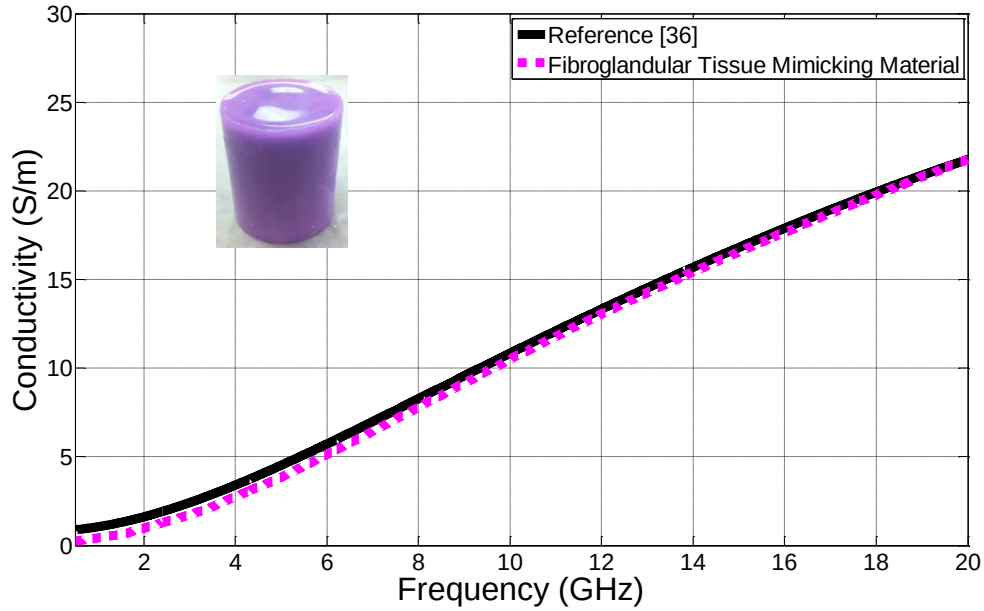

Figure 3.41

Conductivity Comparison of Fibroglandular Tissue Mimicking Material to Reference Data

The graph shows a good agreement obtained between reference data in [36] and measurements of the fibroglandular tissue mimicking material. The characterized fibroglandular tissue mimicking gel maximum deviation from the reference data from 500 MHz to 20 GHz is 2.13 for the relative permittivity and 0.71 S/m for conductivity.

3.4.3 Shelf Life Study of the Fibroglandular Tissue Mimicking Material with 0-30% Adipose Tissue

The steps previously described in Chapter 3.1.3 are applied to two fibroglandular tissue mimicking materials to investigate the material's shelf life and the effects refrigeration has on the electrical properties of the tissue mimicking material for a period of eight weeks. Figures 3.42-3.45 show the electrical properties of both the refrigerated and non-refrigerated material, respectively. After week 1, the non-refrigerated fibroglandular tissue mimicking gel spoiled. Because of this, the measurements on the non-refrigerated sample are not performed for the weeks following.

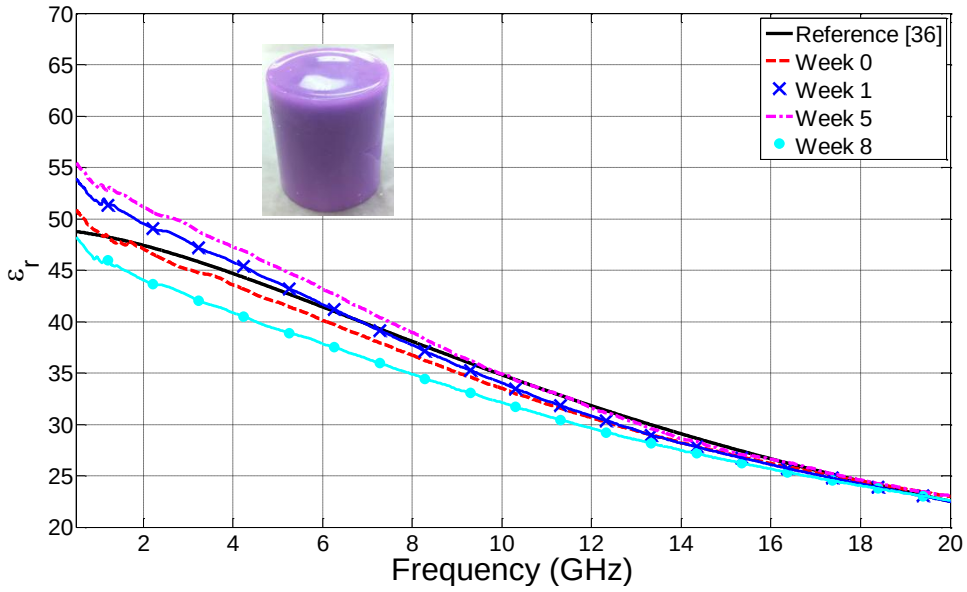

Figure 3.42

Relative Permittivity of Refrigerated Fibroglandular Tissue Mimicking Material

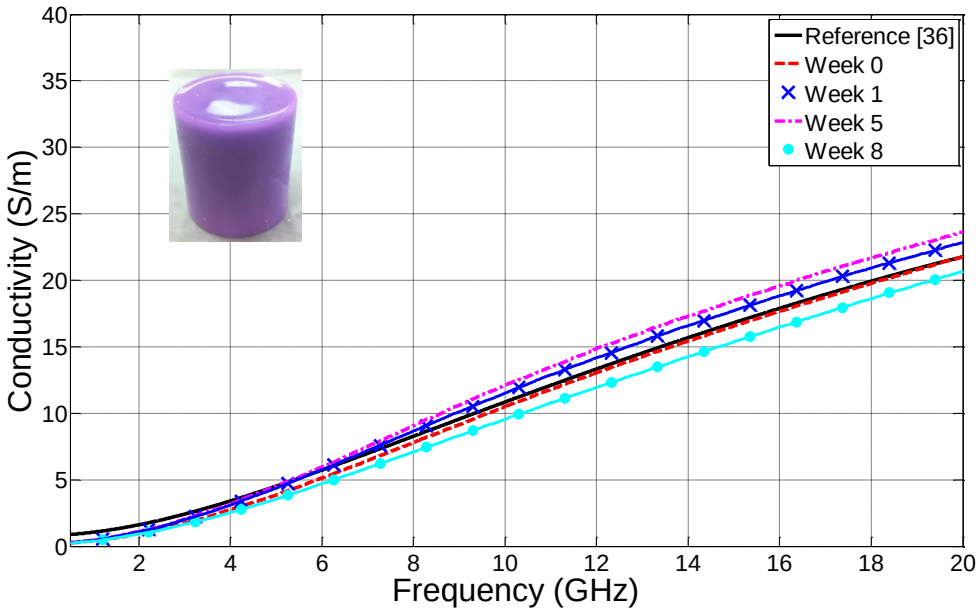

Figure 3.43

Conductivity of Refrigerated Fibroglandular Tissue Mimicking Material

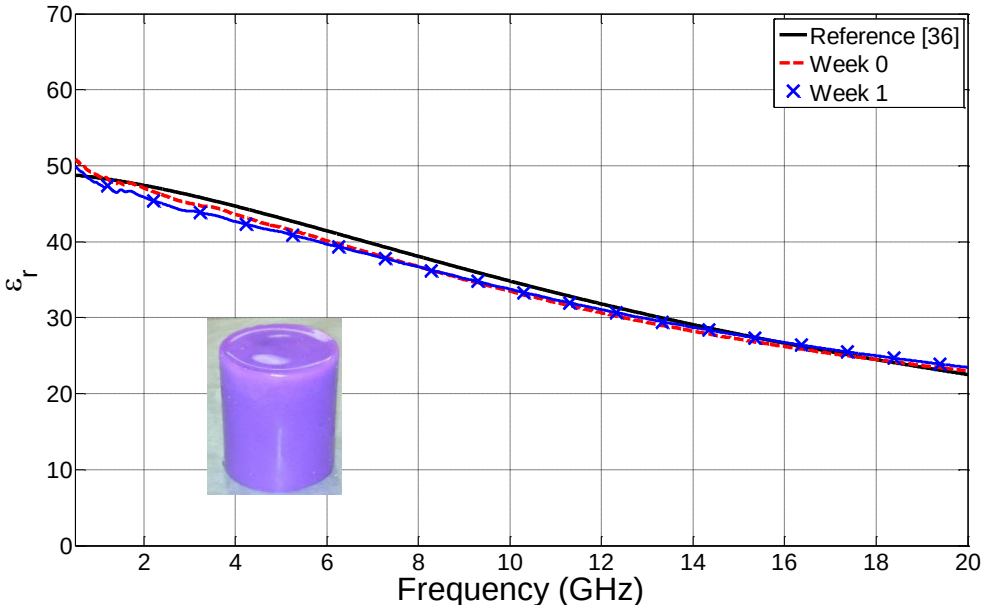

Figure 3.44

Relative Permittivity of Non-Refrigerated Fibroglandular Tissue Mimicking Material

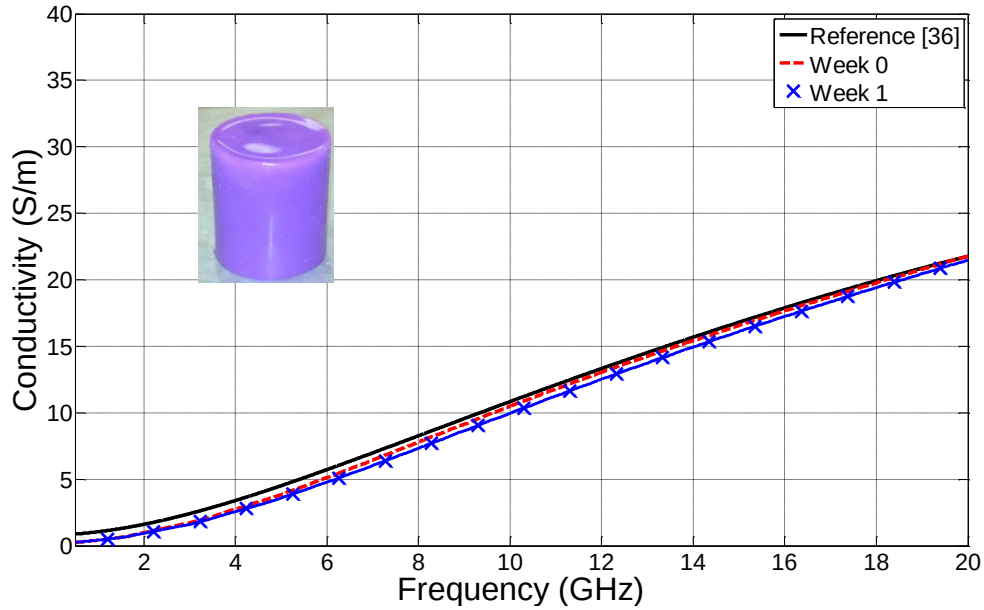

Figure 3.45

Conductivity of Non-Refrigerated Fibroglandular Tissue Mimicking Material

3.4.4 Absorption of the Fibroglandular Tissue Mimicking Material with 0-30% Adipose Tissue

Shown in Figure 3.46, the horn antenna set-up described in Chapter 3.1.4 is used to measure the absorption of power because of the interference or presence of a square fibroglandular tissue mimicking sample. The dimensions of the square sample are 26.5 cm in height, 26.5 cm in length, and 1.3 cm in thickness. Figure 3.47 shows S12 and S21 from 7-11 GHz of the antennas with and without the interference of the fibroglandular tissue mimicking sample. The absorption by the fibroglandular tissue mimicking material is shown in Figure 3.48.

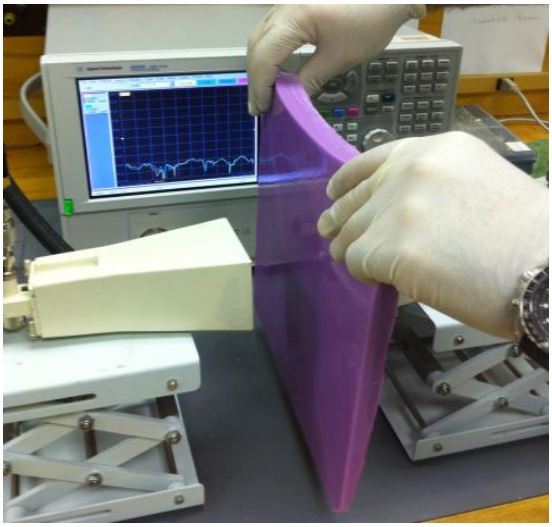

Figure 3.46

S12 and S21 Measurement Set-Up

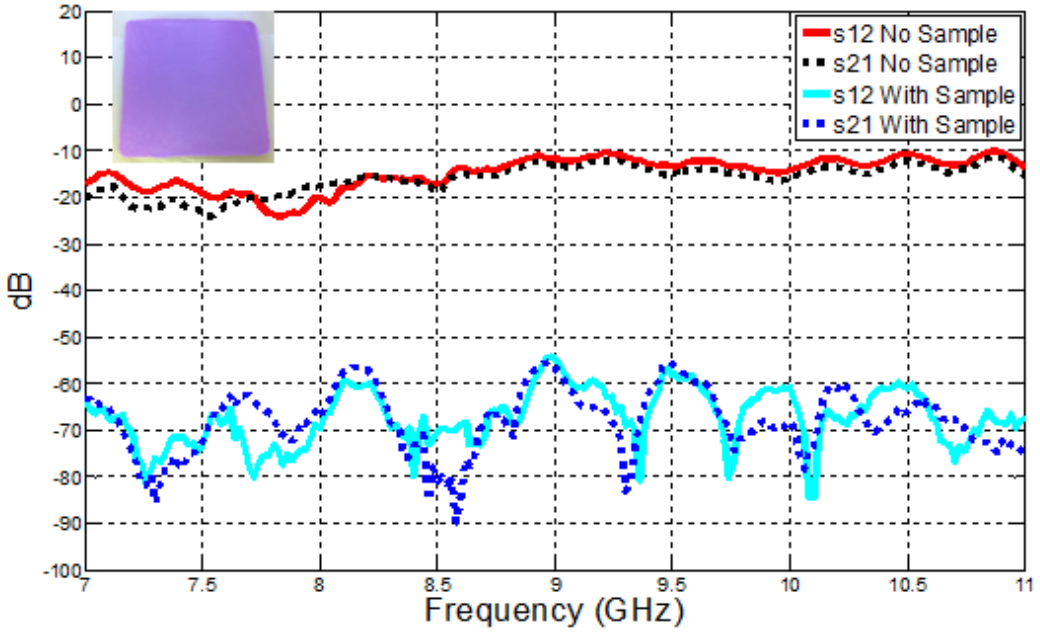

Figure 3.47

S12 and S21 With and Without the Interference of the Fibroglandular Tissue Mimicking Sample

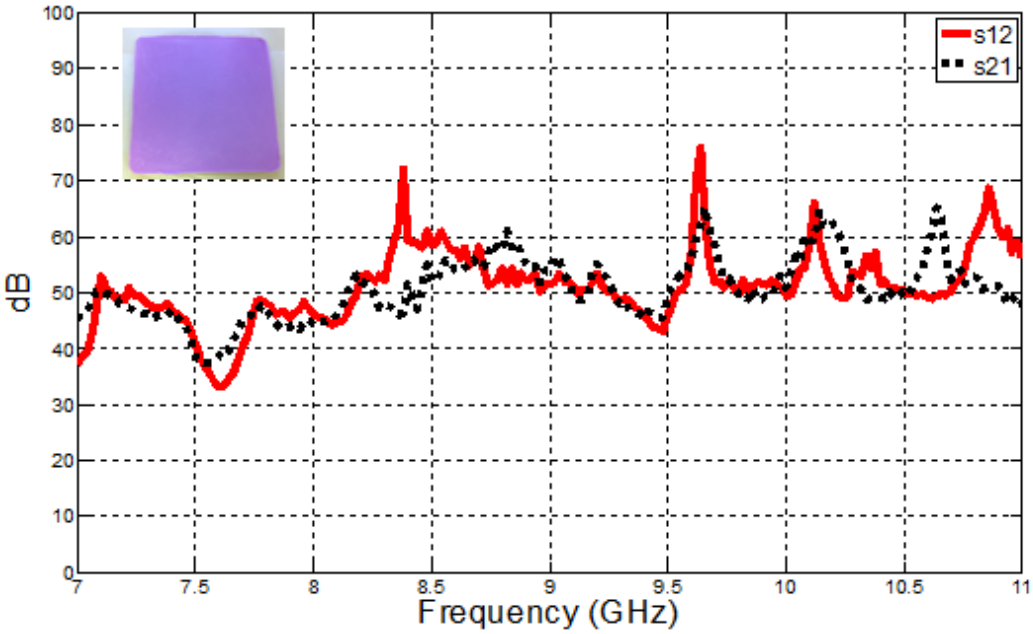

Figure 3.48

Absorption of Fibroglandular Tissue Mimicking Material

3.5 Fibroglandular Tissue Mimicking Material with 31-84% Adipose Tissue

3.5.1 Characterization of Fibroglandular Tissue Mimicking Material with 31-84% Adipose Tissue

A material that mimics fibroglandular tissue with 31-84% adipose tissue is characterized by mixing de-ionized water, vegetable oil, Ultra Ivory® hand soap, Gelatin A, Triton X-100, and purple food coloring. The steps described in Chapter 3.4.1 are followed to characterize the fibroglandular tissue mimicking material. Table 3.5 shows the list of ingredients along with their percent volume, and Figure 3.49 shows the formed mimicking material.

Table 3.5

Recipe for Fibroglandular Tissue Mimicking Material with 31-84% Adipose Tissue

Ingredient	Percent Volume
De-ionized Water	65.54
Vegetable Oil	21.85
Gelatin A	10.92 (ρ=1.2 g/mL)
Ultra Ivory Soap	1.09
Triton X-100	0.41
Purple Food Coloring	0.18 (1 drop= 0.0417 mL)

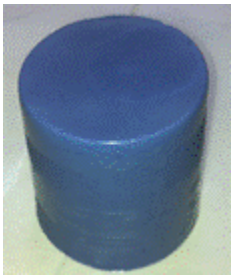

Figure 3.49

Characterized Fibroglandular Tissue Mimicking Material

3.5.2 Fibroglandular Tissue Mimicking Material with 31-84% Adipose Tissue Dielectric Probe Measurements

The relative permittivity and conductivity are measured from 500 MHz to 20 GHz as described in Chapter 3.1.2. The average of the measured electrical properties is compared with the human fibroglandular tissue with 31-84% adipose tissue reference data obtained from [36]. Figure 3.50 and Figure 3.51 show a graphical comparison between fibroglandular tissue's relative permittivity and conductivity of measured and reference data in [36]. The graph shows a good agreement obtained between reference data in [36] and measurements of the fibroglandular tissue mimicking material. The characterized fibroglandular tissue mimicking gel maximum deviation from the reference data from 500 MHz to 20 GHz is 2.77 for the relative permittivity and 0.57 S/m for conductivity.

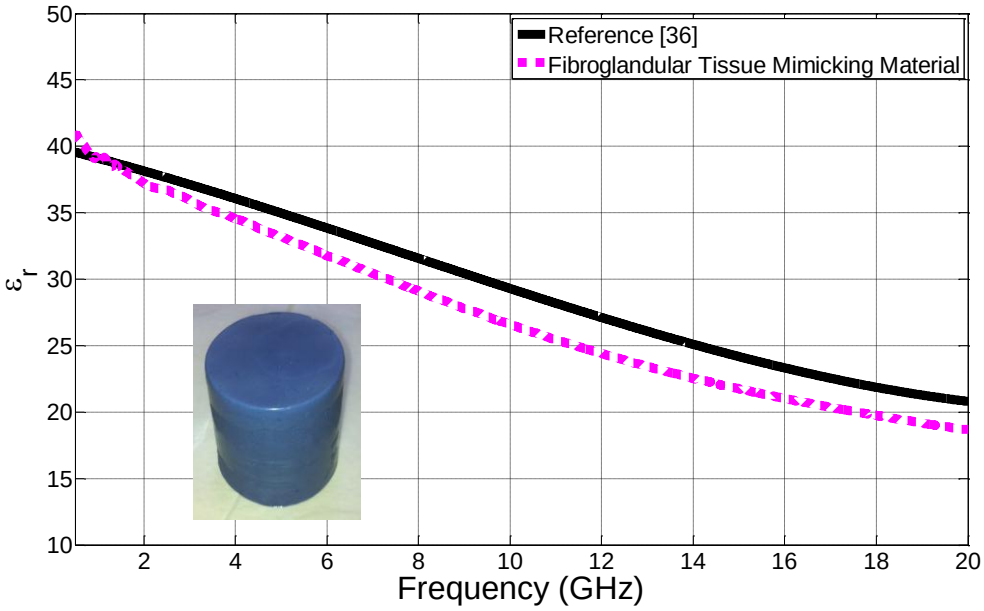

Figure 3.50

Relative Permittivity Comparison of Fibroglandular Tissue Mimicking Material

to Reference Data

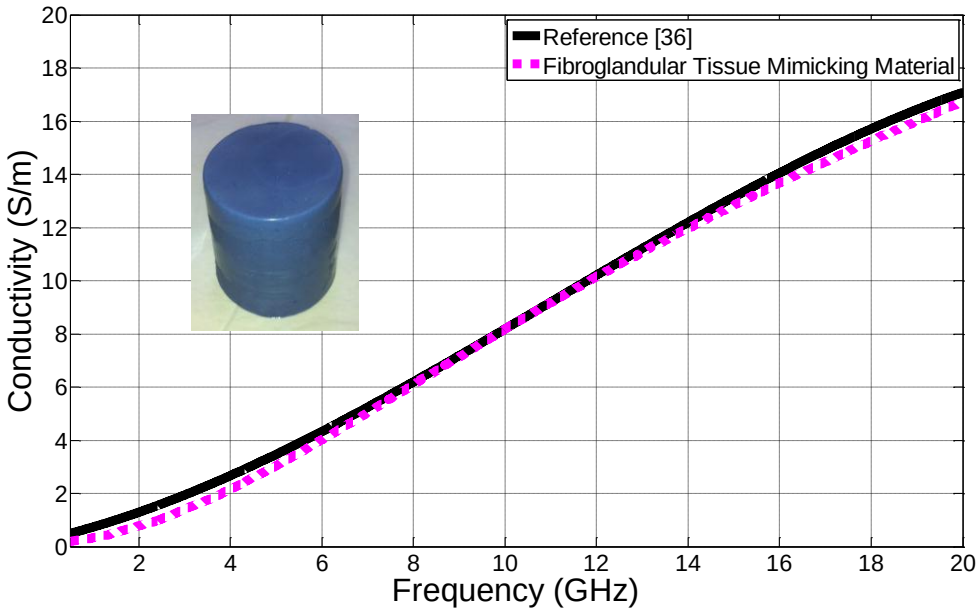

Figure 3.51

Conductivity Comparison of Fibroglandular Tissue Mimicking Material to Reference Data

3.5.3 Shelf Life Study of the Fibroglandular Tissue Mimicking Material with 31-84% Adipose Tissue

The steps previously described in Chapter 3.1.3 are applied to two fibroglandular tissue mimicking materials to investigate the material's shelf life and the effects refrigeration has on the electrical properties of the tissue mimicking material for a period of eight weeks. Figures 3.52-3.55 show the electrical properties of both the refrigerated and non-refrigerated material, respectively. After week 2, the non-refrigerated fibroglandular tissue mimicking gel spoiled. Because of this, the measurements on the non-refrigerated sample are not performed for the weeks following.

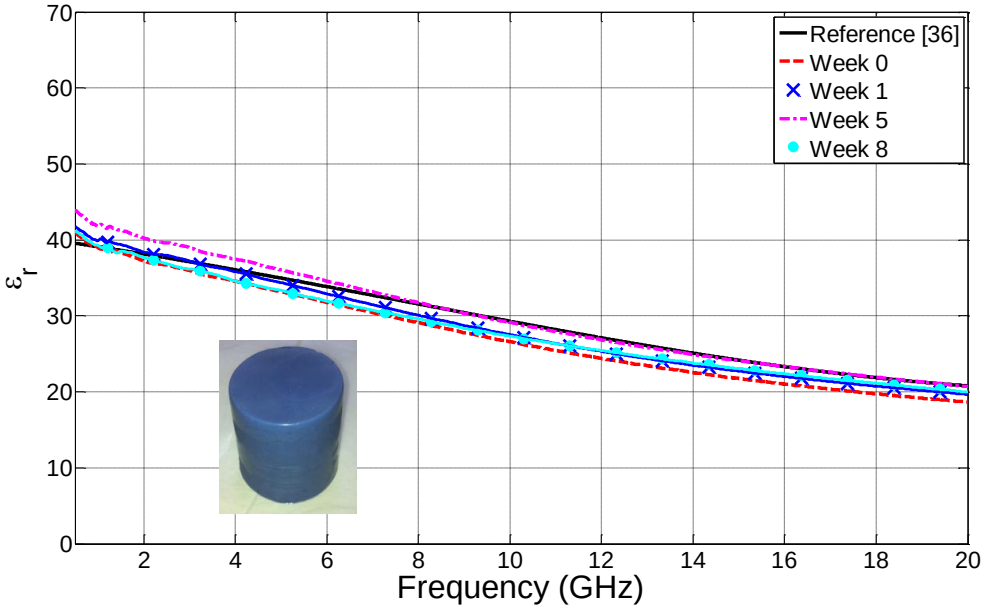

Figure 3.52

Relative Permittivity of Refrigerated Fibroglandular Tissue Mimicking Material

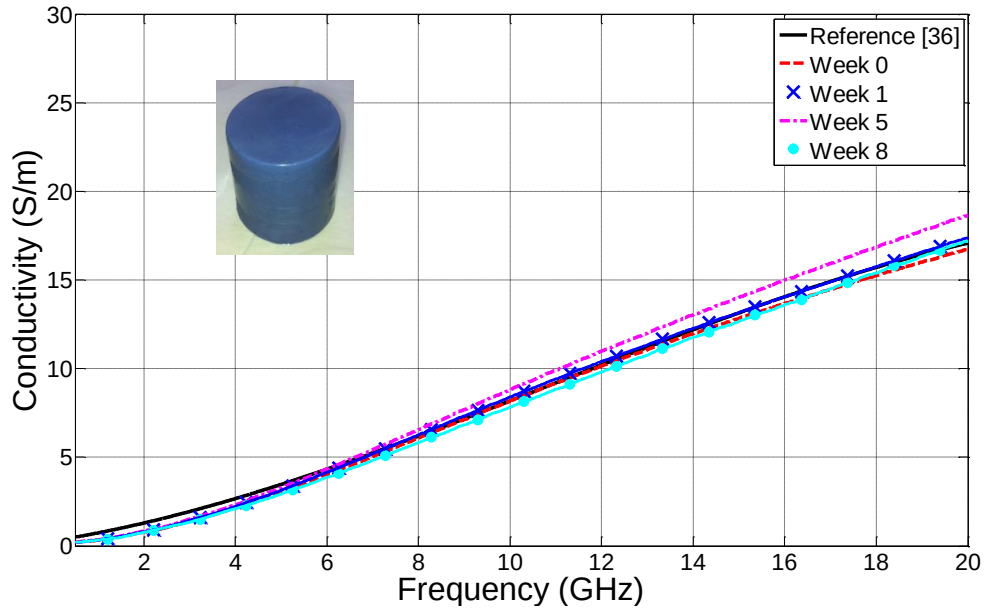

Figure 3.53

Conductivity of Refrigerated Fibroglandular Tissue Mimicking Material

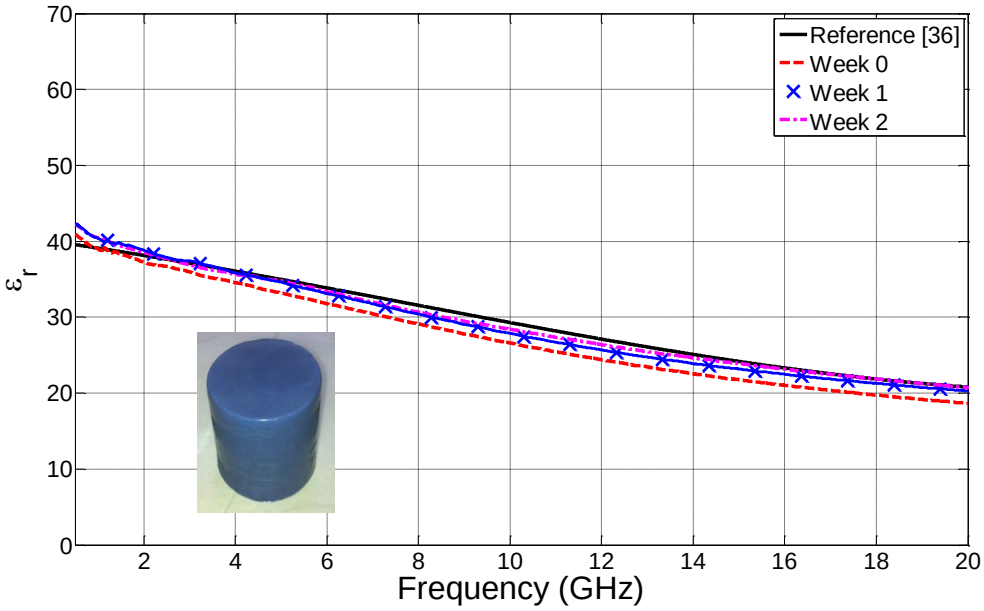

Figure 3.54

Relative Permittivity of Non-Refrigerated Fibroglandular Tissue Mimicking Material

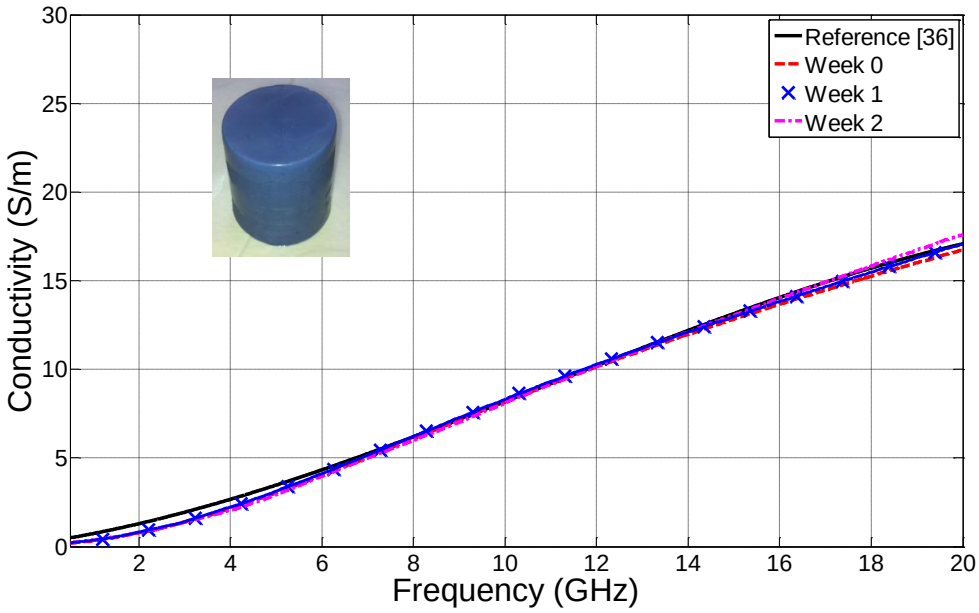

Figure 3.55

Conductivity of Non-Refrigerated Fibroglandular Tissue Mimicking Material

3.6 Malignant Fibroglandular Tissue Mimicking Material with 0-30% Adipose Tissue

3.6.1 Characterization of Malignant Fibroglandular Tissue Mimicking Material with 0-30% Adipose Tissue

A gel that mimics the electrical properties of malignant fibroglandular tissue with 0-30% adipose tissue is characterized by mixing de-ionized water, vegetable oil, Ultra Ivory® hand soap, Gelatin A, Triton X-100, Sodium Chloride, and green food coloring. Table 3.6 shows the list of ingredients along with their percent volume. The steps described in Chapter 3.1.1 are followed to characterize the muscle mimicking material. The formed malignant fibroglandular tissue mimicking gel is shown in Figure 3.56.

Table 3.6

Recipe for Malignant Fibroglandular Tissue Mimicking Material with 0-30% Adipose Tissue

Ingredient	Percent Volume
De-ionized Water	75.09
Vegetable Oil	13.24
Gelatin A	8.83 (ρ=1.2 g/mL)
Ultra Ivory Soap	1.77
Triton X-100	0.88
Sodium Chloride	0.12 (ρ=2.165 g/mL)
Green Food Coloring	0.15 (1 drop= 0.0417 mL)

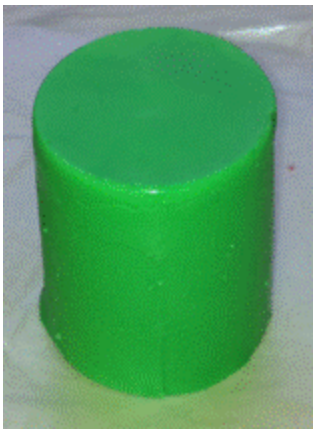

Figure 3.56

Characterized Malignant Fibroglandular Tissue Mimicking Material

3.6.2 Malignant Fibroglandular Tissue Mimicking Material with 0-30% Adipose Tissue Dielectric Probe Measurements

The relative permittivity and conductivity of the synthesized mimicking material are measured from 500 MHz to 20 GHz as described in Chapter 3.1.2. The average of the six sets of measured electrical properties is compared with the human malignant fibroglandular tissue with 0-30% adipose tissue average reference data obtained from [37]. In [37] the electrical property measurements from 500 MHz to 20 GHz of three types of malignant fibroglandular tissue defined by percentage adipose tissue present in samples are given: 0-30% adipose, 31-84% adipose, and 85-100% adipose fat. The measurements are taken from breast tissue from 196 patients undergoing lumpectomies, mastectomies, and biopsies. Figure 3.57 and Figure 3.58 show a graphical comparison between the malignant fibroglanduar tissue's relative permittivity and conductivity of measured and reference data in [37], respectively.

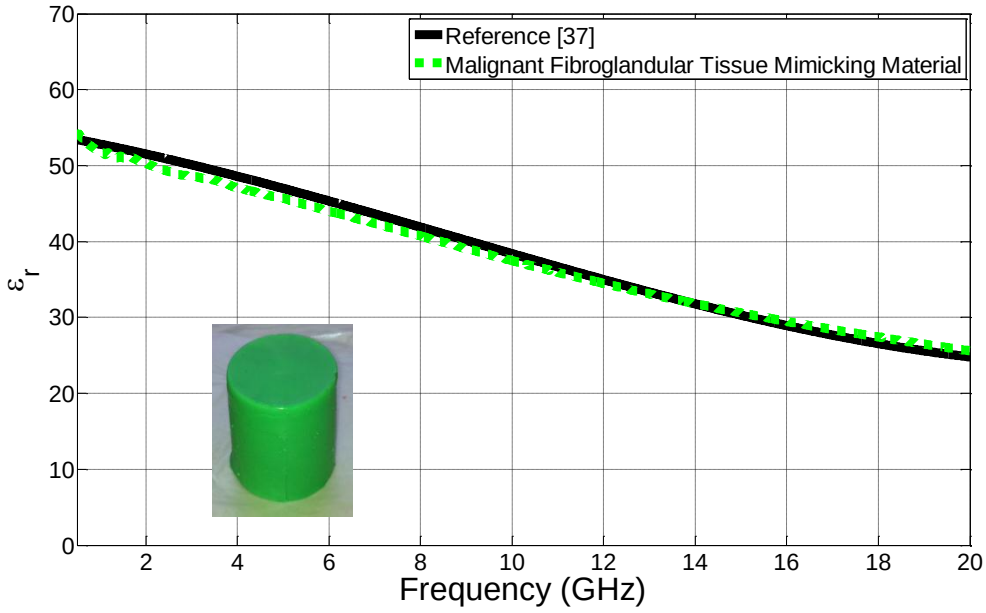

Figure 3.57

Relative Permittivity Comparison of Malignant Fibroglandular Tissue Mimicking Material to Reference Data

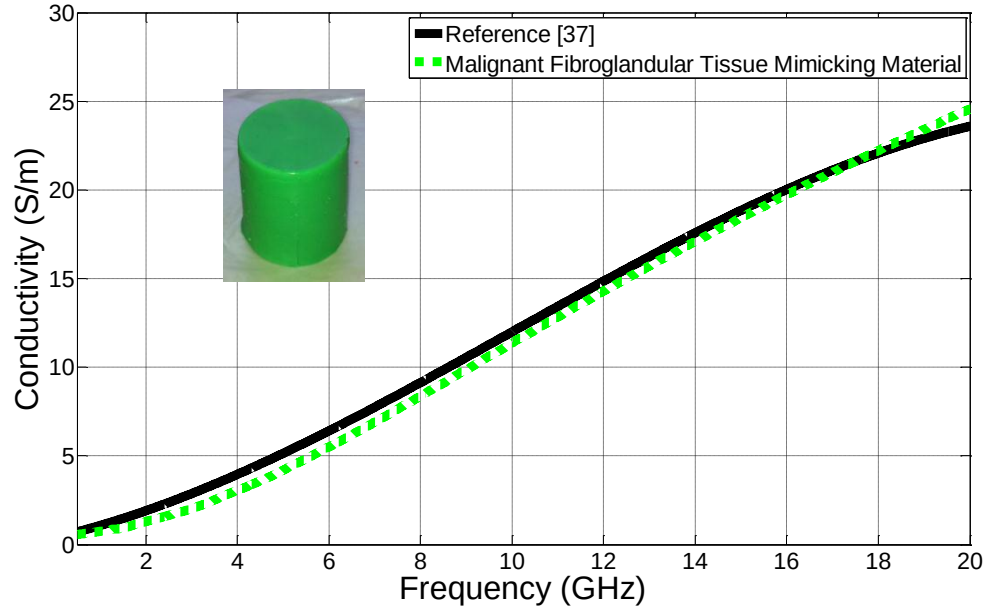

Figure 3.58

Conductivity Comparison of Malignant Fibroglandular Tissue Mimicking Material to Reference Data

The graph shows a good agreement obtained between reference data in [37] and measurements of the malignant fibroglandular tissue mimicking material. The characterized tissue mimicking gel maximum deviation from the reference data from 500 MHz to 20 GHz is 1.68 for the relative permittivity and 0.97 S/m for conductivity.

3.6.3 Shelf Life Study of the Malignant Fibroglandular Tissue Mimicking Material with 0-30% Adipose Tissue

The steps previously described in Chapter 3.1.3 are applied to two fibroglandular tissue mimicking materials to investigate the material's shelf life and the effects refrigeration has on the electrical properties of the tissue mimicking material for a period of eight weeks. Figures 3.59-3.62 show the electrical properties of both the refrigerated and non-refrigerated material. After week 2, the unrefrigerated malignant fibroglandular tissue mimicking gel spoiled. Thus, the measurements are not performed for the weeks following.

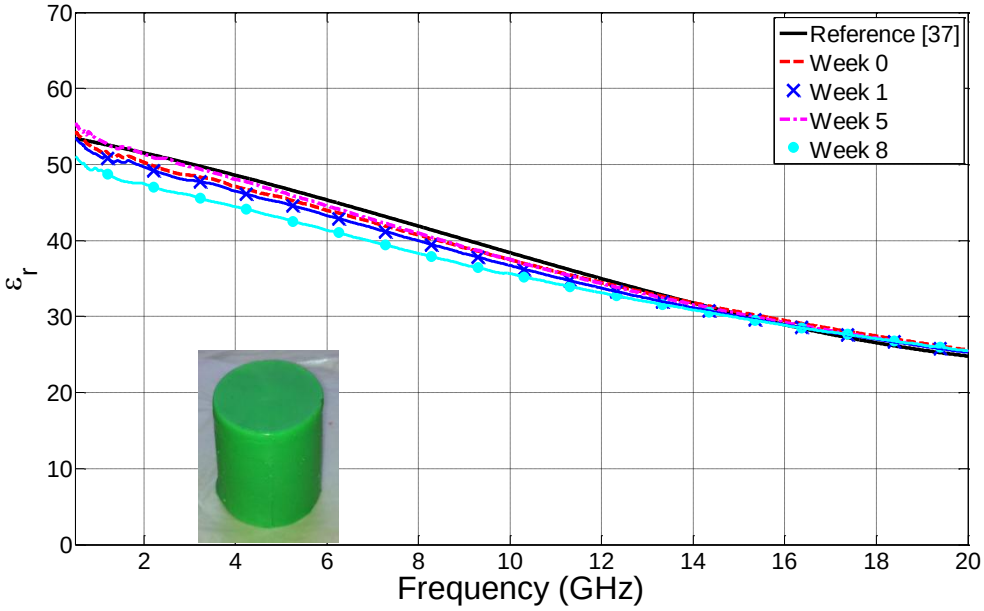

Figure 3.59

Relative Permittivity of Refrigerated Malignant Fibroglandular Tissue Mimicking Material

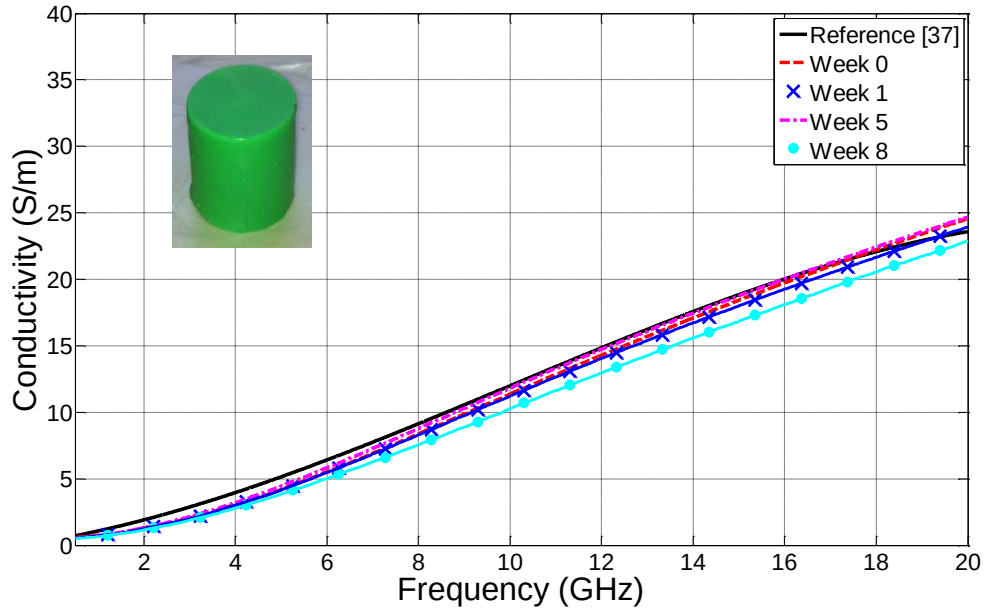

Figure 3.60

Conductivity of Refrigerated Malignant Fibroglandular Tissue Mimicking Material

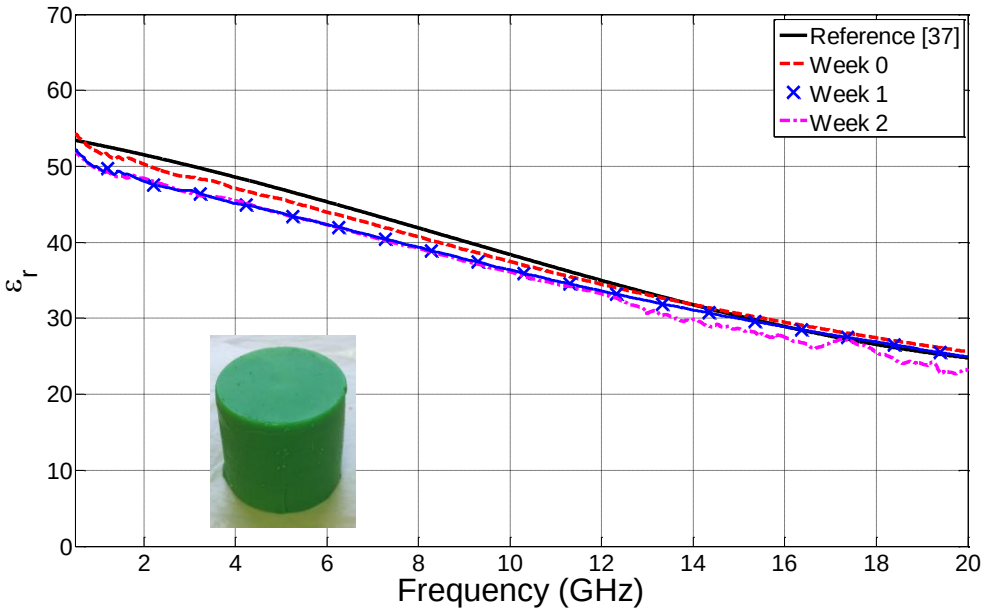

Figure 3.61

Relative Permittivity of Non-Refrigerated Malignant Fibroglandular Tissue Mimicking Material

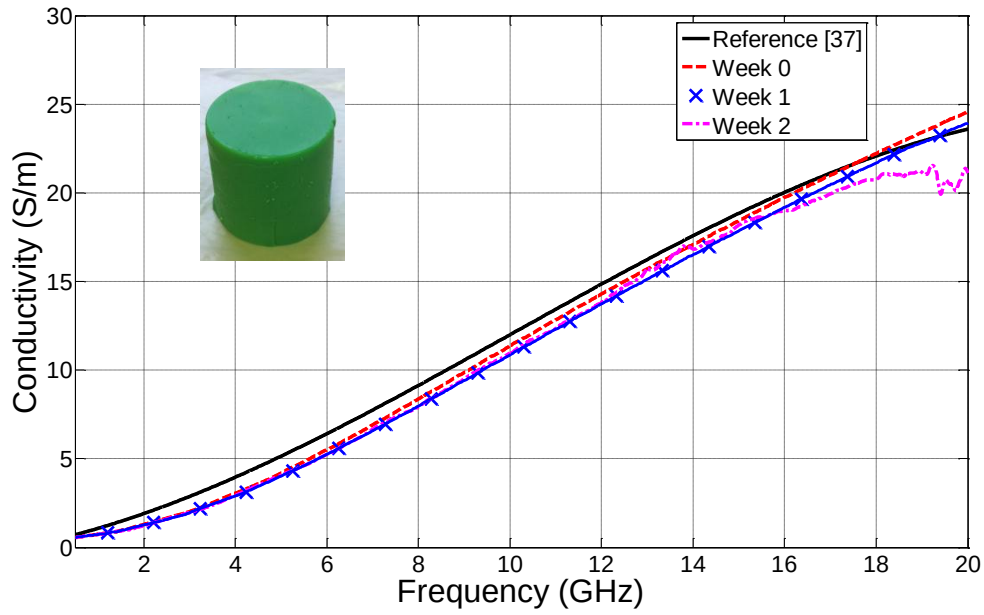

Figure 3.62

Conductivity of Non-Refrigerated Malignant Fibroglandular Tissue Mimicking Material

3.6.4 Absorption of the Malignant Fibroglandular Tissue Mimicking Material with 0-30% Adipose Tissue

The horn antenna set-up described in Chapter 3.1.4 is used to measure the absorption of power because of the interference or presence of a square malignant fibroglandular tissue mimicking sample. The dimensions of the square sample are 26.5 cm in height, 26.5 cm in length, and 1.45 cm in thickness. The measurement set-up with the malignant fibroglandular tissue mimicking sample is shown in Figure 3.63. Figure 3.64 shows S12 and S21 from 7-11 GHz of the antennas with and without the interference of the malignant fibroglandular tissue mimicking gel sample. The absorption by the malignant fibroglandular tissue mimicking material is shown in Figure 3.65.

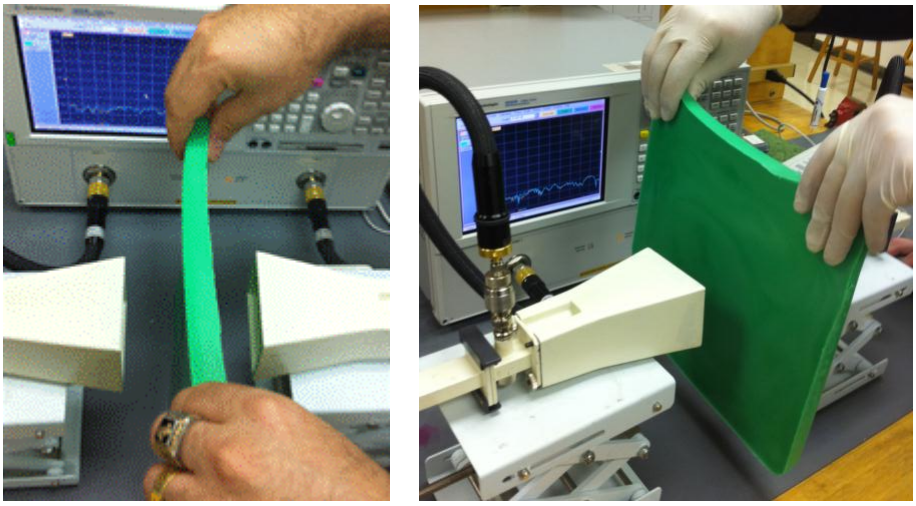

Figure 3.63

S12 and S21 Measurement Set-Up

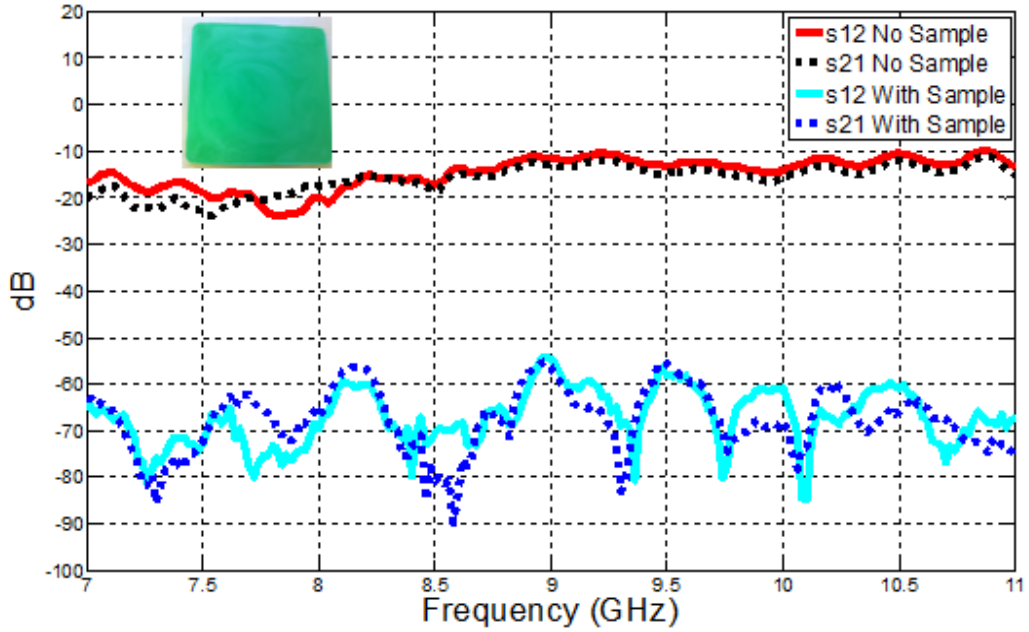

Figure 3.64

S12 and S21 With and Without the Interference of the Malignant Fibroglandular Tissue Mimicking Sample

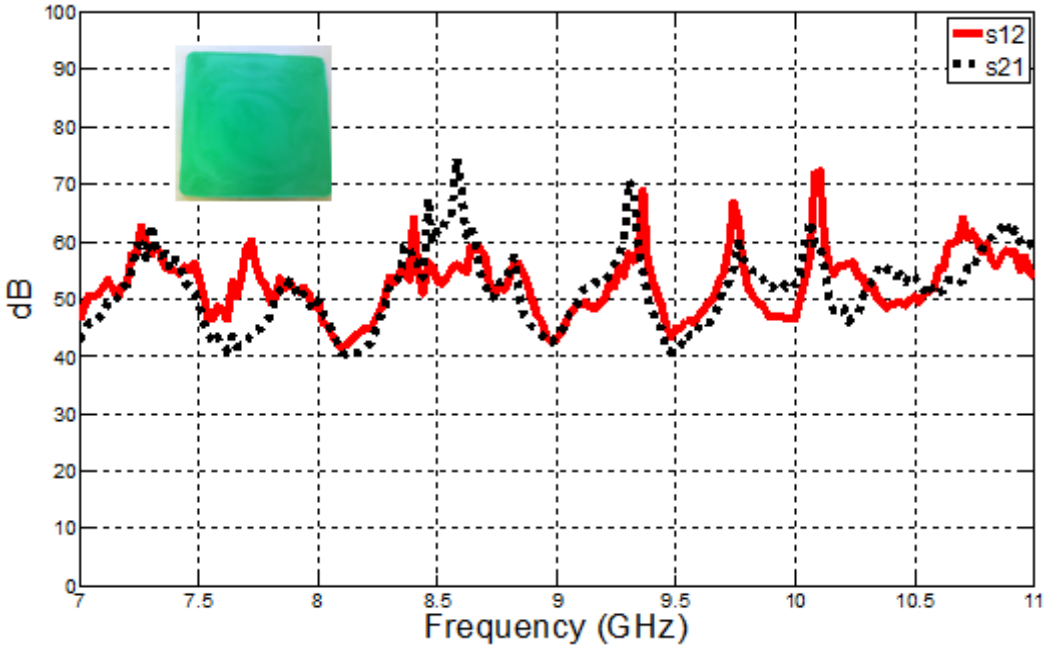

Figure 3.65

Absorption of Malignant Fibroglandular Tissue Mimicking Material

3.7 Malignant Fibroglandular Tissue Mimicking Material with 31-84% Adipose Tissue

3.7.1 Characterization of Malignant Fibroglandular Tissue Mimicking Material with 31-84% Adipose Tissue

A gel that mimics the electrical properties of malignant fibroglandular tissue with 31-84% adipose tissue is characterized by mixing de-ionized water, vegetable oil, Ultra Ivory® hand soap, Gelatin A, Triton X-100, and green food coloring. Table 3.7 shows the list of ingredients along with their percent volume. The steps described in Chapter 3.1.1 are followed to characterize the tissue mimicking material. The formed tissue mimicking gel is shown in Figure 3.66.

Table 3.7

Recipe for Malignant Fibroglandular Tissue Mimicking Material with 31-84% Adipose Tissue

Ingredient	Percent Volume
De-ionized Water	45.89
Vegetable Oil	40.15
Gelatin A	11.47 (ρ=1.2 g/mL)
Ultra Ivory Soap	1.15
Triton X-100	1.15
Lime Green Food Coloring	0.19 (1 drop= 0.0417 mL)

Figure 3.66

Characterized Malignant Fibroglandular Tissue Mimicking Material

3.7.2 Malignant Fibroglandular Tissue Mimicking Material with 31-84% Adipose Tissue Dielectric Probe Measurements

The relative permittivity and conductivity of the synthesized mimicking material are measured from 500 MHz to 20 GHz by following the steps described in Chapter 3.1.2. The average of the six sets of measured electrical properties is compared with the human malignant fibroglandular tissue with 0-30% adipose tissue average reference data obtained from [37]. Figure 3.67 and Figure 3.68 show a graphical comparison between the malignant fibroglanduar tissue's relative permittivity and conductivity of measured and reference data in [37], respectively.

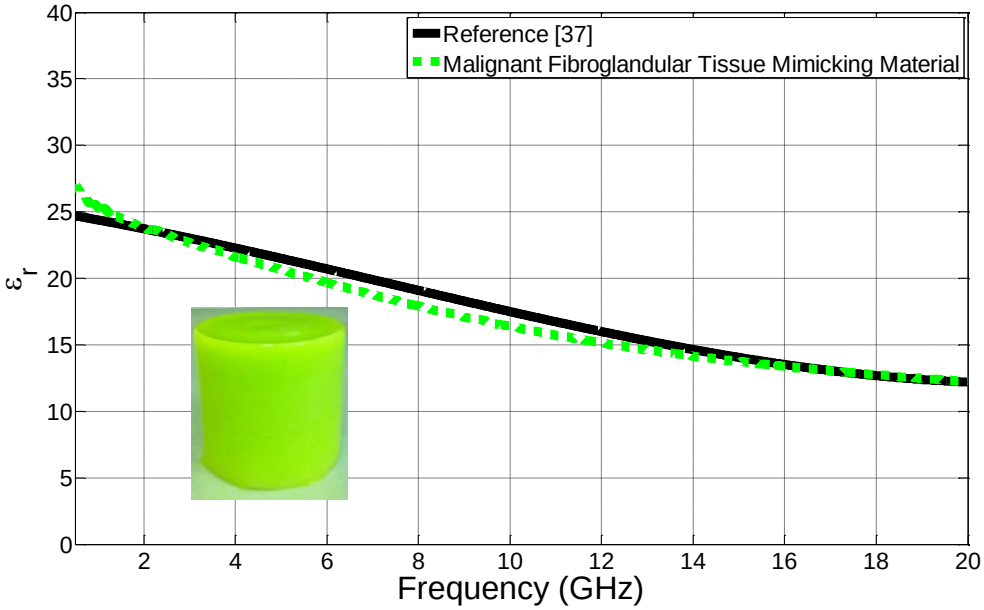

Figure 3.67

Relative Permittivity Comparison of Malignant Fibroglandular Tissue Mimicking Material to Reference Data

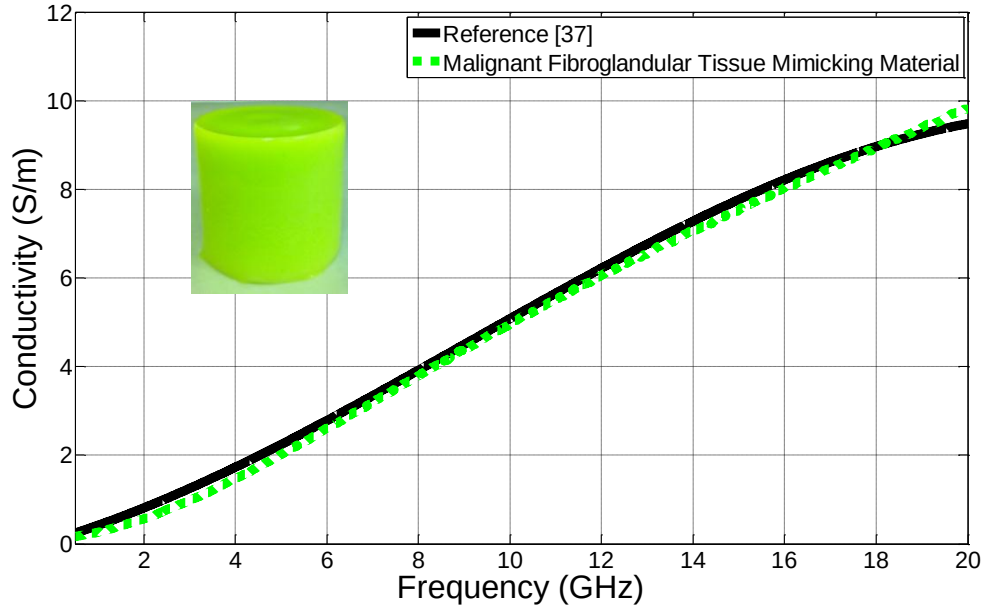

Figure 3.68

Conductivity Comparison of Malignant Fibroglandular Tissue Mimicking Material to Reference Data

The graph shows a good agreement obtained between reference data in [37] and measurements of the fibroglandular tissue mimicking material. The characterized adipose tissue mimicking gel maximum deviation from the reference data from 500 MHz to 20 GHz is 2.33 for the relative permittivity and 0.34 S/m for conductivity.

3.7.3 Shelf Life Study of the Malignant Fibroglandular Tissue Mimicking Material with 31-84% Adipose Tissue

The steps previously described in Chapter 3.1.3 are applied to two malignant fibroglandular tissue mimicking materials to investigate the material's shelf life and the effects refrigeration has on the electrical properties of the tissue mimicking material for a period of eight weeks. Figures 3.69-3.72 show the electrical properties of both the refrigerated and non-refrigerated material. After week 1, the unrefrigerated malignant fibroglandular tissue mimicking gel spoiled. Because of this, the measurements on the unrefrigerated sample are not performed for the weeks following.

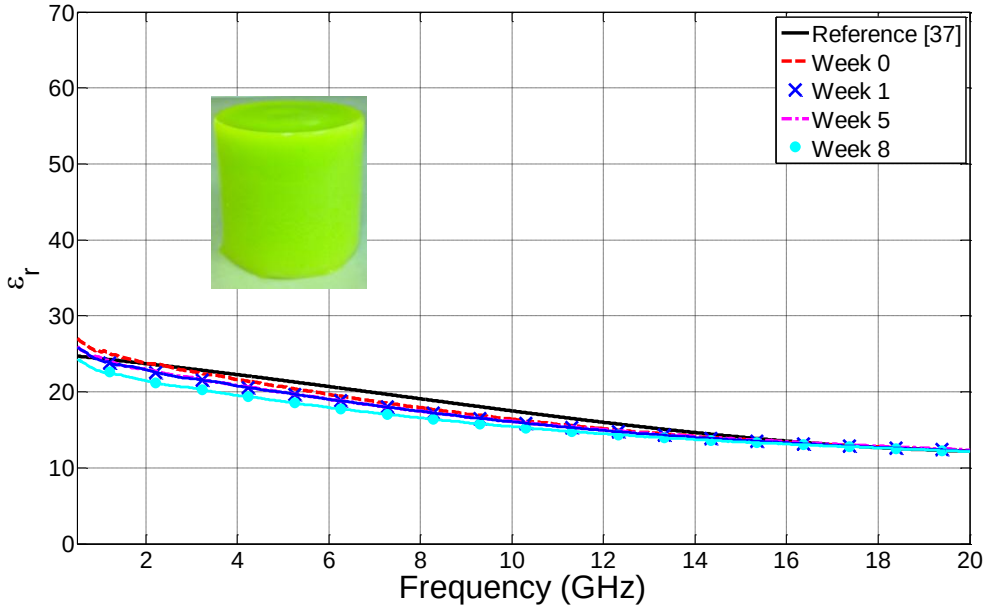

Figure 3.69

Relative Permittivity of Refrigerated Malignant Fibroglandular Tissue Mimicking Material

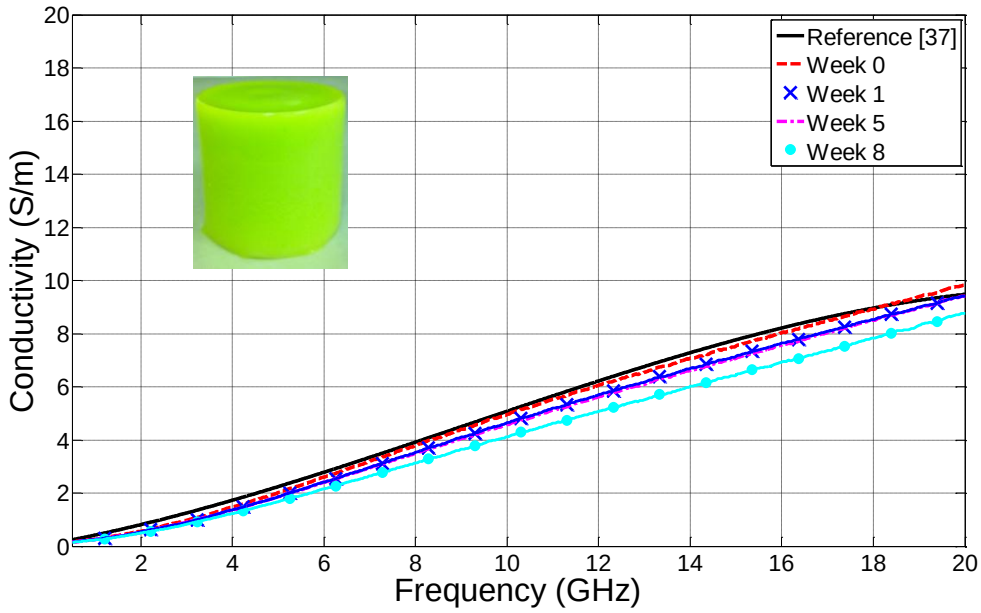

Figure 3.70

Conductivity of Refrigerated Malignant Fibroglandular Tissue Mimicking Material

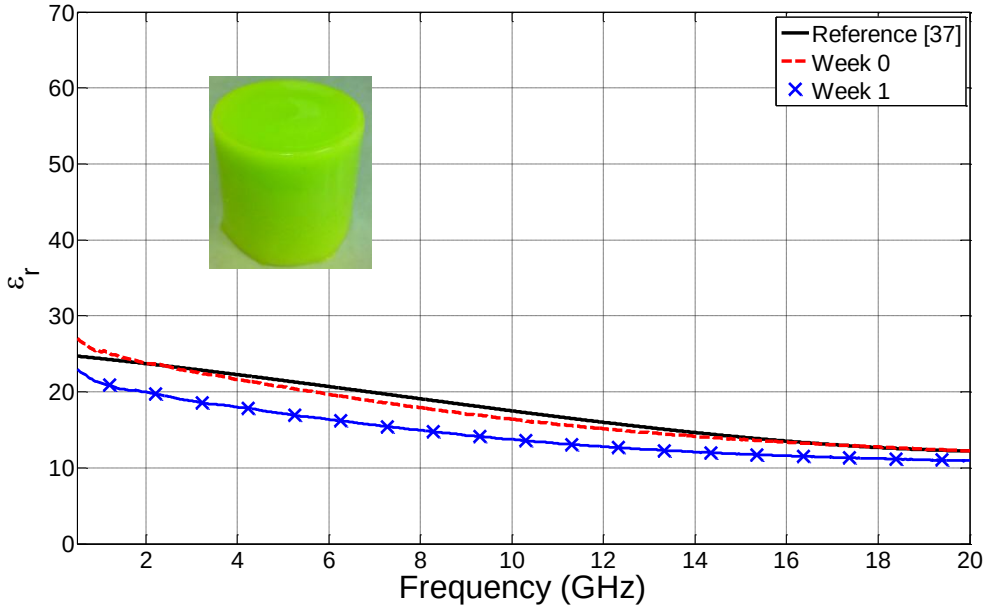

Figure 3.71

Relative Permittivity of Non-Refrigerated Malignant Fibroglandular Tissue Mimicking Material

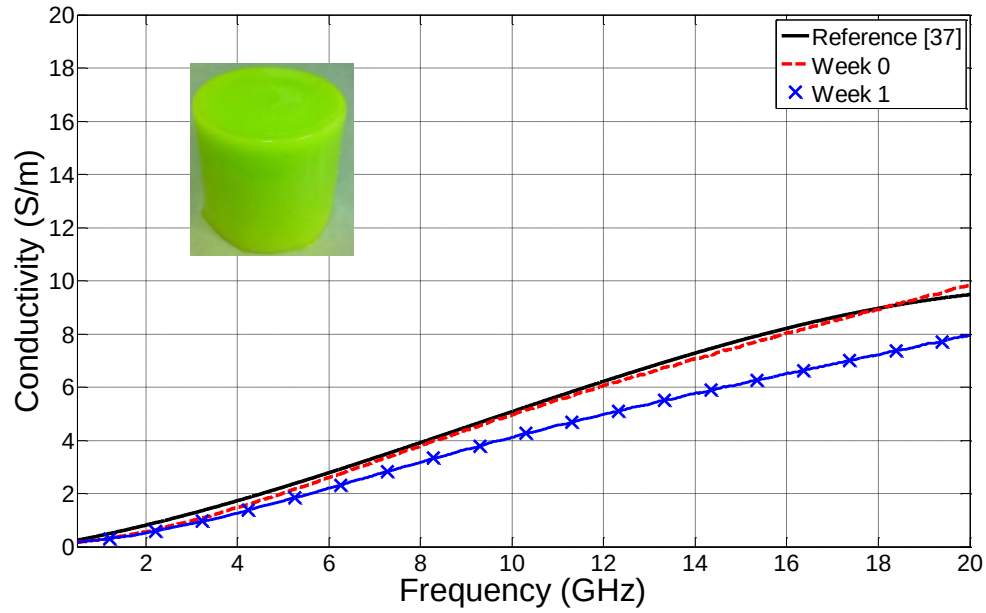

Figure 3.72

Conductivity of Non-Refrigerated Malignant Fibroglandular Tissue Mimicking Material

3.8 Liver Mimicking Material

3.8.1 Characterization of Liver Mimicking Material

A liver material is characterized by mixing de-ionized water, vegetable oil, Gelatin A, Ultra Ivory® hand soap, Triton X-100, sodium chloride, and orange food coloring. Table 3.8 shows the list of ingredients along with their percent volume. The steps described in Chapter 3.1.1 are followed to characterize the tissue mimicking material. The formed liver mimicking gel is shown in Figure 3.73.

Table 3.8

Recipe for Liver Mimicking Material

Ingredient	Percent Volume
De-ionized Water	68.33
Vegetable Oil	20.68
Gelatin A	8.99 (ρ=1.2 g/mL)
Ultra Ivory Soap	0.899
Triton X-100	0.899
Sodium Chloride	0.166 (ρ=2.165 g/mL)
Pink Food Coloring	0.037 (1 drop= 0.042 mL)

Figure 3.73

Characterized Liver Mimicking Material

3.8.2 Liver Mimicking Material Dielectric Probe Measurements

The relative permittivity and conductivity of the liver mimicking material are measured from 500 MHz to 20 GHz by following the steps described in Chapter 3.1.2. The average of the obtained measurements is compared with the human liver reference data obtained from [34-35]. Figure 3.74 and Figure 3.75 show a graphical comparison between a liver's relative permittivity and conductivity of measured and reference data in [34-35], respectively.

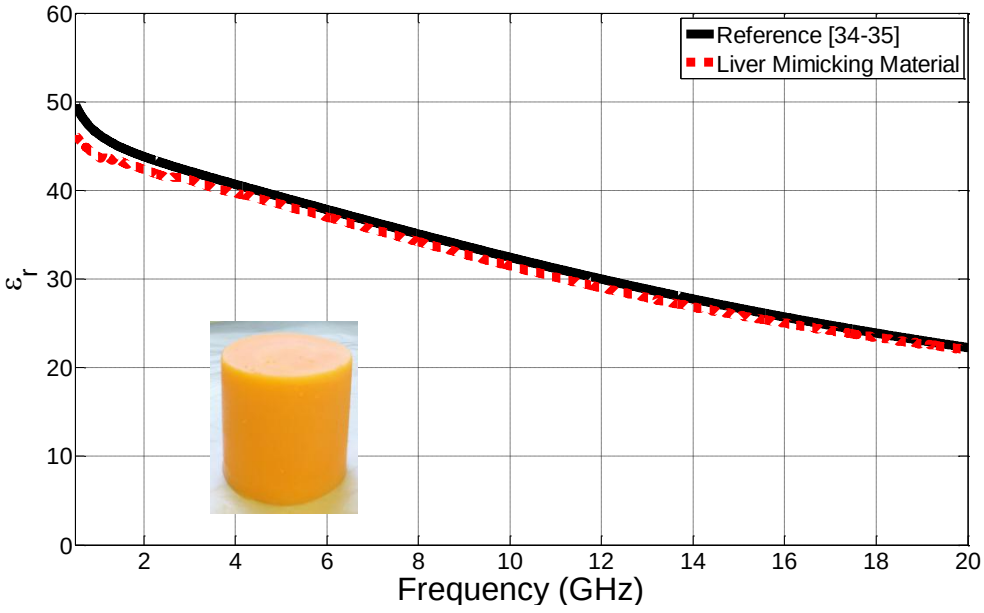

Figure 3.74

Relative Permittivity Comparison of Liver Mimicking Material to Reference Data

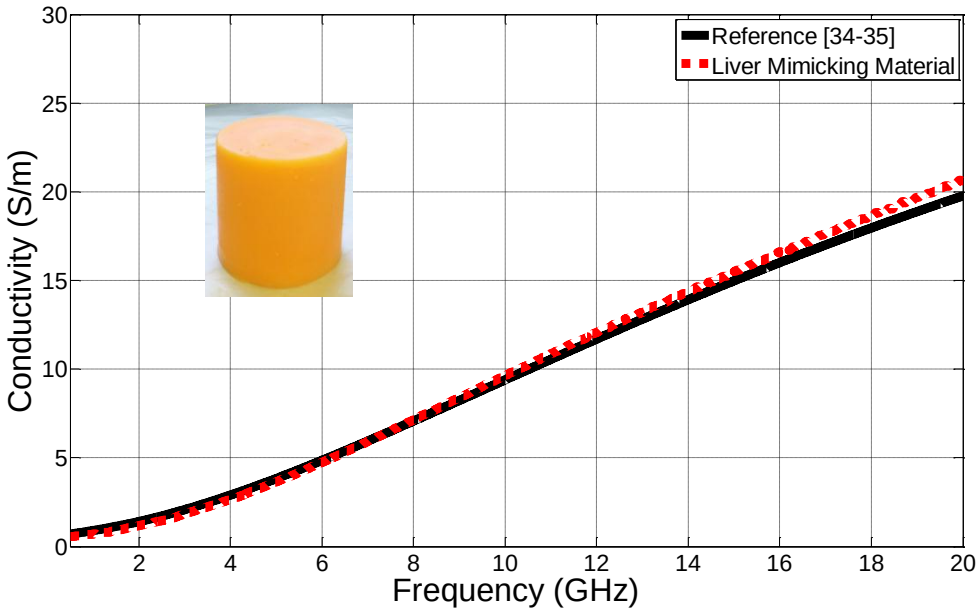

Figure 3.75

Conductivity Comparison of Liver Mimicking Material to Reference Data

As shown in the graphs, a good agreement is obtained between reference data in [34-35] and measurements of the liver mimicking material. The characterized tissue mimicking gel maximum deviation from the reference data from 500 MHz to 20 GHz is 3.49 for the relative permittivity and 0.96 S/m for conductivity.

3.8.3 Absorption of the Liver Mimicking Material

Shown in Figure 3.76, the previously described horn antenna set-up in Chapter 3.1.4 is performed to measure the absorption of power by the interference or presence of a square liver mimicking gel sample. The dimensions of the square sample are 26.5 cm in height, 26.5 cm in length, and 1.02 cm in thickness. Figure 3.77 shows S12 and S21 from 7-11 GHz of the antennas with and without the interference of the liver mimicking gel sample, and the absorption by the liver mimicking material is shown in Figure 3.78.

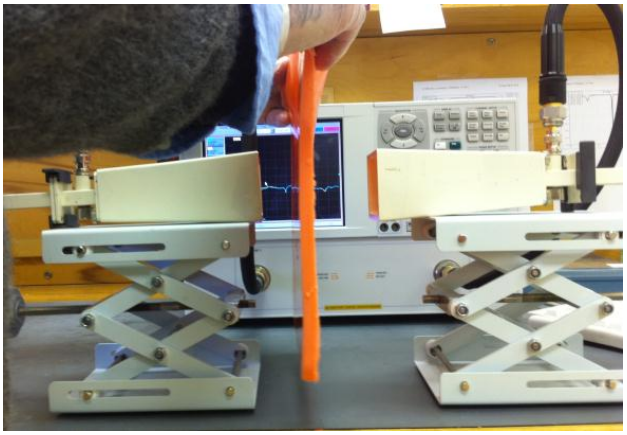

Figure 3.76

S12 and S21 Measurement Set-Up

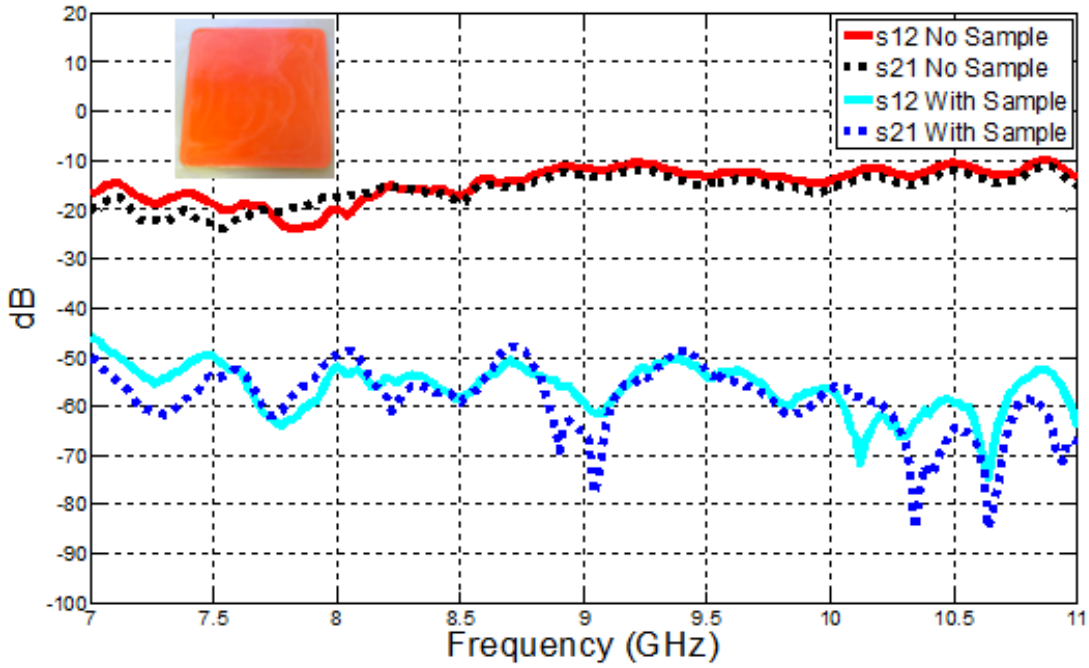

Figure 3.77

S12 and S21 With and Without the Interference of the Liver Mimicking Sample

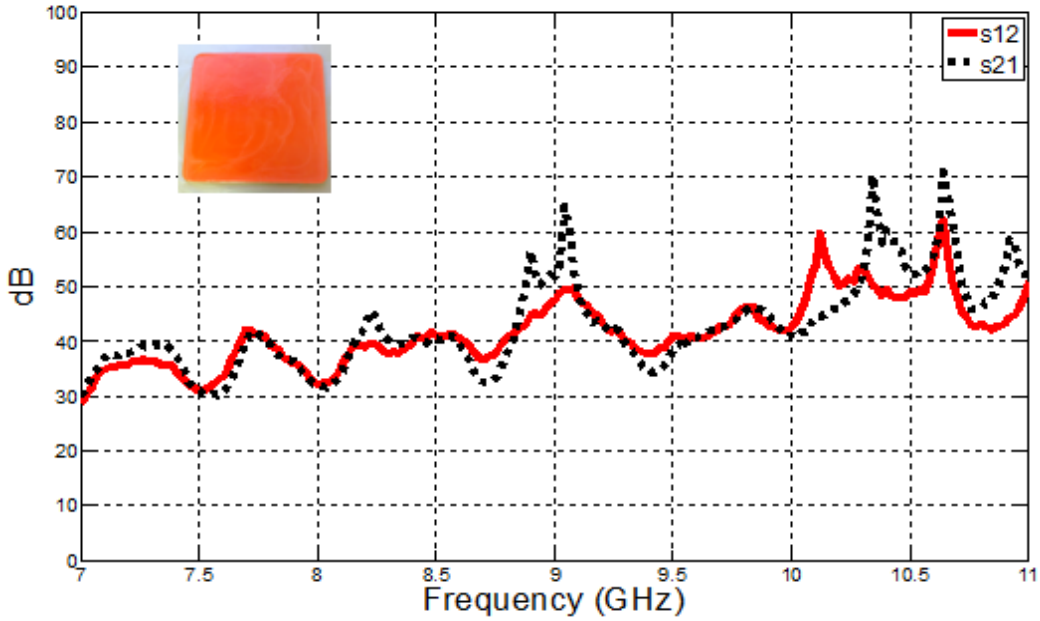

Figure 3.78

Absorption of Liver Mimicking Material

3.9 Pancreas Mimicking Material

3.9.1 Characterization of Pancreas Mimicking Material

A pancreas mimicking material is characterized by mixing de-ionized water, Gelatin A, Triton X-100, sodium chloride, and blue food coloring. Table 3.9 shows the list of ingredients along with their percent volume.

Table 3.9

Recipe for Pancreas Mimicking Material

Ingredient	Percent Volume
De-ionized Water	87.62
Gelatin A	10.95 (ρ=1.2 g/mL)
Triton X-100	1.095
Sodium Chloride	0.15 (ρ=2.165 g/mL)
Blue Food Coloring	0.18 (1 drop= 0.042 mL)

First, sodium chloride is mixed in a beaker with the de-ionized water. The beaker is covered with Syran® wrap and placed an 80ºC water bath. In a separate beaker, Triton X-100 is mixed into 12g of Gelatin A to completely coat the granules. The Gelatin A compound and blue food coloring are added to the saline solution. The beaker is placed back into the 80ºC water bath for 20 minutes. The Gelatin A compound is quickly poured into a 500 mL Whip Mix Vac-U-Mixer and is mixed for 15 seconds. Lastly, the homogeneous mixture is poured into a beaker and set to form in the refrigerator for 30 minutes. The formed pancreas mimicking gel is shown in Figure 3.79.

Figure 3.79

Characterized Pancreas Mimicking Material

3.9.2 Pancreas Mimicking Material Dielectric Probe Measurements

The relative permittivity and conductivity are measured from 500 MHz to 20 GHz following the steps described in Chapter 3.1.2. The average of the obtained measurements is compared with the human pancreas reference data obtained from [34-35]. Figure 3.80 and Figure 3.81 show a graphical comparison of pancreas's electrical properties from measured and reference data in [34-35].

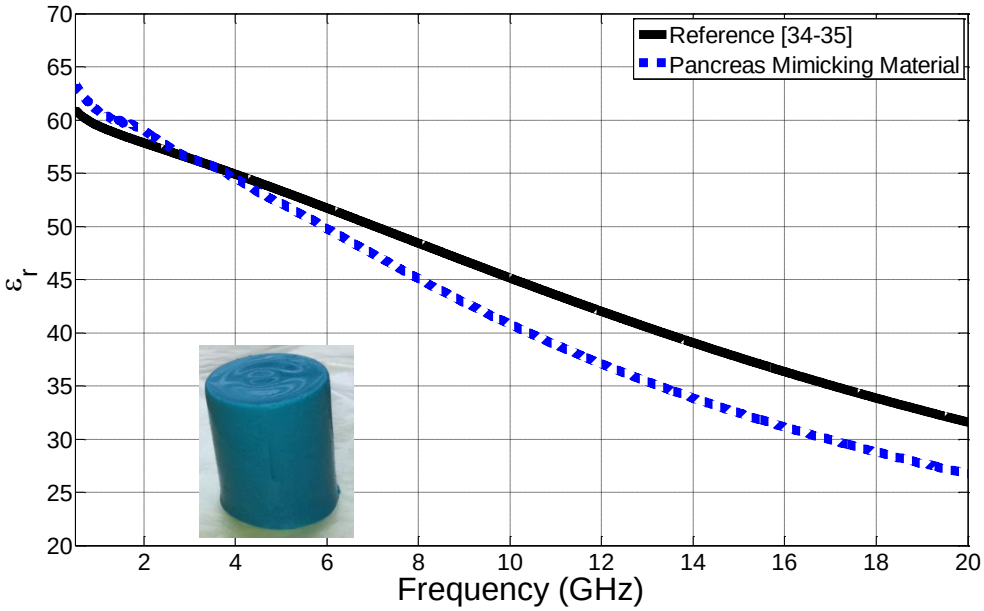

Figure 3.80

Relative Permittivity Comparison of Pancreas Mimicking Material to Reference Data

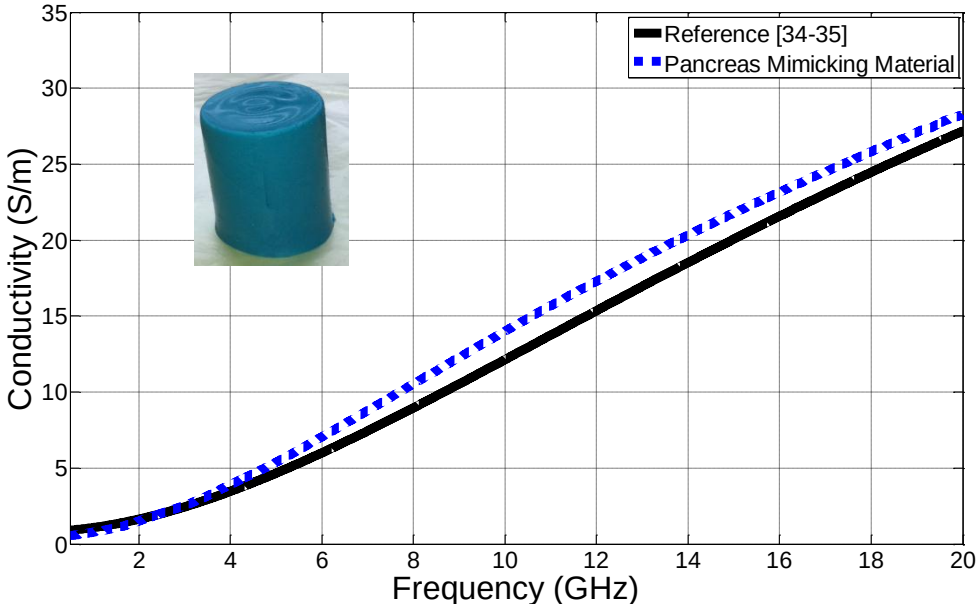

Figure 3.81

Conductivity Comparison of Pancreas Mimicking Material to Reference Data

As shown in the graphs, a good agreement is obtained between reference data in [34-35] and measurements of the pancreas mimicking material. The characterized pancreas mimicking gel maximum deviation from the reference data from 500 MHz to 20 GHz is 5.26 for the relative permittivity and 1.96 S/m for conductivity.

3.9.3 Absorption of the Pancreas Mimicking Material

The previously described horn antenna set-up in Chapter 3.1.4 is performed to measure the absorption of power by the interference or presence of a square pancreas mimicking sample. The dimensions of the square sample are 26.5 cm in height, 26.5 cm in length, and 1.6 cm in thickness. The measurement set-up with the pancreas mimicking gel sample is shown in Figure 3.82. Figure 3.83 shows S12 and S21 from 7-11 GHz of the antennas with and without the interference of the pancreas mimicking gel sample, and the absorption by the pancreas mimicking material is shown in Figure 3.84.

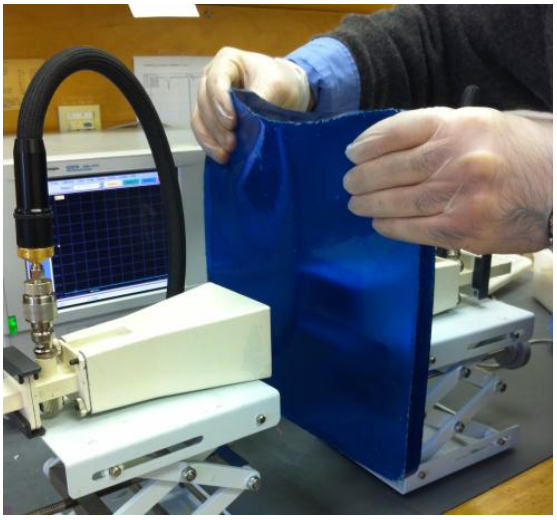

Figure 3.82

S12 and S21 Measurement Set-Up

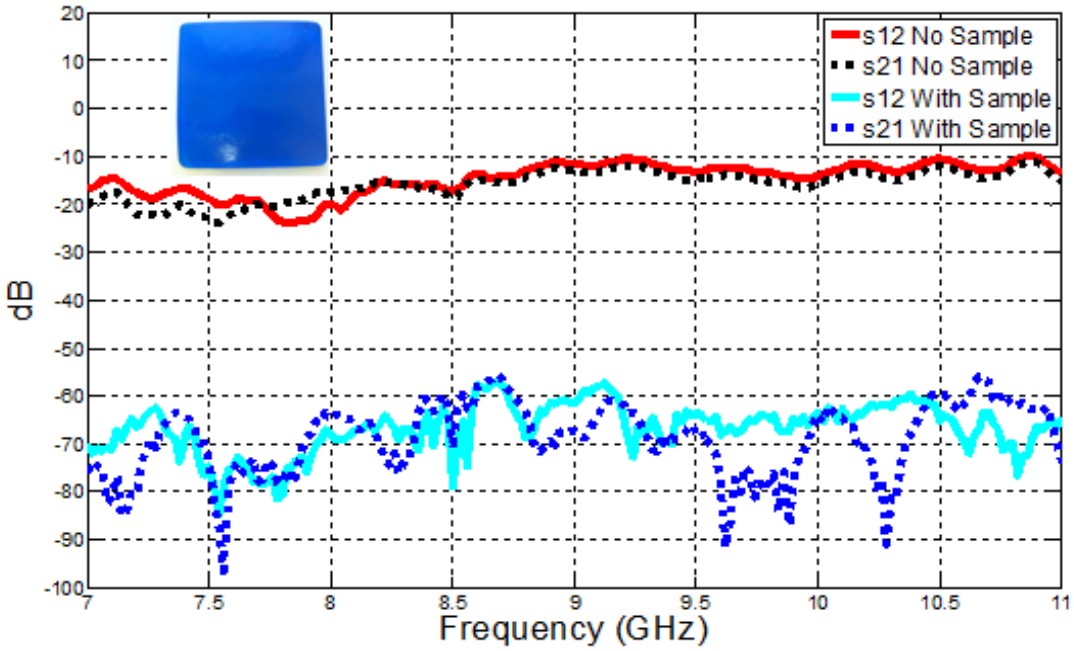

Figure 3.83

S12 and S21 With and Without the Interference of the Pancreas Mimicking Sample

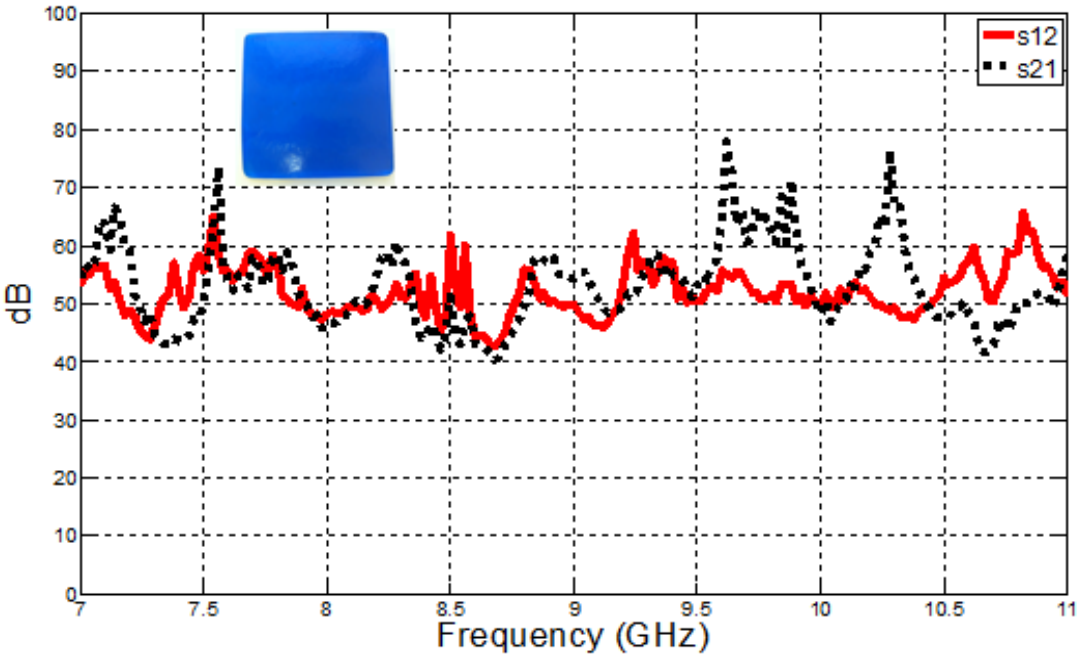

Figure 3.84

Absorption of Pancreas Mimicking Material

3.10 Kidney Mimicking Material

3.10.1 Characterization of Kidney Mimicking Material

A kidney mimicking material is characterized by mixing de-ionized water, vegetable oil, Ultra Ivory® hand soap, Gelatin A, Triton X-100, sodium chloride, and brown food coloring. Table 3.10 shows the list of ingredients along with their percent volume. The steps described in Chapter 3.1.1 are followed to characterize the tissue mimicking material. The formed kidney mimicking gel is shown in Figure 3.85.

Table 3.10

Recipe for Kidney Mimicking Material

Ingredient	Percent Volume
De-ionized Water	72.47
Vegetable Oil	13.59
Gelatin A	9.06 (ρ=1.2 g/mL)
Ultra Ivory Soap	2.72
Triton X-100	0.91
Sodium Chloride	0.13 (ρ=2.165 g/mL)
Brown Food Coloring	1.13 (1 drop= 0.042 mL)

Figure 3.85

Characterized Kidney Mimicking Material

3.10.2 Kidney Mimicking Material Dielectric Probe Measurements

The relative permittivity and conductivity of the kidney mimicking material are measured from 500 MHz to 20 GHz following the steps described in Chapter 3.1.2. The average of the obtained measurements is compared with the human kidney reference data obtained from [34-35]. Figure 3.86 and Figure 3.87 show a graphical comparison between a kidney's relative permittivity and conductivity of measured and reference data in [34-35] respectively. As shown in the graphs, a good agreement is obtained between reference data in [34-35] and measurements of the kidney mimicking material. The characterized pancreas mimicking gel maximum deviation from the reference data from 500 MHz to 20 GHz is 4.97 for the relative permittivity and 1.62 S/m for conductivity.

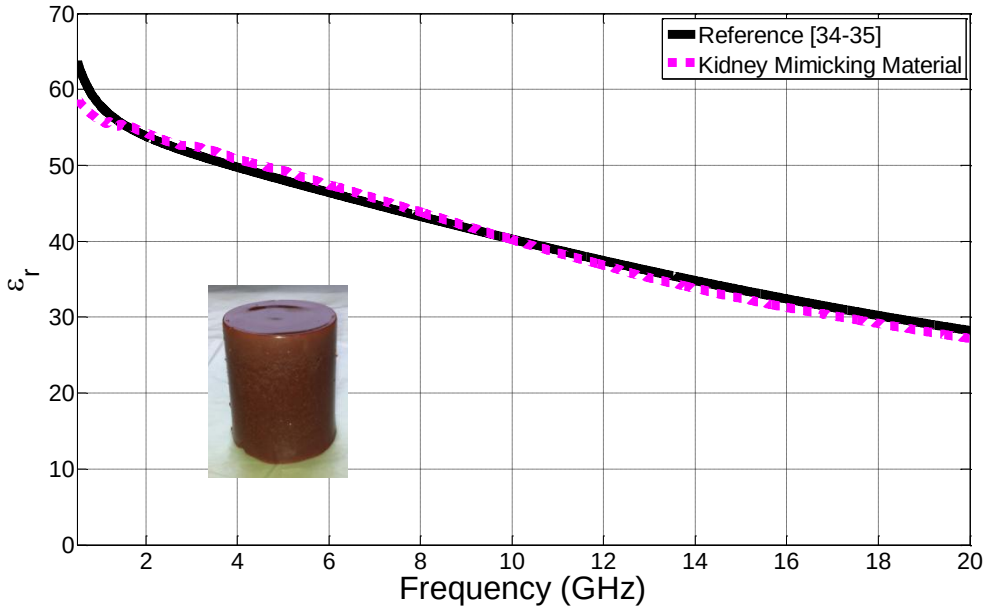

Figure 3.86

Relative Permittivity Comparison of Kidney Mimicking Material to Reference Data

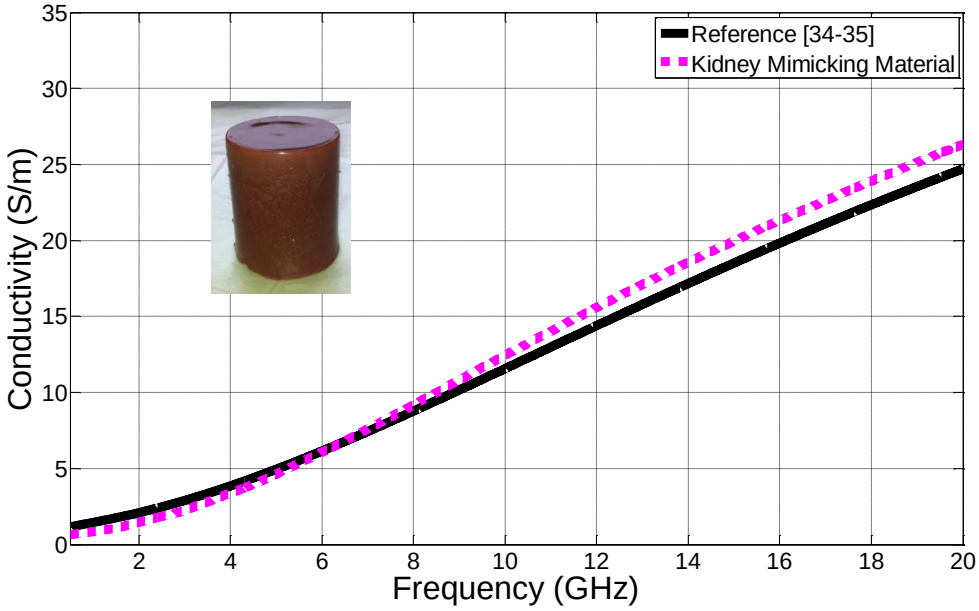

Figure 3.87

Conductivity Comparison of Kidney Mimicking Material to Reference Data

3.10.3 Absorption of the Kidney Mimicking Material

The previously described horn antenna set-up in Chapter 3.1.4 is performed to measure the absorption of power by the presence of a square kidney mimicking gel sample. The dimensions of the square sample are 26.5 cm in height, 26.5 cm in length, and 0.84 cm in thickness. The measurement set-up with the kidney mimicking sample is shown in Figure 3.88. Figure 3.89 shows S12 and S21 from 7-11 GHz of the antennas with and without the interference of the kidney mimicking sample, and the absorption by the kidney mimicking material is shown in Figure 3.90.

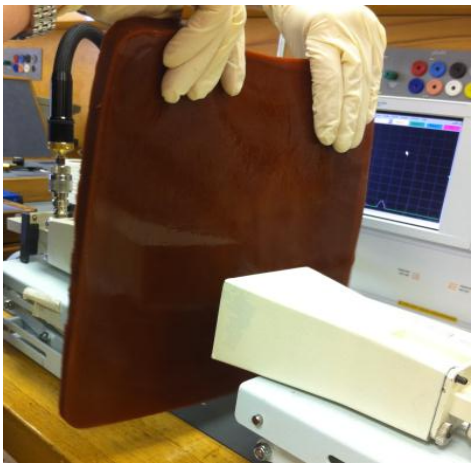

Figure 3.88

S12 and S21 Measurement Set-Up

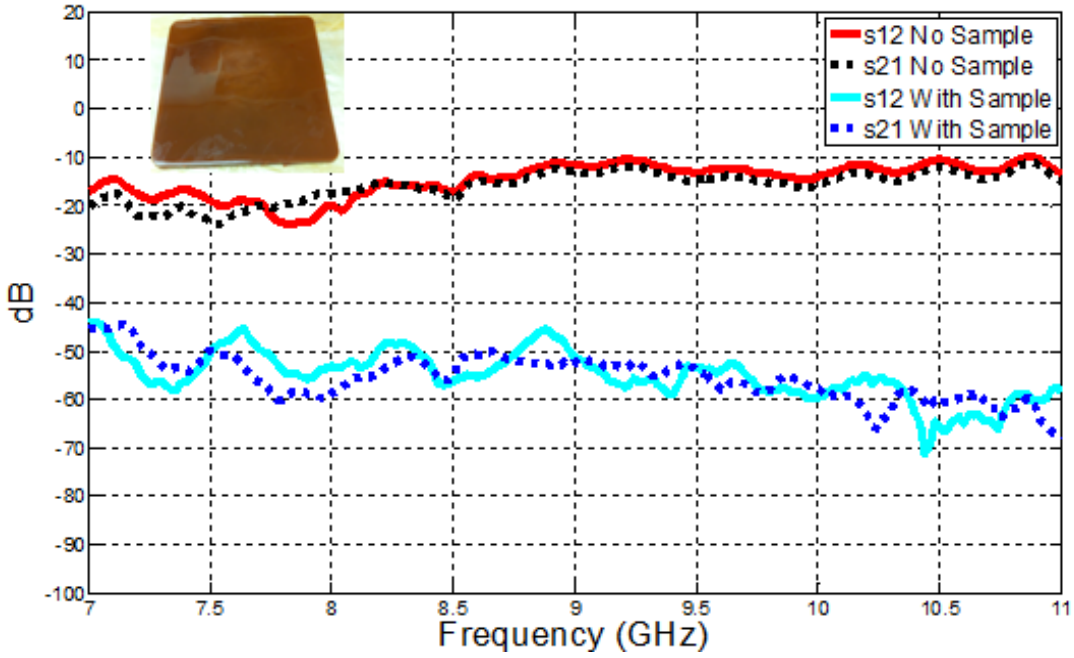

Figure 3.89

S12 and S21 With and Without the Interference of the Kidney Mimicking Sample

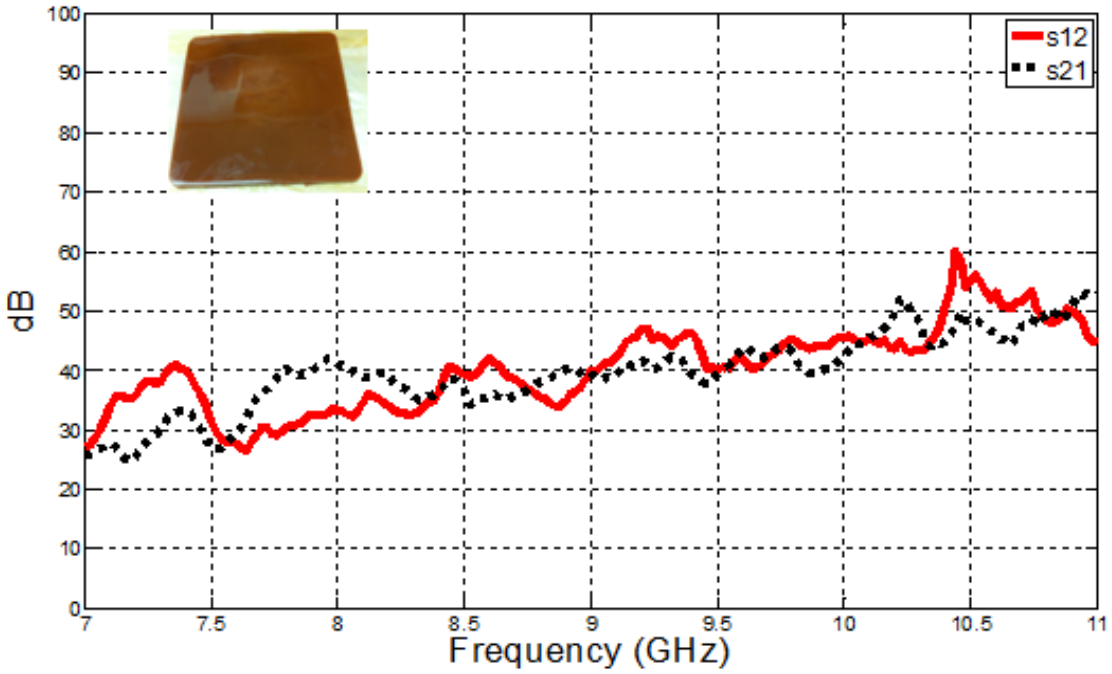

Figure 3.90

Absorption of Kidney Mimicking Material

CHAPTER IV

THE USE OF TISSUE MIMICKING MATERIAL IN MEDICAL TELEMETRY AND EARLY DETECTION OF BREAST CANCER

The characterized tissue mimicking gels are implemented to fabricate phantoms for *in vitro* testing of electromagnetic applications. Various phantoms have been created for the testing of medical telemetry applications and a breast cancer detection system.

4.1 Medical Telemetry

One of the emerging electromagnetic applications in medicine is wireless telemetry systems that continuously monitor physiological parameters of the body such as glucose, blood pressure, and body temperature over a distance through radiofrequency [38-41]. As shown in Figure 4.1, a mutli-sensor device implanted within the patient measures the body's physiological parameters. A transmitter on the patient then sends the information to a receiver that is within close proximity. The data is sent over a distance through radiofrequency to a central monitoring station at a medical vicinity where the data is interpreted. The system allows for continuous health monitoring of patients without physical contact and rigorous schedules.

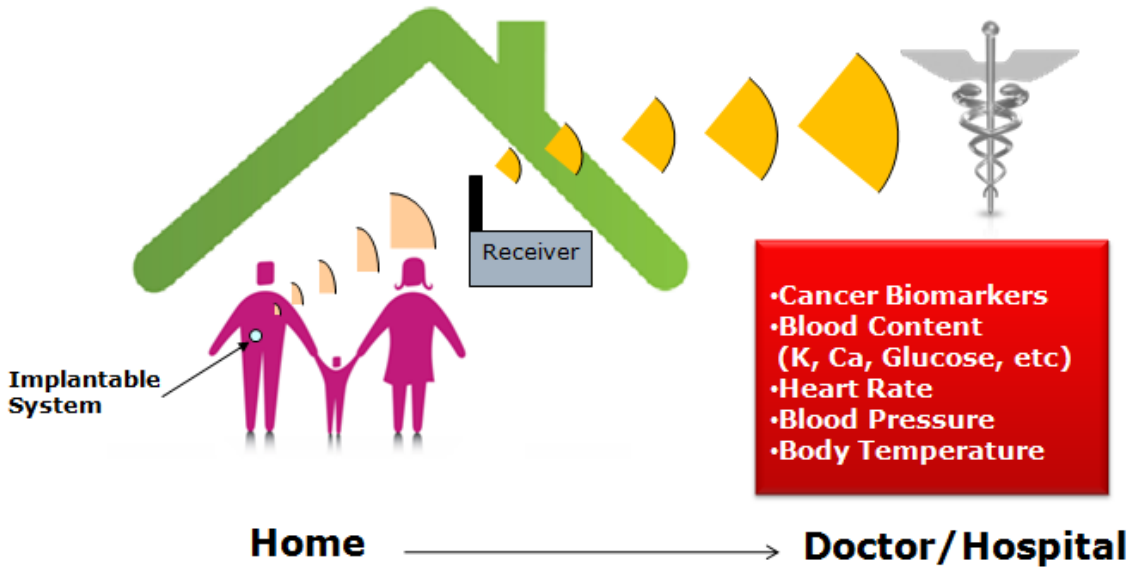

Figure 4.1

Diagram of Wireless Medical Telemetry System

Studies that are intended for monitoring of the physiological parameters require implantation of a wireless data telemetry unit in the interstitial fluid under the skin. As shown in Figure 4.2, the implantable RF unit is composed of a biosensor that will measure the parameters, fully integrated circuits, and an implantable antenna that will transmit the information. For the device to be fully implanted within the patient, it needs to be relatively small in size, biocompatible, and have an extended lifetime. The integrated circuits should require low power, and the antenna needs to operate at multiple bands while maintaining the required radiation characteristics.

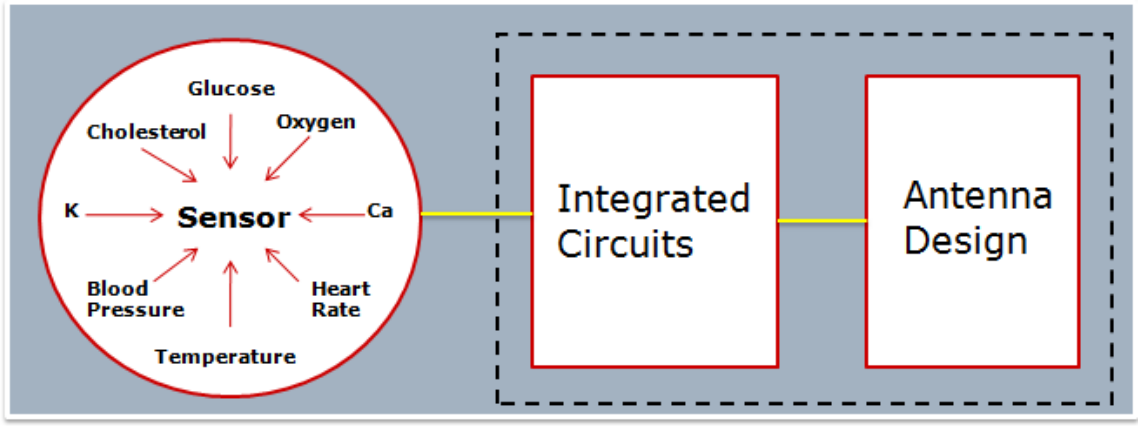

Figure 4.2

Components of Implantable RF Unit

The antenna plays a major role in implantable systems since it provides communication of the implant with the external equipment [38-39]. A small size dual Medical Implant Communications Service (MICS) (402-405 MHz) and Industrial, Scientific, and Medical (ISM) (2.4-2.48 GHz) band implantable antenna that will stay functional when implanted in a patient is created to be integrated into a continuous medical telemetry system. The dual band design allows the implant to switch between sleep and wake-up modes, thus conserving energy and extending the lifetime of the implant. A wake-up signal is sent to the antenna through the ISM band, while the MICS band transmits information to a receiver. As shown in Figure 4.3, the implantable antenna is embedded in a three-tissue phantom layer composed of the skin, adipose tissue, and muscle mimicking materials described in Chapter 3.1-3.3.

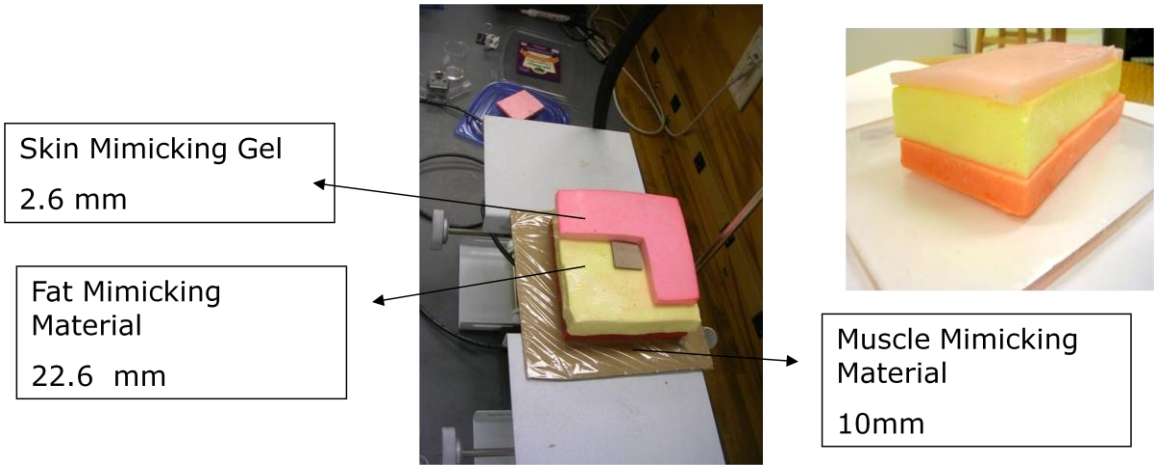

Figure 4.3

Implanted Antenna in Three Tissue Layer Phantom

The network analyzer is used to simulate the antenna's performance in the presence of three different human tissue layers (skin, fat, and muscle) from 200 MHz to 3 GHz. Figure 4.4 shows that the implanted antenna functionally operates at both MICS and ISM bands. There is not a significant change in the resonant characteristics between the measured implanted antenna in the synthetic tissue mimicking phantom than the simulated antenna in a phantom model. Therefore, the antenna can effectively transmit electromagnetic waves within and outside of the body.

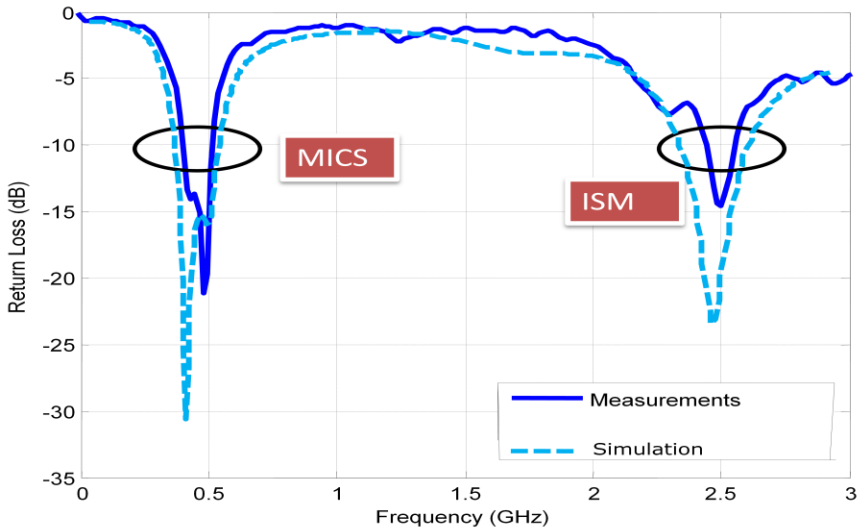

Figure 4.4

Return Loss of Operating Implanted Antenna

4.2 Early Detection of Breast Cancer

A new upcoming technique to detect breast cancer is through microwave breast imaging where the breast is illuminated by electromagnetic waves, and the scattered data is collected to identify the malignant tissue. Conventional techniques to screen for breast cancer today such as x-ray mammography, ultrasound, and magnetic resonance imaging behold several disadvantages. During mammograms, images are taken by pressing the breast tissue between a flat imaging array causing most women pain and discomfort. In addition, the patient is exposed to radiation which can itself lead to cancer. Ultrasound produces false positive results, and the procedure is inaccurate for small tumors. Though magnetic resonance imaging is effective and accurate, it is very costly and not all hospitals and health care centers are equipped for the procedure. The application of microwaves can be an alternative technique for detecting and monitoring breast cancer

with the purpose of eliminating these disadvantages. Because the electrical properties of the malignant and healthy tissue vary significantly at microwave frequencies, one can potentially detect the malignant tissue during the early stages of the cancer development. In a previous study, we investigated this technique by using two horn antennas to detect a tumor mimicking inclusion within a synthesized breast phantom.

First, a breast phantom is constructed to mimic the electrical properties of nonmalignant healthy tissues within the breast. The breast phantom consisted of various layers of gels that mimic the electrical properties of the following tissues: skin, adipose fat, fibroglandular tissue with 0-30% adipose tissue, and muscle. The phantom is constructed in a breast mold modeling an actual human breast. Figure 4.5 shows the breast mold that is used to construct the breast phantom.

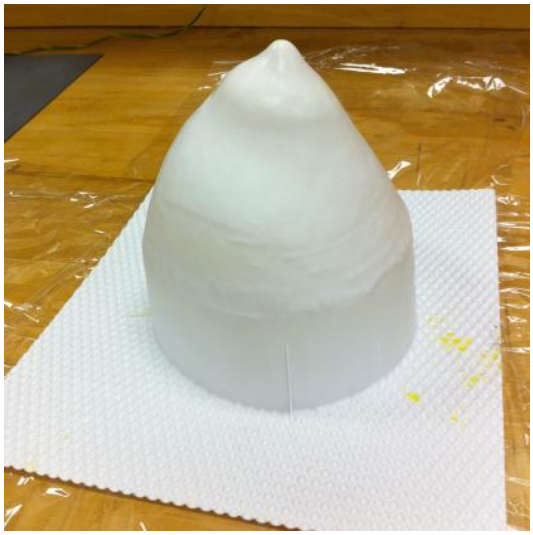

Figure 4.5

Breast Mold

In order to create such a phantom, a 111.23 mL total volume skin mimicking material is created by following the procedure described in Chapter 3.1.1. As soon as the material is thoroughly mixed, it is poured into the breast mold and rotated until the gel has lined the entire walls of around 2 mm in thickness. The skin's thickness around the breast can range from 0.5-2.7 mm [42]. The mold is then set to finish forming in the refrigerator for 30 minutes. Figure 4.6 shows the skin after it is formed within the mold.

Figure 4.6

Skin Lining of the Breast Phantom

A 300 mL total volume mixture that mimics fibroglandular tissue with 0-30% adipose tissue is created by following the procedure described in Chapter 3.4.1. Once thoroughly mixed, the mixture is poured into a martini glass and set to form in the refrigerator for 30 minutes.

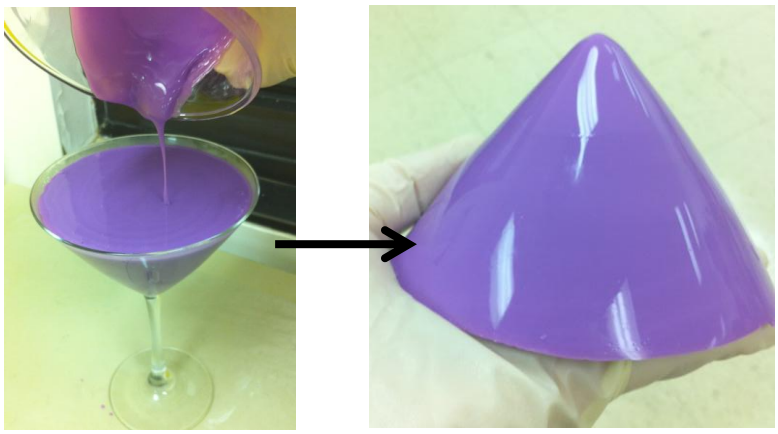

Figure 4.7

Fibroglandular Tissue Phantom

A 522.32 mL total volume mixture that mimics adipose tissue is created by following the procedure described in Chapter 3.2.1. Once thoroughly mixed, approximately 2/5th of the mixture is poured into the bottom of the breast mold (Figure 4.8(a)). The fibroglandular tissue mold is immerged within the adipose tissue (Figure 4.8(b)), and the remainder adipose tissue mimicking material is poured in the mold to completely cover the fibroglandular tissue phantom (Figure 4.8 (c-d)). The breast mold is set in the refrigerator for 2 hours to completely form.

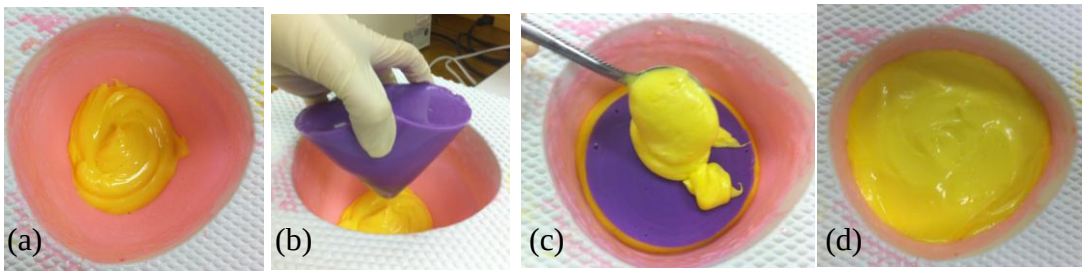

Figure 4.8

Steps (a-d) in Adding Adipose and Fibroglandular Tissue into the Breast Phantom

A 110.38 mL total volume muscle mimicking gel is created by following the procedure described in Chapter 3.3.1. Once the material is thoroughly mixed, the mixture is poured on top of the adipose tissue mimicking gel within the breast mold and set to form in the refrigerator for 30 minutes. Figure 4.9 shows the process with the fabricated breast phantom.

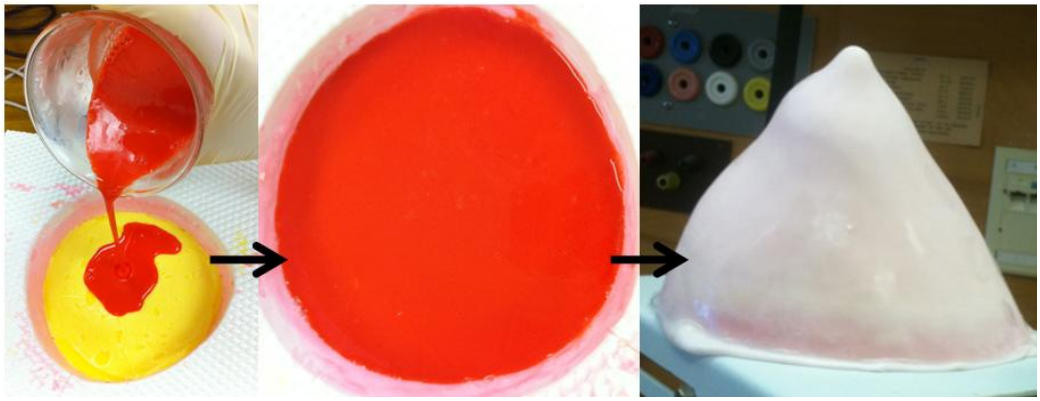

Figure 4.9

Steps in Adding Muscle Tissue into the Breast Phantom

Once fabricated, the nonmalignant breast phantom is wrapped in Syran® wrap and placed in the refrigerator to preserve it until measurements are made. In order to understand the effectiveness of the microwave imaging technology as a tool for early detection of breast cancer, the scattering characteristics of a tumor inclusion in a realistic breast phantom is studied. The fabrication process of the phantom is mostly similar to the previously discussed procedures other than the creation the tumor inclusion within the fibroglandular tissue. After the skin is formed around the lining of the breast mold, a 56.65 total volume mixture that mimics malignant fibroglandular tissue with 0-30% adipose tissue is created according to the steps described in Chapter 3.6.1. Once

thoroughly mixed, the material is poured into a 50 ml beaker and set to form in the refrigerator for 30 minutes. As shown in Figure 4.10, the top of the gel is cut off so that the dimension of the cylindrical tumor is 3.75 cm in height and 3.75 cm in diameter.

(a) (b)

Figure 4.10

(a) Height and (b) Diameter of Cylindrical Malignant Fibroglandular Tissue Phantom

A 258.58 mL total volume mixture that mimics fibroglandular tissue with 0-30% adipose tissue is created by following the steps described in Chapter 3.4.1. Once thoroughly mixed, 20 mL of the mixture is poured into a martini glass and set in the refrigerator for 10 minutes to form. While in the refrigerator, the remaining mixture is kept out at room temperature to cool down the material so that it will not cause the tumor phantom to melt when it comes in contact with it. The tumor mimicking gel is placed at the center of the formed fibroglandular tissue mimicking within the martini glass (Figure 4.11(a)), while the remaining mixture is poured on top of the tumor until it is completely concealed (Figure 4.11 (b-c)). The phantom is set in the refrigerator to form for 30 minutes. Once formed, the final steps involved in creating the breast phantom coincide with the procedure previously described for the fabrication of the nonmalignant breast phantom.

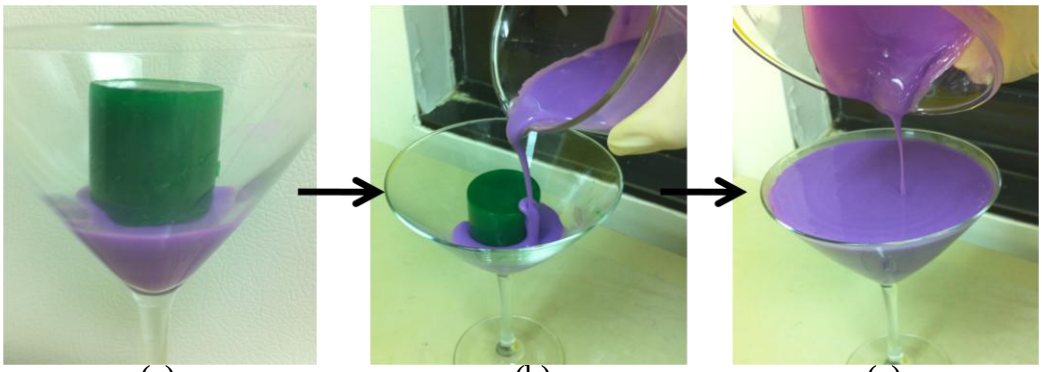

(a) (b) (c)

Figure 4.11

Steps (a-c) in Creating the Malignant Fibroglandular Tissue Phantom

The fabricated breast phantoms are then used to investigate the advantages of microwave imaging technology to detect breast cancer by studying the scattering characteristics of tumor inclusions in the realistic breast phantoms. In order to perform the study, the previous two horn antennas, operating at 7 to 11 GHz, are located 14 cm apart. Each phantom was placed between the horns while the appropriate measurements are made. Figure 4.12 shows the experimental set-up. For each breast phantom, four measurements are made with the sides at a 90° change in orientation. As shown in Figures 4.13-4.15, S12 and S21 of each breast phantom are compared to the measurements made with no sample interaction, and lastly the malignant breast phantom is compared with the phantom with no tumor inclusion.

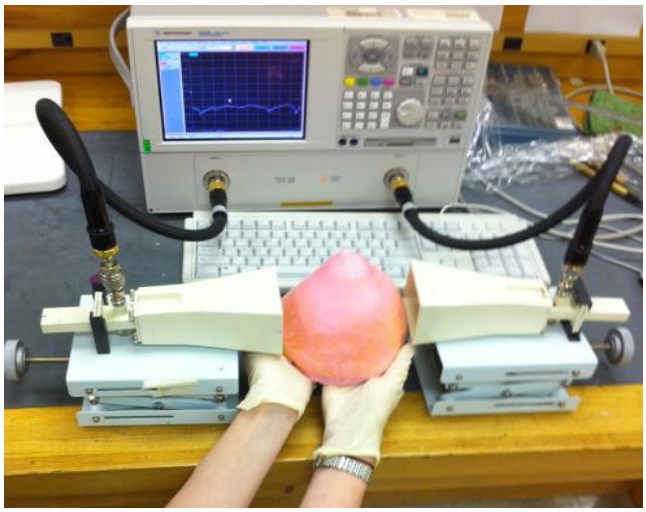

Figure 4.12

Horn Measurement Set-Up with Interference of the Breast Phantom

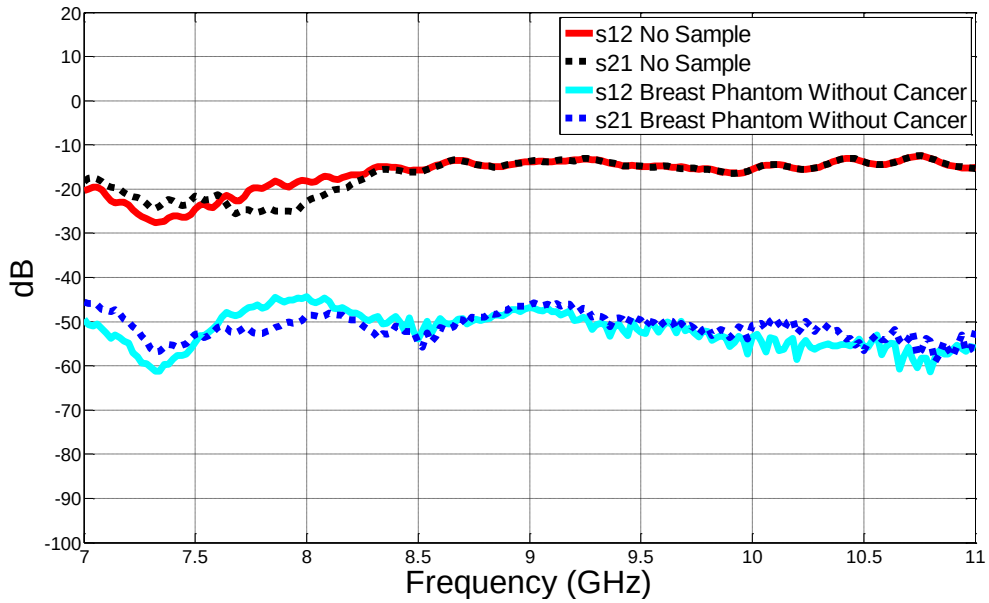

Figure 4.13

S12 and S21 of Non-Malignant Breast Phantom

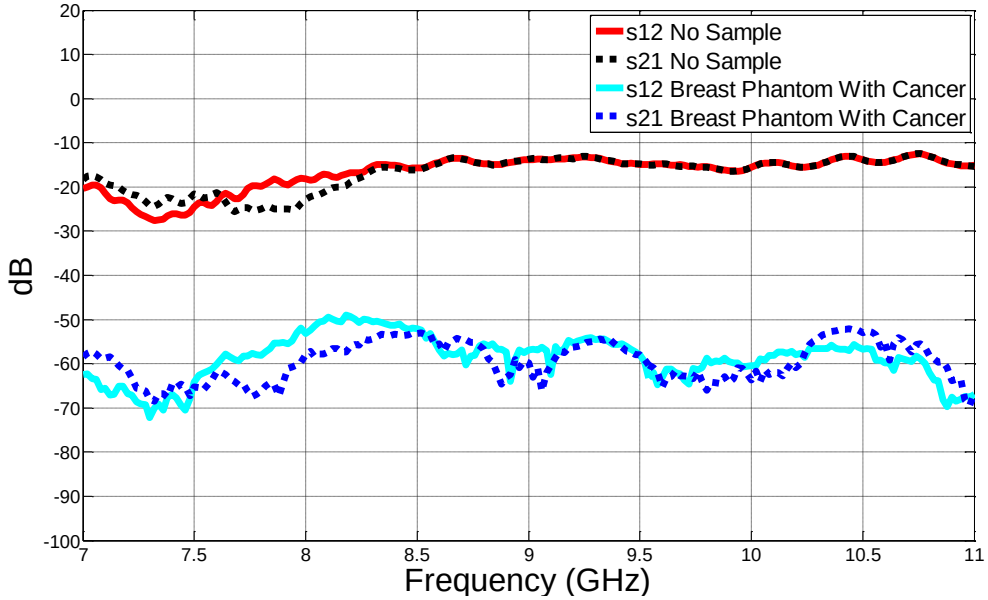

Figure 4.14

S12 and S21 of Malignant Breast Phantom

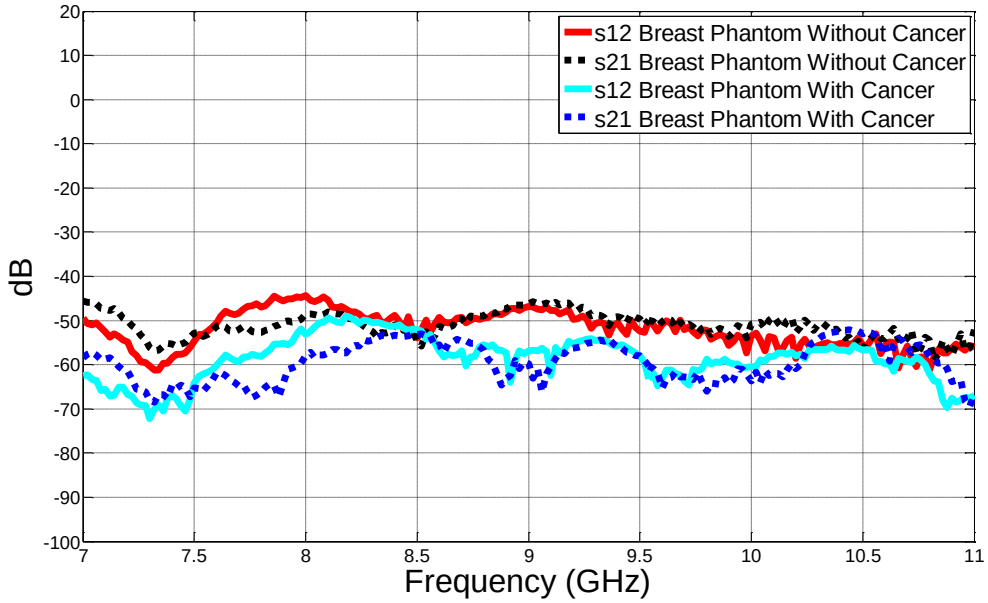

Figure 4.15

S12 and S21 Comparison of Both Breast Phantoms

Figure 4.15 shows that there is around a -12 dB drop in the malignant breast phantom at 7 GHz. This drop occurs because the electrical properties of malignant tissue vary significantly from healthy tissue. The relative permittivity of malignant tissue has higher relative permittivity at microwave frequency ranges than healthy tissue. With a higher relative permittivity, the phantom is more dielectric and therefore absorbs more of the radiating energy. The absorption of energy detects the presence of the malignant tissue. Figure 4.16 shows a cross-section of the breast phantom, validating the presence of the malignant fibroglandular tissue inclusion.

Figure 4.16

Cross-Section of Malignant Breast Phantom

4.3 Other Potential Applications

Hyperthermia is a new and upcoming option for treating several different types of deep-seated cancer within biological tissues such as the liver, pancreas, or kidney. Microwaves can be radiated at frequencies of 200-3000 MHz to heat the malignant tissue and potentially destroy it. The device can either be a direct simple applicator coupled with a cooling water bag, or a complex arrangement of phase array antennas [43].

Since the characterized material mimics the dielectric properties of tissues within the microwave frequency range of 500 MHz- 20 GHz, they are applicable for *in vitro* measurements of new and upcoming microwave hyperthermia techniques. Tissue mimicking phantoms have been used in recent studies to test microwave hyperthermia systems [44-46]. These studies have involved the creation of a liver phantom [45] and a kidney phantom [46] to use in place of real tissue when measuring the SAR around medical devices such as hyperthermia that operate at a microwave range. Our characterized liver, pancreas, and kidney mimicking material can be utilized to create tissue mimicking phantoms that can be used in the development and testing of microwave hyperthermia applications that will treat and, in hopes, ultimately destroy deep seated tumors.

CHAPTER V

CONCLUSION

Gelatin-based tissue mimicking phantoms efficiently aid in the development and testing of microwave medical devices. For future human studies, we characterized semi-solids materials that mimic the dielectric properties of human skin, adipose tissue, muscle, malignant and healthy fibroglandular tissue that contains 0-30% adipose tissue, malignant and healthy fibroglandular tissue that contains 31-84% adipose tissue, liver, pancreas, and kidney within the frequency range of 500 MHz to 20 GHz. These materials are all gelatin-based with varying amounts of vegetable oil and de-ionized water.

These tissue mimicking materials are used to create synthetic tissue mimicking phantoms for the testing of wireless medical telemetry and breast cancer detection applications. A three-tissue layer phantom consisting of skin, fat, and muscle is developed to simulate the performance of the dual MICS and ISM band antenna that is to be integrated into a continuous physiological parameters monitoring system by embedding it within the tissue layers. The implanted antenna worked accurately within the layers of the tissue mimicking phantom. In another study, two human breast phantoms are created that are to be implemented in the testing of a microwave device that detects breast cancer. A study was performed to investigate this detection technique by using two horn antennas to detect the presence of a tumor mimicking inclusion within a breast phantom. By comparing the antennas' return loss due to the presence of both

breast phantoms that contain malignant or healthy tissue, we are able to detect the presence of the tumor within the breast phantom. This is because the electrical properties of the malignant and healthy fibroglandular tissue vary significantly at microwave frequencies.

Our future work will involve the investigation of microwave hyperthermia. Hyperthermia is a new and upcoming option for treating several different types of deep-seated cancer within biological tissues such as the liver, pancreas, or kidney. The characterized liver, pancreas, and kidney mimicking materials are to be used to create phantoms that will aid in the testing of microwave hyperthermia which has the potential to treat and destroy deep seated tumors within biological tissues.

REFERENCES

[1] D. A. Christensen, C. Furse, C.H. Durney, "Electromagnetic in Medicine: Today and Tomorrow," *Basic Introduction to Bioelectromagnetics*, CRC Press, pp. 229-251, 2009.

[2] J. A. Von Arx, W. R. Mass, S. T. Mazar, and M. D. Amundson, "Antenna for an implantable pacemaker," U.S. Patent 6 708 065, Mar. 16, 2004.

[3] D. Panescu, "Wireless communication systems for implantable medical devices," *IEEE Engineering in Medicine and Biology Magazine*, vol. 27, Issue 2, pp. 96-101, March/April 2008.

[4] M. A. Al-Joumayly, S. M. Aguilar, N. Behdad, and S. C. Hagness, "Dual-band miniaturized patch antennas for microwave breast imaging," *IEEE Antennas and Wireless Propagation Letters*, vol. 9, pp. 268-271, 2010.

[5] P. Togni, J. Vrba, L.a Vannucci, "Microwave applicator for hyperthermia treatment on *in vivo* melanoma model," *Medical and Biological Engineering and Computing*, vol. 48, Issue 3, pp. 285-292, March 2010.

[6] M. Ballen, M. Kanda, C. K. Chou, and Q. Balzano, "Formulation and characterization of tissue simulating liquids used for SAR measurement," *Proc. 23rd Annu. Bioelectromagn. Soc. Meeting*, vol. 14-3, p. 80, 2001.

[7] A. Peyman and C. Gabriel, "Tissue equivalent liquids for SAR measurement at microwave frequencies," *Proc. 24th Annu. Bioelectromagn. Soc. Meeting*, vol. P-53, pp. 184–185, 2002.

[8] K. Fukunaga, S.Watanabe, and Y. Yamanaka, "Dielectric properties of tissue equivalent liquids and their effects on specific absorption rate," *IEEE Trans. Electromagn. Compat.*, vol. 46, no. 1, pp. 126–129, Februaray 2004.

[9] K. Fukunaga1, S. Watanabe, H. Asou and K. Sato, "Dielectric properties of non-toxic tissue-equivalent liquids for radiowave safety tests," *IEEE International Conference on Dielectric Liquids*, pp. 425-428, August 2005.

[10] J. Kim and Y. Rahmat-Samii, "Implanted antennas inside a human body: Simulations, designs, and characterizations," *IEEE Transaction Microwave Theory Tech.*, vol. 52, no. 8, pp. 1934–1943, August 2004.

[11] J. T. Chang, M.W. Fanning, P. M. Meaney, and K. D. Paulsen, "A conductive plastic for simulating biological tissue at microwave frequencies," *IEEE Trans. Electromagn. Compat.*, vol. 42, pp. 76–81.

[12] A. W. Guy, "Analysis of electromagnetic fields induced in biological tissue by thermographic studies on equivalent phantom models," *IEEE Trans. Microw. Theory Tech.*, vol. 19, pp. 189–217, 1971.

[13] L. E. Maggi, M. A. von Kruger, W. C. A. Pereira, and E. Monteiro, "Development of silicon-based materials for ultrasound biological phantoms," *IEEE International Ultrasonics Symposium*, pp. 1962-5, 2009.

[14] H. Chio, H. Shim, K. Cho, H. Lee, C. Park, and H. Yoon, "Electromagnetic and electromagnetic wave-absorbing properties of the SrTi03-epoxy composite", *Journal Appl. Polytii. Sci.*, vol. 72, pp. 75-83, 1999.

[15] Y. Nikawa, M. Chino, and K. Kikuchi, "Soft and dry phantom modeling material using silicone rubber with carbon fibre," *IEEE Trans. Microw. Theory Tech.*, vol. 44, pp. 1949–53, 1996.

[16] C. Gabriel, "Tissue equivalent material for hand phantoms," *Phys. Med. Biol.*, vol. 52, pp. 4205-4210, 2007.

[17] T. Kobayashi, T. Nojima, and K. Yamada, "Dry phantom composed of ceramics and its application to SAR estimation," *IEEE Trum Microit. Theory Ted.*, vol. 41, pp. 136-140, 1993.

[18] S. S. Stuchly, "Specific absorption rate distributions in a heterogeneous model of the human body at radio frequencies," *EPA Project Summary*, pp. 89, 1987.

[19] S. S. Stuchly, A. Kraszewski, M. A. Stuchly, G. Hartsgrove, and R. J. Spiegel, "RF energy deposition in a heterogeneous model of man: Far-field exposures," *IEEE Trans. Biomed. Eng.*, vol. BME-34, no. 12, pp. 951–957, Dec. 1987.

[20] S. R. H. Davidson and M. D. Sherar, "Measurement of the thermal conductivity of polyacrylamide tissue-equivalent phantom," *Int. J. Hyperthermia*, vol. 19, pp. 551–62, 2003.

[21] A. Surowiec, P. N. Shrivastava, M. Astrahan, and Z. Petrovich," Utilization of a multilayer polyacrylamide phantom for evaluation of hyperthermia applicators," *Int. J. Hyperthermia,* vol. 8, pp. 795–807, 1992.

[22] C. K. Chou, G. W. Chen, A. W. Guy, and K. H. Luk, "Formulas for preparing phantom muscle tissue at various radiofrequencies," *Bioelectromagnetics*, vol. 5 pp. 435–41, 1984.

[23] K. Ito, K. Furuya, Y. Okano, and L. Hamada, "Development and characteristics of a biological tissue-equivalent phantom for microwaves," *Electron. Commun. Japan 1*, vol. 84, pp. 1126–35, 2001.

[24] Mark W. Groch, John A. Urbon, William D. Erwin, and Sulaiman Al-Doohan, "An MRI tissue equivalent lesion phantom using a novel polysaccharide material," *Magnetic Resonance Imaging,* vol. 9, iss. 3, pp. 417-421, 1991.

[25] K. J. Surry, H. J. B. Austin, A. Fenster, and T. M. Peters, "Poly(vinyl alcohol) cryogel phantoms for use in ultrasound and MR imaging," *Phys. Med. Biol.*, vol. 49, pp. 5529–46, 2004.

[26] C. Marchal, M. Nadi, A. J. Tosser, C. Roussey, and M. L. Gaulard, "Dielectric properties of gelatin phantoms used for simulations of biological tissues between 10 and 50 MHz," *Int. J. Hyperthermia,* vol. 5, pp. 725–32, 1989.

[27] T. Sunaga, H. Ikehira, S. Furukawa, M. Tamura, E. Yoshitome, T. Obata, H. Shinkai, S. Tanada, M. Hajime, and Y. Sasaki, "Development of a dielectric equivalent gel for better impedance matching for human skin," *Bioelectromagnetics*, vol. 24, pp. 214–17, 2003.

[28] M. Lazebnik, E. L. Madsen, G. R. Frank, and S. C. Hagness, "Tissue mimicking phantom materials for narrowband and ultrawideband microwave applications," Phys. Med. Biol., vol. 50, pp. 4245–4258, 2005.

[29] E. L. Madsen, J. A. Zagzebski, and G. R. Frank, "Oil-in-gelatin dispersions for use as ultrasonically tissue-mimicking materials," *Ultrasound Med. Biol.*, vol. 8, pp. 277–87, 1982.

[30] D. Miklavčič, N. Pavšelj, and F. X. Hart, "Electric properties of tissues," *Wiley Encyclopedia of Biomedical Engineering*, John Wiley & Sons, pp. 1-12, 2006.

[31] S. Gabriel, R. W. Lau, and C. Gabriel, "The dielectric properties of biological tissues: III. Parametric models for the dielectric spectrum of tissues," *Phys. Med. Biol.*, vol. 41, pp. 2271–2293, 1996.

[32] M. Mrozowski and M. A. Stuchly, “Parametrization of media dispersive properties for FDTD,” *IEEE Trans. Antennas Propag.*, vol. 45, no. 9, pp. 1438–1439, Sep. 1997.

[33] M. Lazebnik, M. Okoniewski, J. H. Booske, and S. C. Hagness, “Highly accurate Debye models for normal and malignant breast tissue dielectric properties at microwave frequencies,” *IEEE Microw. Wireless Compon. Lett.*, vol. 17, no. 12, pp. 822–824, Dec. 2007.

[34] C. Gabriel, S. Gabriel, and E. Corthout, “The dielectric properties of biological tissues: I. Literature survey,” Phys. Med. Biol., vol. 41, pp. 2231–2249, 1996.

[35] S. Gabriel, R. W. Lau, and C. Gabriel, “The dielectric properties of biological tissues: II. Measurements in the frequency range 10 Hz to 20 GHz,” Phys. Med. Biol., vol. 41, pp. 2251–2269, 1996.

[36] M. Lazebnik, L. McCartney, D. Popovic, C. B. Watkins, M. J. Lindstrom, J. Harter, S. Sewall, A. Magliocco, J. H. Booske, M. Okoniewski, and S. C. Hagness, "A large-scale study of the ultrawideband microwave dielectric properties of normal breast tissue obtained from reduction surgeries," *Physics in Medicine and Biology*, vol. 52, pp. 2637-2656, 2007.

[37] M. Lazebnik, D. Popovic, L. McCartney, C. B. Watkins, M. J. Lindstrom, J. Harter, S. Sewall, T. Ogilvie, A. Magliocco, T. M. Breslin, W. Temple, D. Mew, J. H. Booske, M. Okoniewski, and S. C. Hagness, "A large-scale study of the ultrawideband microwave dielectric properties of normal, benign, and malignant breast tissues obtained from cancer surgeries," *Physics in Medicine and Biology*, vol. 52, pp. 6093-6115, 2007.

[38] R. D. Beach, F. v. Kuster, and F. Moussy, “Subminiature implantable potentiostat and modified commercial telemetry device for remote glucose monitoring,” *IEEE Trans. Instrument. Meas.*, vol. 48, no. 6, Dec. 1999.

[39] R. D. Beach, R. W. Conlan, M. C. Godwin, and F. Moussy, “Towards a miniature implantable *in vivo* telemetry monitoring system dynamically configurable as a potentiostat or galvanostat for two- and three-electrode biosensors,” *IEEE Trans. Instrument. Meas.*, vol. 54, no. 1, Feb. 2005.

[40] T. Yilmaz, T. Karacolak, and E. Topsakal, “Characterization and Testing of a Skin-Mimicking Material for Implantable Antennas Operating at ISM Band (2.4 GHz-2.48 GHz),” *IEEE Antennas and Wireless Propagation Letters*, vol. 7, pp. 418-420, 2008.

[41] T. Karacolak, A. Z. Hood, and E. Topsakal, "Design of a dual band implantable antenna and development of skin mimicking gels for continuous glucose monitoring," *IEEE Trans. MTT*, vol. 56, no. 4, pp. 1001-1008, April 2008.

[42] T. L. Pope, M. E. Read, T. Medsker, A. J. Bushchi, and A. N. Brenbridge, "Breast skin thickness: Normal range and causes of thickening shown on film-screen mammography," *Journal of the Canadian Association of Radiologists,* vol. 35 (4), pp. 365-368, December 1984.

[43] Paul Moroz, Stephen K. Jones, and Bruce N. Gray, "Status of hyperthermia in the treatment of advanced liver cancer," *Journal of Surgical Oncology*, vol. 77, pp. 259-269, 2001.

[44] K. Demura, S. Morikawa, K. Murakami, K. Sato, H. Shiomi, S. Naka, Y. Kurumi, T. Inubushi, and T. Tani, "An easy-to-use microwave hyperthermia system combined with spatially resolved MR temperature maps: Phantom and animal studies," *Journal of Surgical Research*, vol. 134 (1), pp. 179-186, September 2006.

[45] Punit Prakash, Mark C. Converse, David M Mahvi, and John G Webster, "Measurement of the specific heat capacity of liver phantom," *Physiological Measurement*, vol. 27, pp. 41-46, 2006.

[46] X. He, S. McGee, J. E. Coad, F. Schmidlin, P. A. Iaizzo, D.J. Swanlund, S. Kluge, E. Rudie, and J. C. Bishof, "Investigation of the thermal and tissue injury behavior in microwave thermal therapy using a porcine kidney model", *Int. J. Hyperthermia*, vol. 20, no. 6, pp. 567-593, September 2004.